THESIS

BACKYARD TO BATTLEFIELD: MULTIFUNCTIONAL MEDICAL FOAM FOR ENHANCED WOUND MANAGEMENT

Submitted by

Amelia Stoner

Department of Mechanical Engineering

In partial fulfillment of the requirements

For the Degree of Master of Science

Colorado State University

Fort Collins, Colorado

Spring 2025

Master's Committee:

Advisor: Kirk McGilvray

Sing-Wan Wong
Lynn Pezzanite

ABSTRACT

BACKYARD TO BATTLEFIELD: MULTIFUNCTIONAL MEDICAL FOAM FOR ENHANCED WOUND MANAGEMENT

Acute open wounds as a result of traumatic injuries are a prevalent issue for civilians and military personnel across the world. Unfortunately, advanced hospital care for these severe injuries is not always readily available, leaving the morbidity and mortality outcomes of people who suffer these injuries to rely on primary wound care, hopefully applied before it is too late. A complete understanding of traumatic injury's effect on the body remains elusive. However, known complications include hemorrhage and infection of wounds if not treated quickly and effectively. Many primary wound care products exist, but few can perform more than one function. For example, packing a wound with gauze can help stop bleeding, but will not do anything to combat infection.

Thus, this work sought to generate a multifunctional therapeutic approach to primary wound care that includes bleeding (tranexamic acid) and infection (vancomycin) control agents delivered through a biopolymer carboxymethyl cellulose foam. This non-solidifying, volume-filling foam was hypothesized to improve the quality of care for those who sustain open wounds from traumatic injuries, especially those who are injured in rural or austere environments without immediate access to advanced care.

This work is comprised of four aims that will contribute to the field of emergency wound care. The first aim included generating and characterizing the base foam responsible for delivering selected bleeding and infection control therapeutics topically to the wound. 200% tunability in

temporal stability and volumetric expansion was demonstrated, indicating precise control over physical properties. The second aim was to evaluate the *in vitro* safety of the foam through monolayer live/dead staining of fibroblasts, one of the most prevalent cell types in skin. The foam and its constituents were found to be non-cytotoxic to both murine and human fibroblasts *in vitro*, indicating base-level safety of the material and potential for successful *in vivo* experimentation. The third aim focused on *in vitro/ex vivo* efficacy evaluation of antifibrinolytic and hemostatic properties of the foam on ovine blood with the chosen bleeding control therapeutic. Delivery with the foam demonstrated low clot lysis rates and mechanically robust blood clot rheology compared to other treatment formulations, indicating potential for successful *in vivo* experimentation in future work. The fourth and final aim evaluated the foam's *in vitro/ex vivo* antibiotic efficacy on methicillin-resistant *Staphylococcus aureus* with the selected infection control therapeutic. Delivery with the foam demonstrated 3-4 log bacterial killing of methicillin-resistant *Staphylococcus aureus*, indicating potential for successful *in vivo* experimentation in future work. Together, these aims provide novel preliminary data crucial to the product development process and *in vivo* implementation of the foam as a staple of primary wound care in acute open traumatic injuries.

ACKNOWLEDGEMENTS

I am extremely grateful to my graduate committee, fellow graduate students, OBRL co-workers, friends, and family for supporting me in this academic endeavor.

Firstly, I thank my advisor Dr. Kirk McGilvray for his continual patience and professional guidance. His enthusiasm for engineering is inspiring and contagious, and I could not have been successful in my role as a graduate student without him. Next, I would like to thank my committee members Dr. Sing-Wan Wong and Dr. Lynn Pezzanite for offering unique perspectives on the work described herein. Dr. Steven Dow was responsible for much of the inspiration behind this work, and his extensive expertise in biologic development was instrumental to this work. I would especially like to acknowledge Dr. Lynn Pezzanite for her generous assistance and guidance with many biological concepts unfamiliar to me as a mechanical engineer. She is an inspiration to me and everyone she works with. I would next like to acknowledge the support of the OBRL graduate students. The completion of this work would have been nearly impossible without camaraderie and the continual exchange of ideas. I would like to extend specific thanks to Jaci Linn, Abby Waugh, and Sam Winston for directly encouraging me through the duration of this work. Next, I would like to acknowledge the support of the Orthopedic Bioengineering Research Laboratory and the staff responsible for assisting me and my fellow graduate students in our research efforts, namely research engineers Ryan Foslien and Lucas Nakamura. Finally, I would like to thank my friends and family for their unwavering support in my academic and personal journey, namely my husband Will Augustine. I gratefully acknowledge the support of the Department of Mechanical Engineering and COEDIT for their financial support of this work.

TABLE OF CONTENTS

LIST OF TABLES

LIST OF FIGURES

Chapter 1 - Background

1.0 Open Traumatic Injuries

1.1 Overview

Annually, approximately 5-6 million deaths globally are a result of trauma [1]. In the United States, trauma is the leading cause of death for individuals between 1-45 years old and is the fourth leading cause of death accounting for all age groups [2]. As of 2020, the Center for Disease Control (CDC) estimates the total cost of injury in the United States to be $4.6 trillion [3], making trauma management an expensive endeavor for both healthcare corporations and patients alike.

There are many types of traumatic injuries, but overall, they can be categorized into three main groups: blunt, deceleration, and penetrating trauma [4]. Penetrating trauma accounts for approximately 15% of traumatic injury deaths worldwide [5] and 18.8% of injuries sustained by personnel in Iraq and Afghanistan, predominantly from blast wounds in war zones [6]. Direct injury of internal organs and/or the formation of open wounds created by penetrating trauma can lead to a multitude of both primary complications (hemorrhage, shock, contamination, etc.) and secondary complications (infection, ischemia, oxidative stress, etc.) if not treated quickly and efficiently [5, 7, 8].

1.2 The Golden Hour of Care

In casualty care, the “golden hour” of care is the first 60 minutes after injury. The level of injury care and treatment within this time frame has been found to be directly related to morbidity and mortality of those who suffer traumatic injuries [9, 10], making timely and effective care extremely important when treating traumatic injuries, especially penetrating injuries susceptible

to the primary and secondary complications. If not mitigated quickly, blood loss and sepsis from infection are especially problematic and are deemed to be the most significant dangers in civilian and combat related injuries [11].

1.3 Trauma-Induced Coagulopathy (TIC) and Hyperfibrinolysis

Severe penetrating trauma interferes with the natural clotting pathway in extremely complex ways, and the range of systemic changes that occur during traumatic injury and their consequences are still poorly understood [12].

Trauma-induced coagulopathy (TIC) is the overarching complication that describes abnormal coagulation processes after traumatic injury. TIC is a complicated condition that consists of bleeding (hypocoagulability), thrombotic (hypercoagulability), or mixed phenotypes dependent on factors such as wound type, injury severity, and, especially, time passed since the trauma first occurred. Generally, hypocoagulation occurs during the early stages of TIC (<6 hours of injury) whereas hypercoagulation typically occurs during later stages (>24 hours of injury). Unique challenges accompany all phenotypes; however, early TIC complications include acute blood loss, shock, impaired clot formation, and hyperfibrinolysis [13]. Hyperfibrinolysis is the direct result of the release of tissue plasminogen activator (tPA) by the body as a response to hemorrhage and shock. Blood clots that are able to form after injury are quickly dissolved due to the breakdown of fibrinogen and fibrin initiated by tPA [14]. With this breakdown comes a stark decrease in blood clot strength. This loss of strength can cause re-bleeding or dislodged clots, both of which can be detrimental to patients and have been shown to be linked to poor outcomes in trauma patients [15]. Thus, focusing emergency care efforts on mitigating hemorrhage from hypocoagulation and inhibiting the hyperfibrinolysis of clots that do form immediately after traumatic injuries is crucial for survival outcomes.

1.4 Infection and sepsis potential

Objects responsible for wounds, especially penetrating wounds, can introduce pathogens directly into the body's interior that are often driven deep into tissues or the bloodstream [16]. It is approximated that between 5%-32% of acute wounds become infected [17]. Wound irrigation and debridement along with antibiotic administration are common methods employed for infection prevention, but infections that develop can be difficult to treat. In extreme cases, infections that are untreated or insufficiently treated can lead to sepsis, organ disfunction, organ failure, and death [11, 18]. Thus, focusing emergency care on infection prevention and treatment is also crucial for survival outcomes concerning penetrating injuries and their resulting wounds.

2.0 Advancing Primary Wound Care: Gaps in Medical Standards of Care (SOCs)

Hospitals and advanced care settings are generally well-equipped to treat open wounds sustained from penetrating traumatic injuries, however this care is not always readily accessible within the "golden hour" of care. Rural environments for civilians and remote, austere, or delayed evacuation environments for military personnel lead to increased travel times to advanced care settings, making the quality and timeliness of primary wound care especially important for improved morbidity and mortality [10].

2.1 Department of Defense (DoD)

Many of the DoD's research proposal calls center around improvements to existing combat casualty care protocols, specifically for traumatic injuries that occur in prolonged, austere, remote, and/or expeditionary field settings.

The following are example statements of such proposal calls, each outlined by the Medical Technology Enterprise Consortium Military Prototype Advancement Initiative (MTEC-MPAI)

or the Congressionally Directed Medical Research Programs Peer Reviewed Medical Research Program (CDMRP-PRMRP):

MTEC-MPAI - Prophylactic to Prevent Infection in Battlefield Wounds from Complex Traumatic Penetrating Injuries in a Far-Forward, Austere Environment: This focus area of interest seeks the development of materiel solutions that have the following required solution characteristics:

- Must be able to conform to 3-dimensional wound shape (i.e., not a bandage)
- Must be self-absorbing or removable through wound irrigation
- Must be effective against at least one, but preferably multiple, high priority pathogens: Pseudomonas aeruginosa, Klebsiella pneumoniae, Acinetobacter baumannii, Staphylococcus aureus

… In addition, it is strongly preferred that proposed solutions provide the following desired solution characteristics:

- Integration of novel antibiotic drug classes against Gram-negative pathogens
- Single solution with ability to provide antibiotics, pain analgesics, and/or hemostasis compounds

CDMRP-PRMRP - Musculoskeletal Disorders Related to Acute and Chronic Bone Conditions and Injuries (Prevention): Develop strategies for improved point-of-injury care to mitigate risk of secondary complications and to address joint preservation…Develop and test strategies to prevent bacterial and/or fungal infections that occur with severe fractures or trauma.

CDMRP-PRMRP - Limb Stabilization and Protection: Development of rapid limb stabilization and novel wound protectants for severely or critically wounded limbs to enable prolonged care and eventual transport to the point of definitive treatment.

CDMRP-PRMRP - Retention Strategies (Battlefield Care): Strategies that can be utilized at or near the point of injury to allow an injured Service Member to remain on the battlefield or on mission without the need for evacuation. Treatment strategies that allow return to mission effectiveness within 30 days will be considered.

Current treatment protocols for patients are separated into care categories dependent on the Role of Care facility support level [19, 20] (**Table 1**).

Table 1: Descriptions of the Roles of Medical Care in the military.

	Size/Description	Treatments
Role 1	Unit-level Goal: Return patient to duty OR stabilize for evacuation to higher level care	Immediate life-saving measures (airway, bleeding, shock prevention, wound protection, stabilization) and preventative measures
Role 2	Large unit-level Goal: Stabilize for evacuation to higher level care, specifically for surgical treatment	Advanced trauma management (blood products, limited x-ray, laboratory, dental care) and limited surgical care
Role 3	Division-level Goal: Expand support provided at Role 2 and provide total treatment within evacuation policy	Diagnosis, holding, and total treatment (specialist diagnostic, surgical, preventative treatments) until return to duty
Role 4	Base hospital-level Goal: Definitive care of patients with required treatment longer than evacuation policy OR who need more advanced treatment than Role 3	Highly specialized, time-consuming treatments (specialist surgical and medical procedures, reconstruction, rehabilitation, and convalescence)

According to Joint Trauma System Clinical Practice Guidelines (JTSCPG), two main goals of acute, prolonged, traumatic wound care include hemorrhage control and minimizing infection [21]. Most triage care provided by Role 1 and Role 2 facilities centers around hemorrhage control, utilizing interventions include hemostatic gauzes, bandages, and tourniquets [21]. Although these treatments are well-established and relatively successful, secondary complications like re-bleed from TIC or infection can occur, especially if evacuation to advanced care is not readily available and/or resources are limited. Re-achieving hemostatic control in Role 1 and some Role 2 facilities generally include the use of clamps, sutures, or electrocautery when necessary [21], all of which can damage surrounding tissue. Antibiotic administration in Role 1 and some Role 2 facilities is limited to single dose, broad-spectrum, by mouth (PO) if evacuation is expected to be delayed [22]. Without access to antibiotics that are pathogen-specific, broad-spectrum treatment is either continued or stopped, both of which potentially lead to the development of drug-resistant organisms which are much more difficult to treat when appropriate care becomes available [23].

Thus, it can be reasonably deduced from DoD research proposals and current SOCs that reinforced hemostatic control and infection control are necessary in prolonged care scenarios where evacuation to higher levels of care are heavily delayed or not possible.

To determine if other traumatic wound care personnel identify similar pain points, emergency medical service (EMS) and hospital providers were interviewed as an extension of this research.

2.2 National Science Foundation Innovation Corps – Customer Discovery

To gauge the clinical extent of primary traumatic wound care problems outside of the military, Voice of Customer (VOC) structured interviews were conducted (A. Stoner: January 2024 to March 2024) with a spectrum of healthcare professionals (trauma surgeons, orthopedic surgeons,

paramedics) through the U.S. National Science Foundation Innovation Corps (NSF I-Corp) program.

Generally, EMS personnel serve as primary providers for severe injuries, while physicians and surgeons serve as secondary providers once patients reach the hospital. To identify current SOCs and pain points these customers face, five EMS providers and five surgeons were interviewed, covering a range of specialties related to acute wounds (**Figure 1**).

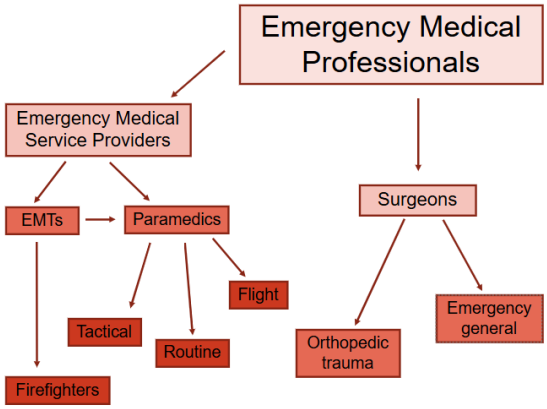

Figure 1: NSF I-Corp Voice of Customer interview profession breakdown. N=10.

2.2.1 EMS Providers

All EMS providers expressed concern for uncontrolled hemorrhage and stated that no antibiotics are currently administered in the field prior to hospital arrival. The primary concern for pre-hospital care revolves around patient stabilization and triage care as outlined by the Airway, Breathing, Circulation, Disability, and Exposure (ABCDE) approach for emergency assessment [24]. Essentially, establishing blood loss control is crucial in emergency evaluation and care, along with establishing a clear airway and sufficient breathing. Current field treatments used for bleeding control include hemostatic gauze, bandages, tourniquets, and blood transfusion, all of which are administered with sterile equipment and personal protective equipment (PPE) when possible to minimize infection risk. Issues with these treatments revolve around unpackable

wounds and potential improper equipment use, leaving personnel open to liability. EMS providers had differing opinions when asked if they thought field administration of antibiotics was necessary. Most agreed that administering antibiotics would be beneficial; however, they believed that the time spent doing so would be better suited for alternate care since hospitals are well-equipped to deal with debridement and infection control. EMS providers that were more concerned with infection prevention and treatment in the field consisted of flight and routine paramedics who provide care in remote or rural areas. Due to longer travel times, patients in these settings have delayed access to care and a much more substantial risk of complications from bleeding and infection.

2.2.2 Surgical Providers

All surgeons expressed the highest amount of in-hospital concern for infection because although pre-and post-operative antibiotics are administered either intravenously (IV) or topically, there are still high rates of infection after surgery. This sentiment was shared by general and orthopedic trauma surgeons operating on emergency trauma patients and scheduled orthopedic patients. Due to the external environment and initial focus of EMS on patient stabilization, elevated concern for potential infection was expressed for incoming trauma patients over non-emergent or elective orthopedic surgeries. However, biofilm formation on surgical hardware (plates, screws, etc.) also leads to relatively high rates of post-operative infection for non-emergent or elective surgeries, despite a well-established regiment of antibiotic administration. If proper hemostatic care is administered by EMS in the field, blood loss during surgery is less of a concern due to the more controlled environment. All surgeons expressed the importance of timely and effective pre-hospital care within the “golden hour” and stated that field administration could be beneficial as long as the antibiotics could be irrigated out at the hospital.

Surgeons also have the benefit of administering anesthesia, thus mitigating patient awareness or discomfort during treatment.

Through these VOC interviews and the NSF I-Corps program, valuable insight into current SOCs and pain points were identified for other sectors of emergency medicine besides military potential combat scenarios.

3.0 The Ideation of Medical Foam

In an attempt to mitigate pain points identified by the military and EMS providers and advance primary traumatic point-of-injury wound care caused by penetrating injuries, the development of a multifunctional, topical Medical Foam (MF) was idealized and pursued.

3.1 Hypothesized characteristics

Concentrated, localized therapeutic delivery to the entire wound geometry: Topical delivery of therapeutics to wounds has demonstrated high local concentrations with minimized systemic complications compared to intravenous and intramuscular injections [25-27]. Unlike bandages, powder, liquid, or gauze formulations, MF would conform to wound geometry and allow for homogenous distribution of therapeutics.

Tailorable temporal stability and therapeutic release: By controlling the temporal stability of the MF, therapeutic release and concentration can be controlled in the wound. As MF begins to lose volume, physical dilution takes effect and the concentration gradient of therapeutic agents increases, presumably reinforcing their respective effects in the wound.

Resource-saving and adjunct therapy compatible: Due to the MF's volumetric expansion, less base material will be used. The MF can be used in conjunction with other forms of wound care, such as gauze, bandages, etc., to not replace current SOCs, but enhance them.

3.2 Material Justification and Mechanisms

3.2.1 Base Material: Carboxymethyl Cellulose

Carboxymethyl cellulose (CMC) was selected as the base material for the MF. CMC is a popular cellulose-derived polymer used in many industries, including food, cosmetics, textiles, paper, and healthcare. CMC is cellulose that undergoes a chemical modification process to enhance its water-solubility, rheological properties, stability, adhesivity, absorption capability and ionic character, making it a versatile material for many applications. Most notably, its unique characteristics, including its ability to form viscous "gel" solutions and act as a stabilizing agent, make it a prevalent component in various medical applications. From pharmaceutical formulations to medical devices, CMC plays a crucial role in drug delivery systems, wound care, and ophthalmic solutions, showcasing its relevance in medical settings [28]. CMC has been shown to be biocompatible both *in vitro* and *in vivo* [29-33]. CMC is commonly found in the form of hydrogels, porous scaffolds, fibers, and gauze, depending on the application, presence of additives, and fabrication method. The ability to precisely adjust characteristics such as viscosity and elasticity allows for the development of wound dressings and topical formulations that cater to specific wound types and stages of healing [34]. The strength and rheological properties contribute to the absorption capacity of CMC, aiding in maintaining an ideal wound environment while controlling the emergence of exudates, both of which are conducive to healing. Moreover, its versatility allows for the incorporation of additional therapeutic agents, such as antimicrobial agents or growth factors, enhancing the overall performance of wound care products [35-37]. The amiable properties of CMC not only facilitate the customization of wound care materials but also contribute significantly to promoting an optimal healing environment for a diverse range of wounds.

3.2.2 Bleeding Control: Tranexamic Acid

Tranexamic acid (TXA) was chosen to act as an antifibrinolytic agent in the MF. TXA attaches to the lysine binding receptors present on plasminogen, thus preventing plasmin (the activated form of plasminogen) from breaking down blood clots. This mechanism of action is especially important when treating cases of TIC and hyperfibrinolysis. The half-life of TXA ranges from 2-11 hours, and the duration of action is 3 hours after the initial dose when applied intravenously [38]. According to a meta-analysis conducted by Mitha et al. (2024) on TXA use in spine surgery, intravenous administration leads to increased nervous system exposure and only a small percentage of intravenous TXA injections reach the target location [39]. This analysis included 18 previously published studies that passed certain search criteria and a risk of bias assessment. A total of 2177 patient outcomes were reported across the studies, and all were human participants with treatments of topical TXA in spine surgeries. This review found that since safety and efficacy for the topical and intravenous methods are comparable, localized treatment could be beneficial for a decreased risk of transfusion-related issues and thromboembolic events in spine surgery [39]. Furthermore, a narrative review by Gkiatas et. al (2022) outlined a range of topical TXA doses typically investigated for *in vitro* and *in vivo* toxicity studies as 0-100 mg/mL [40]. This range supports clinically relevant topical doses of TXA, including 100 mg/mL for acute epistaxis treatment [41], 25 mg/mL for temporary moistening of surgical wounds [42], and 10 mg/mL for sustained treatment of surgical wounds [43].

3.2.3 Infection Control: Vancomycin

Vancomycin was selected as an antibiotic agent in the MF. Vancomycin is a potent gram-positive antibiotic that weakens bacterial cell walls and causes leakage of intracellular components, thus initiating cell death. Vancomycin is one of the few antibiotics that can

effectively treat methicillin-resistant *Staphylococcus aureus* (MRSA) and is particularly effective against streptococci, enterococci, and staphylococci, all of which are common pathogens in penetrating trauma infections [44]. Vancomycin has a rapid onset of action when applied intravenously and has a terminal half-life of 4-6 hours in healthy adults with normal renal function. [45]. Local, topical antibiotics can be administered at higher local concentrations with lower systemic levels, decreasing the risk of nephrotoxicity or ototoxicity [46, 47]. Ostermann et al. (1995) compared the addition of an antibiotic bead pouch versus systemic antibiotics alone in preventing infection in 1085 open fractures and reported infection rates of 3.7% in those treated with the antibiotic bead pouch in addition to systemic antibiotics, compared with 12% in those treated with systemic antibiotics alone [47]. These high local concentrations decrease biofilm formation, bacterial resistance, and infection risk while bypassing impaired blood flow or necrotic tissue that would otherwise hinder intravenous antibiotic delivery [48]. A rat study published by Wei et al. (2023) introduced systemic vancomycin (SV; intraperitoneal injection, 88 mg/kg) or intraoperative intra-wound vancomycin powder (VP0.5: 44 mg/kg, VP1.0: 88 mg/kg, VP2.0: 176 mg/kg) after spinal implant surgery and methicillin-resistant S. aureus (MRSA; ATCC BAA-1026) inoculation in rats. No post-surgical deaths, wound complications or obvious signs of vancomycin adverse effects were observed. Bacterial counts and blood and tissue inflammation were reduced in the VP groups compared with the SV group, indicating that intra-wound VP may be more effective than systemic administration in preventing infection caused by MRSA after spinal implant surgery in a rat model [49]. The VANCO Trial is an ongoing human trial in which intrawound vancomycin safety and efficacy are being evaluated to reduce the rate of surgical site infections. Rather than being introduced topically in solution, 1-2 g of vancomycin powder is being introduced suprafascially into wounds [50-52]. Against

MRSA, the typical minimum inhibitory concentration of vancomycin does not typically exceed 8 μg/mL [53, 54]. Typical intravenous use of vancomycin in solution is not recommended to exceed 5 mg/mL.

3.2.4 Material Integration and Therapeutic Doses

All therapeutics are available in powder form, allowing for a long shelf-life (2-3 years) before integration into the CMC to form MF. Due to the exceptionally wide range of acceptable therapeutic doses of TXA and vancomycin, clinically relevant doses of 10 mg/mL TXA and 1 mg/mL vancomycin were chosen for MF *in vitro/ex vivo* experimentation with the exception of *in vitro* safety evaluations (see section 4.2). All materials are FDA-approved, although use in the MF would be considered off-label.

4.0 Specific Aims

To investigate the hypothesized characteristics of the MF, a series of specific aims were pursued with the goal of evaluating the MF tunability, *in vitro* safety, and *in vitro/ex vivo* efficacy:

4.1 Specific Aim 1: Generate and characterize a medical foam (MF) with tunable temporal stability and volumetric expansion

4.1.1 Outline

Bandages and other 2D treatments currently saturate the wound care market. Thus, the development and characterization of a volumetric treatment was pursued. A parametric study was conducted to define the production boundaries of the MF, while cadaveric boundary experiments were conducted to validate the 3D formulation and compare to alternate treatment formulations. An in-depth analysis of MF breakdown kinetics was conducted, and the effects of sterilization, shelf-life, and therapeutic addition were explored. Finally, viscosity and viscoelastic rheology were performed to characterize the physical properties of the MF.

4.1.2 Hypotheses

It was hypothesized that MF temporal stability would be mainly affected by CMC solution concentration and bubble size, and that sterilization would not alter the temporal stability or volumetric expansion. It was also speculated that MF would use less resources and be more mechanically robust than alternative treatment formulations.

4.2 Specific Aim 2: Evaluate the *in vitro* safety of the MF in murine and human dermal fibroblasts

4.2.1 Outline

Once it was confirmed that MF could be generated and specifically tuned, *in vitro* safety needed to be evaluated to ensure material biocompatibility. Thus, live-dead monolayer staining was conducted over a range of therapeutic concentrations for both murine fibroblasts and human dermal fibroblasts in anticipation of future *in vivo* rodent and human studies. Cytotoxicity was evaluated at 4-, 24-, 48-, and 72-hour treatment time points to simulate acute and prolonged MF application.

4.2.2 Hypotheses

MF was hypothesized to not be cytotoxic to murine or human fibroblasts. When loaded with therapeutics, cell viability with the MF would decrease in a time and dose dependent manner.

4.3 Specific Aim 3: Evaluate the *in vitro/ex vivo* bleeding control efficacy of the MF

4.3.1 Outline

To determine the effectiveness of TXA delivered with the MF, blood clot breakdown inhibition, blood clot viscoelasticity, and blood flow inhibition experiments were conducted using ovine blood. As hyperfibrinolysis is common in traumatic injuries, it is vital to ensure that blood clots that do form do not break down prematurely in the clotting process and are mechanically robust.

Thus, evaluating the antifibrinolytic properties of the TXA and the MF is crucial in anticipation of future *in vivo* studies. TXA efficacy was evaluated at 4-, 24-, 48-, and 72-hour treatment time points to simulate acute and prolonged MF application.

4.3.2 Hypotheses

It was hypothesized that MF with TXA would significantly slow down blood clot lysis and prolong clot formation ability. The MF was not speculated to significantly slow or inhibit active blood flow.

4.4 Specific Aim 4: Evaluate the *in vitro/ex vivo* infection control efficacy of the MF

4.4.1 Outline

To determine the effectiveness of vancomycin delivered with the MF, bacterial killing ability was evaluated against methicillin-resistant *Staphylococcus aureus*. Gram positive bacteria are common pathogens in wounds resulting from penetrating injuries, so ensuring effective vancomycin delivery and bacterial killing of prevalent pathogens is vital to the feasibility of future *in vivo* studies. Vancomycin efficacy was evaluated at 4-, 24-, 48-, and 72-hour treatment time points to simulate acute and prolonged MF application.

4.4.2 Hypotheses

It was hypothesized that MF with vancomycin would demonstrate > 2 log reduction in MRSA bacterial load and that MF would demonstrate superior killing ability compared to alternative treatment formulations.

1.0 Background

Foam is classified as a thermodynamically unstable two-phase system consisting of gas entrapment in a continuous liquid phase. Due to this instability, foam structure begins to decay immediately after creation due to a combination of drainage, coarsening, and coalescence [55, 56].

Drainage occurs when the liquid phase of the foam begins to flow through the borders that separate gas bubbles due to gravity. This process reduces the border thickness between bubbles, leading to coarsening (growth or shrinkage due to gas diffusion) and coalescing (merging due to border rupture) of bubbles [57, 58]. Coarsening and coalescing lead to an increased average bubble size over time, making bubble popping and volumetric loss more likely to occur [59] (**Figure 2**).

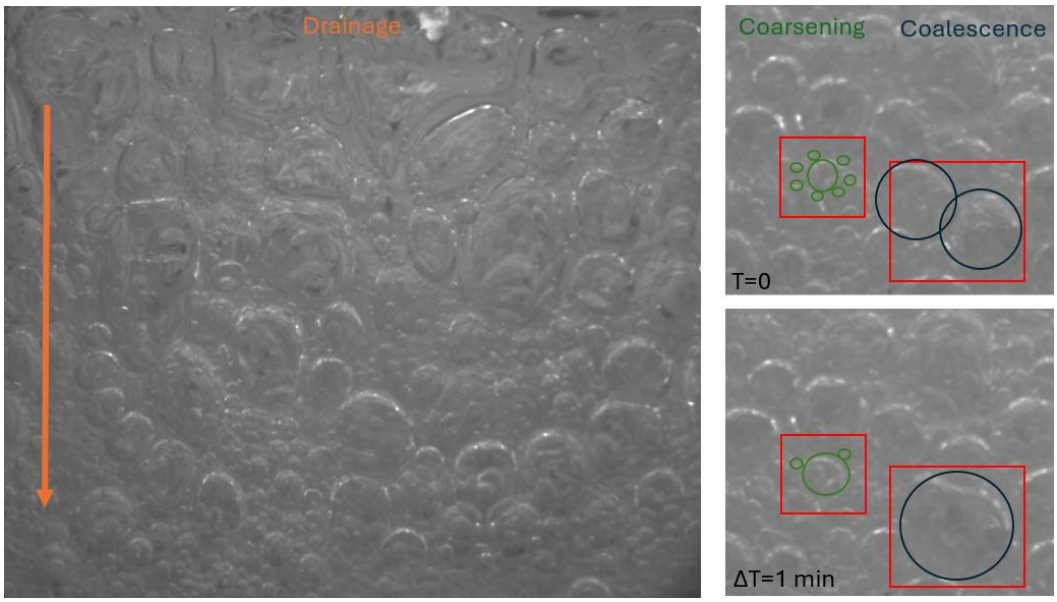

Figure 2: Drainage, coarsening, and coalescence concept demonstration in MF.

Foam can be formed by chemical reaction processes [60-64] or physical processes that include mechanical or induced mixing [65], pressure release [66-68], and/or gas injection (aeration or sparging) [69, 70]. Physical foaming was chosen to produce the foam developed herein to minimize foam production complexity and the introduction of non-biocompatible constituents that may form due to chemical foaming. A commercially available pressurized canister was selected as the MF method of generation, which operates by a combination of pressurized gas injection, mixing, and pressure release principles. Nitrous oxide gas is injected into the canister body which contains the foam's base CMC solution in a viscous liquid form. The canister is then pressurized, and mixing occurs (shaking) to further incorporate gas bubbles into the CMC solution. Finally, the pressure is released by a valve, and the pressure difference from the canister to the atmosphere forces the resulting foam out of a nozzle to be deposited on a surface. The gas bubbles formed in the canister expand when exposed to lower pressure in a classic demonstration of Boyle's law, which states that pressure and volume of a gas have an inverse relationship when temperature is assumed constant (**Equation 1**).

$$\text{Equation 1: } P_1V_1 = P_2V_2$$

This bubble expansion is responsible for a large increase in solution volume due to large gas pockets. Thus foam is formed.

There is no known literature on CMC-based polymer liquid foams. Regardless, established foam parameters can include foam decay, which is widely characterized by bubble size measurements, bubble size distributions, and drainage volume or volumetric loss over time [71-75]. Thus, to determine the validity and versatility of MF generation with this foaming method, a series of foam generation, stability, and characterization experiments were conducted based on accepted foam decay measurement methods and procedures.

2.0 Parametric Study for MF Optimization

To define the working limits of the MF and explore which parameters influenced its characteristics the most, MF was generated at various input conditions, and volumetric stability, breakdown time, and volumetric expansion were recorded for each set of parameters. The MF formulation that optimized increased volumetric stability and expansion was identified.

2.1 Materials and Methods

2.1.1 MF Preparation and Generation

Carboxymethyl cellulose sodium salt powder (Santa Cruz Biotechnology, Santa Cruz, CA, USA) was dissolved into 1x phosphate-buffered saline (PBS) to form the desired weight by volume (w/v) CMC solution concentrations (i.e. 1%, 2%, 3%). These mixtures were homogenized by continual mechanical mixing (300-700 rpm, AM120Z-H Laboratory Mixer) at 25°C until complete CMC dissolution was observed. The resulting solutions were refrigerated at 2°C overnight to allow for complete CMC powder hydration and stored until experimental use. As described above, the base MF was created by adding the hydrated CMC solution into commercially available whipped cream canisters (AmazWhip, China) and pressurizing with nitrous oxide chargers (Whip-it!, San Francisco, CA, USA).

2.1.2 Primary Parametric Study Design

CMC solution concentration, CMC solution temperature, gas introduction position/shaking orientation of the canister, and shaking frequency variables were parameterized to investigate their effects on the MF's volumetric stability and expansion (**Table 2**).

Table 2: Primary input parameters and resulting outputs for factorial design of volumetric stability and expansion parametric study.

Inputs				Outputs
Conc.	Temp.	Intro./Orient.	Freq.	Time to volume loss onset
1%	2°C	1. Top-down/Nozzle-up	50	Breakdown time
2%	20°C	2. Aerated/Nozzle-up	100	Expansion factor
3%		3. Top-down/Nozzle-down	200	
		4. Aerated/Nozzle-down	300	
		5. Top-down/Alternating		
		6. Aerated/Alternating		

Solution concentration refers to the w/v ratio of CMC powder to PBS, while solution temperature refers to the storage temperatures before experimentation. Top-down and aerated gas introduction refers to if N_2O was introduced on top of the solution or through the bottom of the solution, while nozzle-up, nozzle-down, or alternating orientation refers to the canister position during the mixing (shaking) process (**Figure 3**). Mixing frequency refers to how many times the canister was manually shaken up and down.

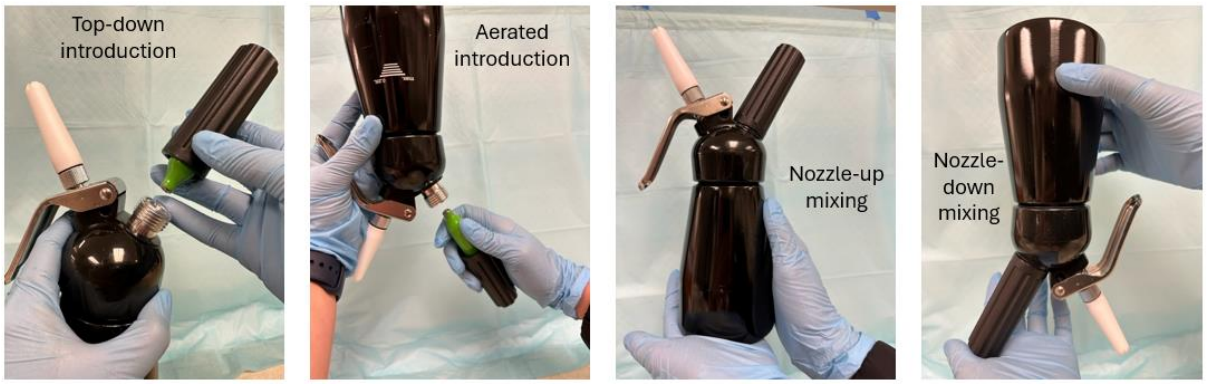

Figure 3: Representative images of gas introduction and mixing orientation parameters.

Time to volumetric loss onset was defined as the time (minutes) of observed volumetric collapse, characterized by visual CMC residue beginning to coat the surface of the observation container. Breakdown time was defined as the time (minutes) at which macroscopic collapse was no longer observed. MF expansion factor was defined as the ratio of initial MF volume (mL) to final solution volume (mL) after complete volume loss.

A primary full factorial design table was generated using these parameters, and the resulting stability and expansion outputs were recorded in duplicate for each combination. The best-performing combinations were further manipulated by introducing the additional variables of pressure and off-gassing (pressure release) cycles and expanding the range of shaking frequencies. Aerated/alternating, 2°C, and 3% inputs were chosen as constants for the secondary input factors (**Table 3**).

Table 3: Secondary input parameters and resulting outputs for factorial design of volumetric stability and expansion parametric study.

Expanded inputs			Outputs
Canister pressure	Release cycles	Mixing frequency	Time to volume loss onset
1 cartridge	0	25	Breakdown time
2 cartridges	1	50	Expansion factor
	2		

2.1.3 Secondary Parametric Study Design

A secondary factorial design table was generated from these parameters, and the resulting stability and expansion outputs were recorded in duplicate for each combination. All input and output combinations were plotted and working stability/expansion limits of the MF were defined. An optimized combination was chosen as a representative MF formulation for further MF generation and experimentation.

Canister pressure was classified in terms of the number of N_2O cartridges per pressure release cycle. Based on nitrous oxide cartridge specifications, MF canister dimensions, and an assumed 100 mL of CMC solution, 1 cartridge was estimated to pressurize the canister to 2 MPa and 2 cartridges was estimated to pressurize the canister to 4 MPa. Pressure relief cycles consisted of N_2O expulsion from the canister without releasing MF, achieved by forcing CMC solution to the bottom of the canister before off-gassing the nitrous oxide via the canister's release valve.

2.2 Results

2.2.1 Primary Parametric Study

The primary input parameters that most drastically impacted volumetric stability and expansion were solution concentration (viscosity) and gas introduction position/shaking orientation combinations. Overall, increased solution concentrations demonstrated high volumetric stability but lower expansion capabilities whereas decreased solution concentrations demonstrated an inverse relationship. This trend persisted across all gas introduction/shaking orientation combinations, temperatures, and shaking frequencies (**Figure 4**).

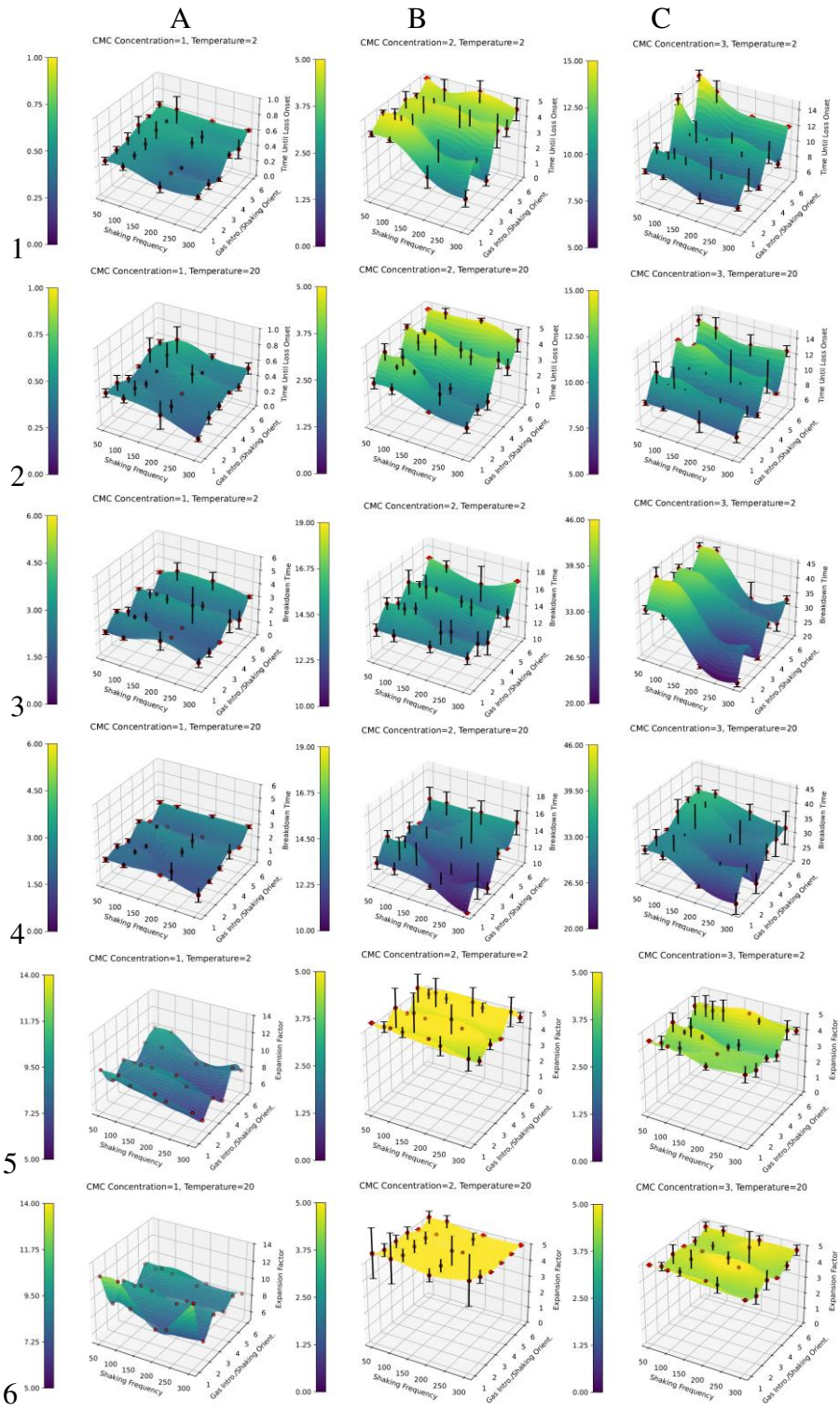

Figure 4: Primary time until loss onset (rows 1-2), breakdown time (rows 3-4), and expansion factor (rows 5-6) plots with shaking frequency and gas introduction/mixing combinations (assigned numeric values based on **Table 2**) on x and y axes at each solution concentration and temperature combination (columns A, B, C).

Higher concentrations of CMC-based polymer solutions generally demonstrate increased viscosity compared to lower concentrations, especially in CMC-based materials [76-83]. As the concentration of polymer chains increases, they begin to overlap and entangle, leading to a restriction in molecular movement [84, 85]. This entanglement is likely why the experimental results demonstrated increased stability (15 minute time until volume loss, 40 minute breakdown time) with 3% CMC solutions (**Figure 4**, C1 and C3) as compared to 1% (0.6 minute time until volume loss, 3 minute breakdown time) and 2% (5 minute time until volume loss, 17 minute breakdown time) CMC solutions (**Figure 4**, A1 and A3, B1 and B3). These data suggest the benefit of higher solution concentrations for subsequent experiments.

Overall, foams that were aerated with the nitrous oxide cartridges demonstrated increased volumetric stability and decreased expansion capabilities as compared to foams where nitrous oxide was introduced top-down into the CMC solution. This behavior is hypothesized to be due to increased N_2O volume contact with and travel time through the CMC solution, although there are no known studies that explore these effects. However, a common method of wet foam generation is diffusion or sparging of gas through a solution in a bottom-up configuration [86-88] (**Figure 5**).

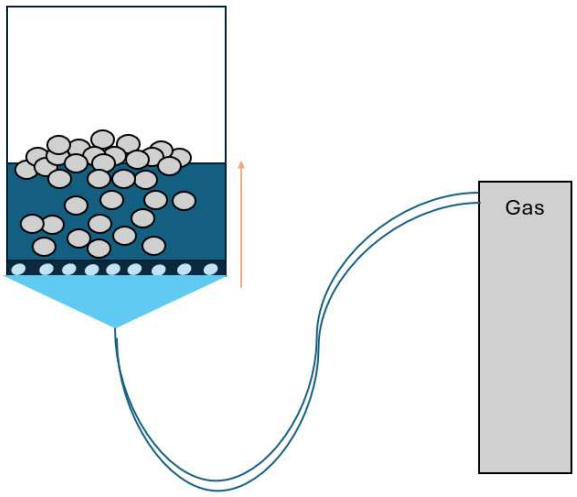

Figure 5: Diagram of gas diffusion or sparging. Gas is introduced into the bottom of a container, and then it travels through a foaming solution to create foam.

Aerated foams shaken in an alternating nozzle up-nozzle down pattern generally demonstrated increased volumetric stability (15 minute time until volume loss, 40 minute breakdown time for 3% CMC solution) as compared to aerated foams shaken in a nozzle-up (10 minute time until volume loss, 40 minute breakdown time for 3% CMC solution) or nozzle-down (13 minute time until volume loss, 38 minute breakdown time for 3% CMC solution) orientation (**Figure 4**, C1 and C3). This is hypothesized to be a function of the inherently increased agitation experienced by the CMC solution with excess mixing introduced by the nozzle up-nozzle down pattern changes. Increased agitation has been shown to be conducive to foam stability, due to further dispersion of the gas into the foaming solution [89, 90]. These trends persisted across higher solution concentrations and shaking frequencies (**Figure 4**, B1:C4).

Generally, volumetric stability decreased, and expansion capability increased slightly in 20°C formulations as compared to 2°C across all solution concentration and gas introduction/shaking orientation groups (**Figure 4**, rows 2, 4, 6). It is well known that temperature affects polymer solution characteristics, especially at high concentrations [91-93]. Interestingly, increased

shaking frequencies led to both decreased volumetric stability and expansion. These results suggest a point of diminishing returns where excessive agitation is detrimental to foam stability. However, this conjecture is difficult to correlate with historical data as literature sources on this behavior in foamed polymer solutions is limited.

2.2.2 Secondary Parametric Study

The secondary input parameter that most impacted volumetric stability and expansion was the number of aeration/off gassing (pressure release) cycles. Increasing the number of pressure release cycles greatly increased the volumetric stability and greatly decreased the expansion ability of the resulting foam (**Figure 6**).

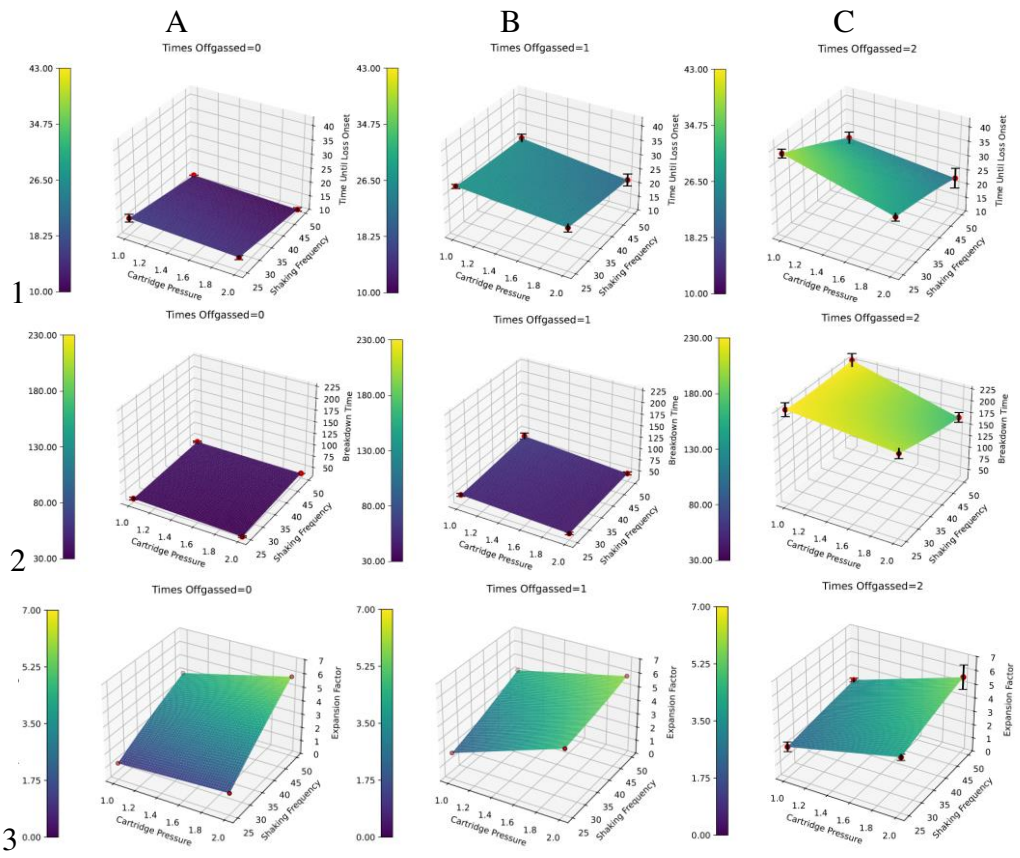

Figure 6: Secondary time until loss onset (row 1), breakdown time (row 2), and expansion factor (row 3) plots with cartridge pressure and shaking frequency on x and y axes at each pressure release (off-gas) value (columns A, B, C).

Inherent to an increased number of pressure release cycles, the CMC solution was aerated multiple times before foam generation with the canister. This process results in more gas becoming trapped in the CMC base solution, forming smaller bubbles and ultimately increasing temporal volume stability upon release from the canister. Increasing the cartridge pressure in the canister demonstrated large increases in expansion factors (**Figure 6** ,row 3), but slight decreases in the volumetric stability of the foam (**Figure 6** ,rows 1-2) at 1 and 2 times off-gassed (**Figure 6**, column B-C). These results are hypothesized to be due to increased shear conditions upon exit of the canister, caused by an increased pressure difference between canister and environment that forces the MF to exit the nozzle at a high exit velocity, potentially rupturing resulting bubbles

and leading to accelerated breakdown (see discussion on rheological data indicating that the foam is a shear thinning material in section 6). Mechanical deformation, including high shear, is commonly utilized as an anti-foamer for processes where foam formation is not desired, such as in bioreactors and during concentrate processing [94, 95], thus supporting these findings. Reduced mixing frequency (25 shakes) yielded limited expansion capabilities and the resultant composition did not truly take on a foam-like formulation. Volumetric stability results at this frequency were unreliable, as the limited expansion made it difficult to determine exactly when breakdown occurred.

From the results of this parametric study, input parameters that yielded the most volumetrically stable and least volumetrically stable MF formulations were determined, and a formulation that optimized volumetric stability and expansion capabilities was chosen to move forward with all future experimentation (**Table 4**).

Table 4: Highest stability, lowest stability, and optimized volumetric stability and expansion parameters and resulting time until loss onset, breakdown time, and expansion factor values.

Highest Stability MF Parameters			
Input Parameters	3% CMC solution	Optimized Output	**39 min ± 1.41** Time until loss onset
	2°C CMC solution		
	2 pressure release/off-gassing cycles		
	1 cartridge pressure		**230 min ± 14.14** Breakdown time
	Aerated gas introduction/alternating shaking		**2.22x** Expansion factor
	25 shakes		
Lowest Stability MF Parameters			
Input Parameters	1% CMC solution	Optimized Output	**0.23 min ± 0.03** Time until loss onset
	20°C CMC solution		
	0 pressure release/off-gassing cycles		
	1 cartridge pressure		**1.37 min ± 0.53** Breakdown time
	Top-down gas introduction/nozzle-up shaking		**12.50x** Expansion factor
	300 shakes		
Optimized MF Parameters			
Input Parameters	3% CMC solution	Optimized Output	**26.5 min ± 2.12** Time until loss onset
	2°C CMC solution		
	2 pressure release/off-gassing cycles		
	1 cartridge pressure		**230 min ± 14.14** Breakdown time
	Aerated gas introduction/alternating shaking		**3.23x** Expansion factor
	50 shakes		

By plotting the upper and lower volumetric stability and expansion limits, minimal and maximal expansion slopes after maximum and minimum volumetric stability were calculated and yielded a 199.5% difference (**Figure 7**).

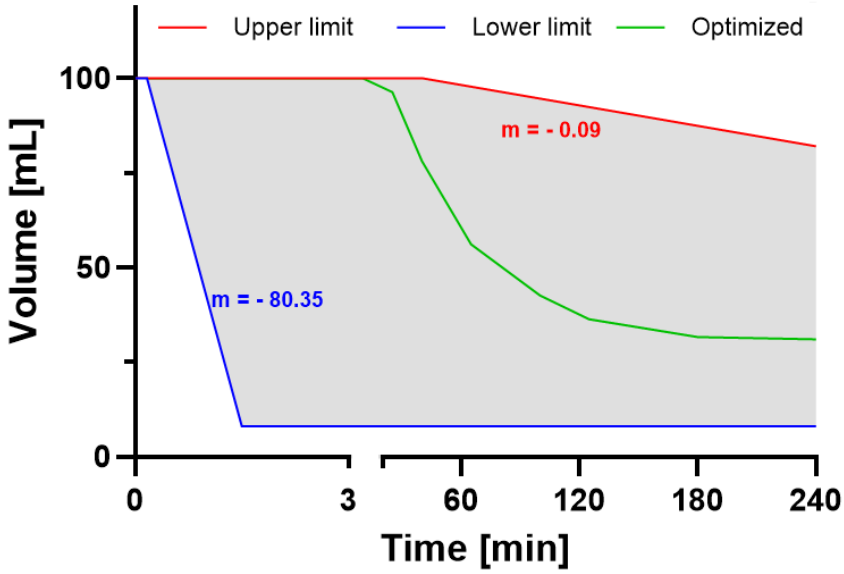

Figure 7: MF volumetric stability and expansion limits. M values represent average rates of volumetric loss.

Limitations of this study design include incomplete exploration of the secondary factors on all combinations of the primary factors (not just the most volumetrically stable formulation) which could give a more comprehensive outline of the MF breakdown under specific conditions. Regardless, culmination of these results demonstrate precise control over the MF's temporal stability and volumetric expansion over a range of input conditions.

3.0 MF Wound-Filling Capabilities and Advantages

To represent the wound-filling capabilities of the optimized MF (**Table 4**, **Figure 7** above) in biological tissues, cadaveric ovine muscle (i.e. the biceps femoris muscle from the hind limb) from unrelated preclinical studies was collected and used to create large volumetric wounds *in vitro*.

3.1 Adhesiveness and Coating Evaluation

3.1.1 Materials and Methods

To visually demonstrate MF tissue adhesiveness and drainage from the wound, MF was deposited into a large cavity wound created in a surgically isolated portion of ovine muscle and suspended at a 90° angle. MF behavior was then visually monitored over 1 minute (**Figure 8**).

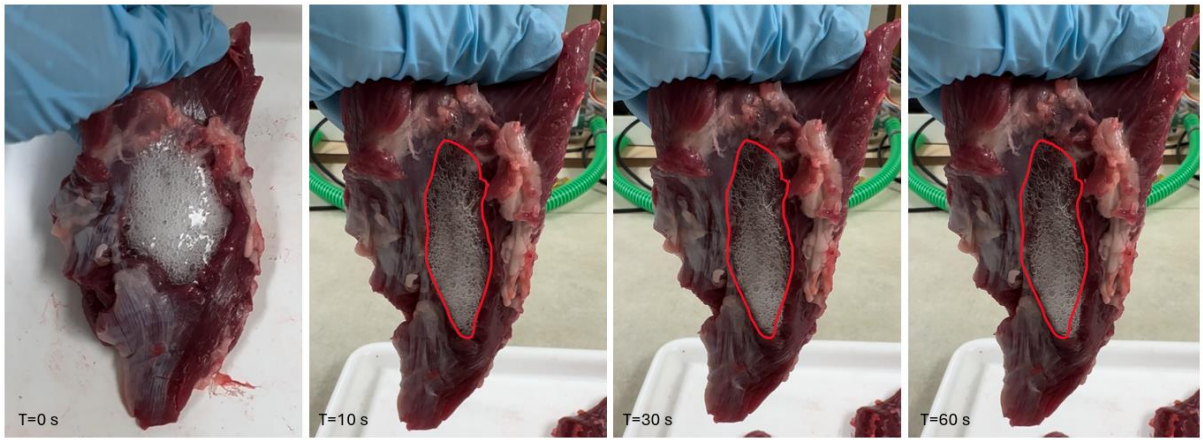

Figure 8: Ovine cavity wound filled with MF and held at 90°. MF behavior was monitored for 1 minute to determine adherence and coating.

3.1.2 Results and Discussion

Over the course of 1 minute, the MF slowly begins to drain from the cavity wound due to gravity, leaving behind a CMC residue on the cavity wall. This is hypothesized to be a desirable quality, as wound beds will not always be in a supine orientation and gravity will not always

keep treatment interventions in place. In the likely event that the patient needs to move to another location or position during the treatment [96, 97], MF can adhere to and coat the tissue if it does run out of the wound. This slow drainage allows for increased contact time of the therapeutic agents embedded in the MF with the wound bed, thus increasing the treatment exposure concentrations and durations. As demonstrated in the parametric study on MF stability, as the MF breaks down it returns to a CMC solution over time and loses volume when doing so. Thus, the ability of MF to coat tissue allows for treatment application even during volumetric breakdown.

3.2 Radiographic Evaluation of Volumetric Filling

3.2.1 Materials and Methods

The MF's volumetric wound bed-filling was determined by x-ray imaging by incorporating 3 mL of an imaging contrast agent (Hexabrix, Mallinckrodt, Lot V188B) into the base CMC solution before MF generation. A large 8cm x 5cm x 5cm cavity wound was created in a cadaveric portion of ovine muscle and radiographs (MyRad, Universal Imaging, CXDI Control Software NE Ver 2.19.0.13) were captured temporally after MF application (**Figure 9**).

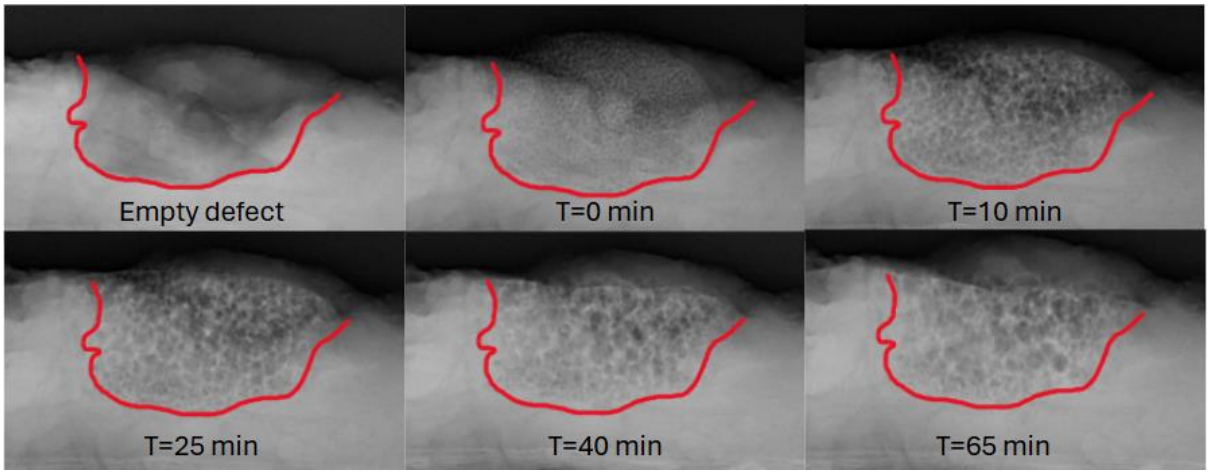

Figure 9: Temporal radiographs of MF-filled cavity wound. Red line outlines the cadaveric boundary wound layer. Dark circles within this outline are bubbles in the MF.

3.2.2 Results and Discussion

The imaging contrast agents in the MF were visible on the radiographs (light) in the liquid borders between bubbles (dark). Thus, further experimentation was pursued to include volume-filling capabilities and material use to alternate formulations of treatment deliveries including CMC powder/paste, CMC solution, and gauze (Quik-Clot Z-fold Vacuum Packed Combat Gauze, Teleflex). Detached ovine hind limbs were utilized, leaving the leg muscles intact but removing the hamstring to improve lateral x-ray imaging (**Figure 10**).

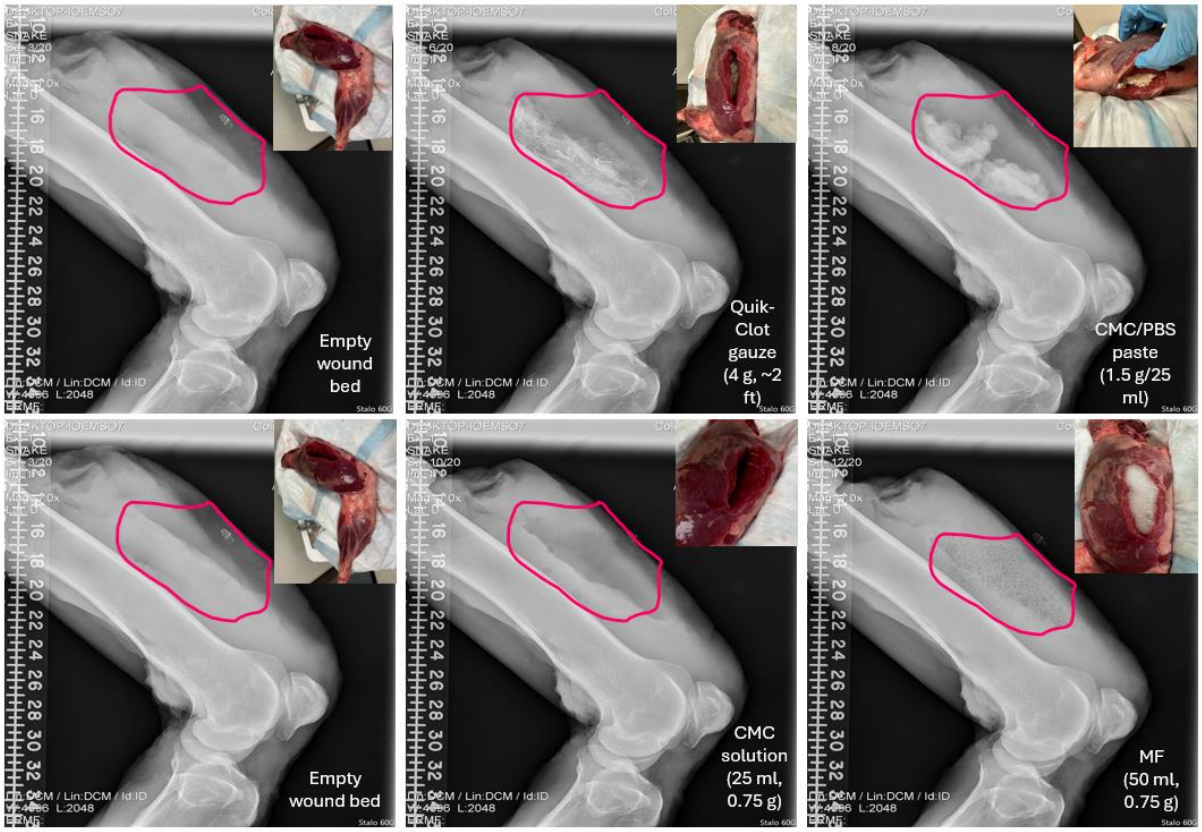

Figure 10: Comparative cadaveric volumetric wound filling. Treatments include an empty cavity wound, Quik-Clot gauze, CMC paste, CMC solution, and MF. Pink line outlines the wound boundary.

MF filled the wound entirely using less material than other treatment modalities. 25 mL of 3% CMC solution (0.75 g CMC powder), 25 mL of CMC paste (1.5 g CMC powder), and 2 ft (4 g Quik-Clot gauze) all provided ~50% volumetric filling of the wound bed, as compared to 100% volumetric filling demonstrated by MF that only used 0.75 g of CMC powder in the base material due to the volumetric expansion. A reduction in material use to fill the wound indicates the potential for the MF to have similar efficacy with decreased material waste and reduced production cost. Reduction in material use may also indicare space-saving opportunities for personnel carrying and applying the MF.

MF adheres to muscle tissue in the wound bedand coats the surface during eventualy uncontained runoff. In addition to these characteristics, MF provides complete volumetric wound

filling while using at least half of the raw material amount of powder, solution, or gauze formulations, thus saving resources and reducing material waste.

One study limitation is the use of simulated open wounds in cadaveric tissue without pressure/closure, blood flow, or an accurate wound environment. These conditions can only truly be evaluated *in vivo*. However, the volumetric filling data is representative of potential wound bed sizes and positioning.

4.0 Sterilization and Therapeutic Addition Effects on Volumetric Breakdown

4.1 Materials and Methods

After choosing an optimal MF formulation, the effects of autoclave sterilization and therapeutic (i.e. TXA and vancomycin) addition on time-dependent volumetric breakdown were determined for the MF. Volumetric loss, solution drainage, bubble distributions, and average bubble sizes at established time points were measured and compared for sterile and non-sterile MFs and vancomycin and TXA-loaded MFs (N = 9). CMC solutions were generated as previously described before autoclaving at 121°C for 15 minutes and storage at 4°C overnight to regain viscosity before experimentation. Powdered vancomycin (Vancomycin Hydrochloride, VANCOCIN, Lot 28420) and TXA (Tranexamic Acid, ChemCruz, Lot H0824) were reconstituted in a small volume (5 mL) of PBS and thoroughly mixed into the base CMC solution immediately before experimental use to achieve the desired therapeutic w/v concentration (10 mg/mL TXA, 1 mg/mL vancomycin).

4.1.1 Volumetric Stability Comparison

Foam breakdown was monitored over 240 minutes, the longest observed experimental time for complete volumetric loss in the previous parametric stability studies. In addition to volumetric loss onset and breakdown times, liquid drainage from the MF was observed and defined as the volume of solution present during MF breakdown [55]. Drainage does not automatically correspond to volume loss, although the final MF volume and final drainage volumes are equivalent. Still images of a clear 20 x 50 x 100 mm container were taken, and MF heights at selected time points were analyzed using ImageJ (ImageJ, Version 1.54m, NIH).). All samples had an initial height of 50 mm, corresponding to a volume of 100 mL. Averages and standard deviations of 9 samples were calculated and reported. Statistical analysis for volume and

drainage measurements were performed using two-way ANOVA with Tukey's multiple comparisons.

4.1.2 Bubble Size and Distribution Comparison

Bubble size throughout the MF was monitored concurrently with volume loss and quantified in the same container over the same time points. Bubble size in foams is well-known to be closely related to volumetric stability through coarsening and coalescence [98-100]. Randomly sampled bubble diameters were measured over a constant 20 x 50 mm area, with sample sizes equaling the corresponding MF volume in mL to keep sampling consistent at each time point (ex. 100 bubbles per 100 mL). Bubble size averages and deviations for 9 samples were calculated, and frequency distributions were determined at each time point to assess the overall homogeneity of each MF (**Figure 11**).

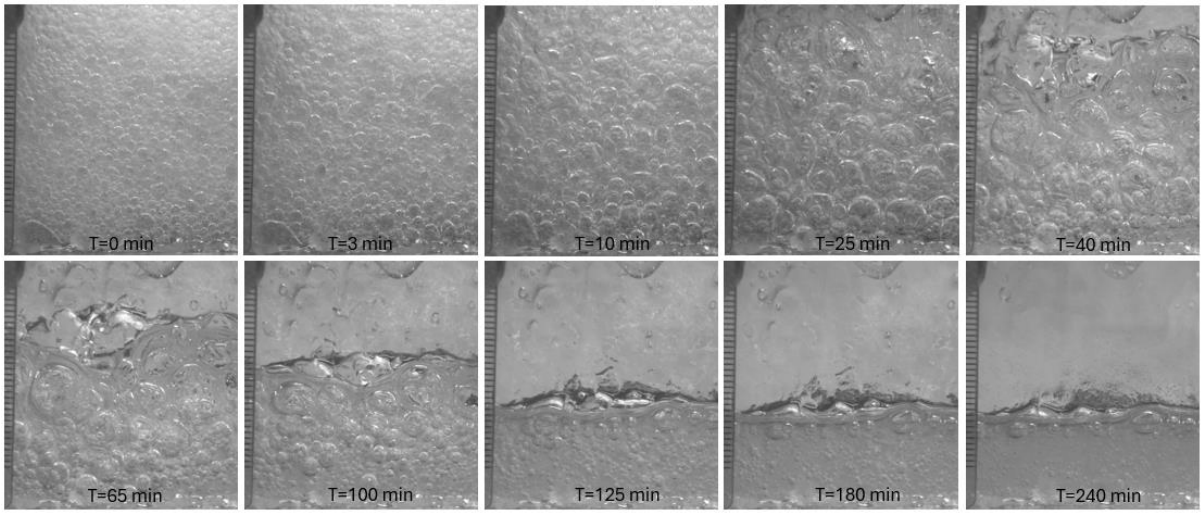

Figure 11: Optimized MF temporal breakdown images to measure average volume loss, drainage, and bubble diameters.

Statistical analysis was conducted using two-way ANOVA with Tukey's multiple comparisons for bubble size and non-parametric Kruskal-Wallis tests with Dunn's multiple comparisons for bubble distribution.

4.2 Results and Discussion

Sterilized MF bubble size, volumetric stability, drainage, and bubble distribution were compared to non-sterile, sterile MF with 10 mg/mL TXA, sterile MF with 1 mg/mL, and sterile MF with 10 mg/mL TXA and 1 mg/mL vancomycin to determine differences in measures of stability and if these differences could be related to bubble size and distribution (**Figure 12**).

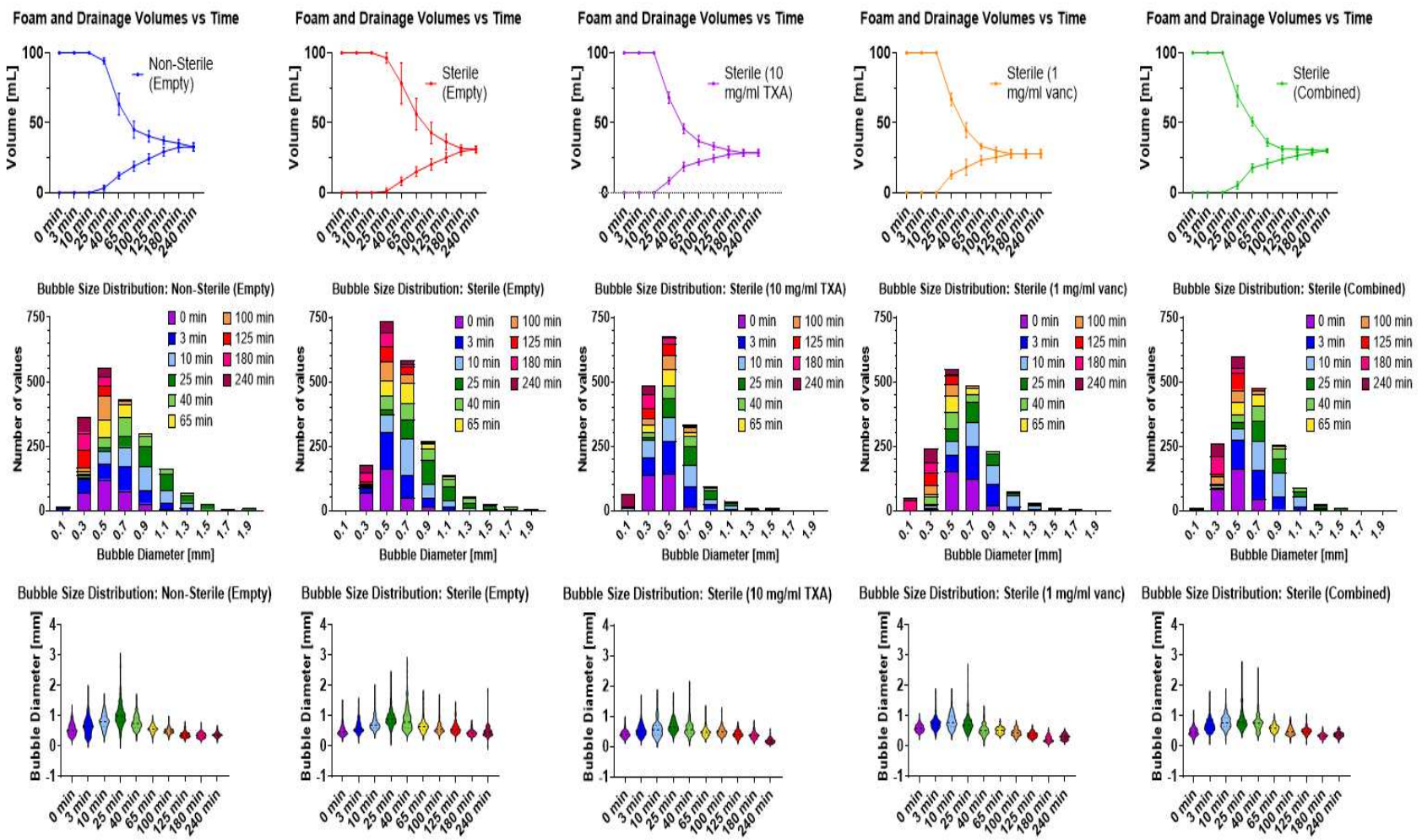

Figure 12: MF average volume loss and drainage with standard deviation (top row), bubble size distribution (middle row), and average bubble size (bottom row) over time for non-sterile, sterile, sterile with TXA, sterile with vancomycin, and sterile with TXA and vancomycin formulations. N=9 samples.

4.2.1 Sterile vs Non-Sterile MF

Compared to non-sterile MF, sterile MF without any therapeutics demonstrated no significant difference in time until volumetric loss onset (volume at 25 minutes, $p = 0.80$) or expansion (final volume, $p = 0.90$), but a lower rate of loss (higher volumes and less drainage) and a more uniform bubble size (tighter distribution curve). These results suggest that sterilizing the CMC solution by autoclave (high temperature and pressure) has some effect on the MF structure. However, the sterile MF remains fundamentally unchanged in volumetric stability and expansion behavior compared to the non-sterile MF generated and used throughout the parametric study. The literature does not currently support or disprove these results, however autoclaving some polymer solutions has been demonstrated to alter the properties at extended sterilization periods [101].

4.2.2 Sterile vs Therapeutic-Loaded Sterile MF

Once the sterile MF was loaded with TXA, vancomycin, or a combination of the two, time until volumetric loss onset and maximum bubble diameter at MF volumetric loss onset (25 min) decreased, while expansion stayed consistent. Bubble size was more uniform for sterile MF than sterile MF with TXA and sterile MF with vancomycin, but sterile MF had similar uniformity to sterile MF with TXA and vancomycin. Due to the large number of sampled time points and desired statistical comparisons, **Table 5** outlines stability, expansion, bubble size, and bubble distribution comparisons determined temporally over 240 minutes.

Table 5: Statistically significant comparisons for non-sterile, TXA, vancomycin, and combined MF formulations as compared to sterile MF formulations. Statistical significance ($p < 0.05$*, $p < 0.01$ **, $p < 0.001$***, $p < 0.0001$****) was determined using two-way ANOVA with Tukey's multiple comparisons for volume, drainage, and bubble size and Kruskal-Wallis tests with Dunn's multiple comparisons for distribution.

Comparison	Outcome	T=0	T=3	T=10	T=25	T=40	T=65	T=100	T=125	T=180	T=240
Non-Sterile (Empty) vs Sterile (Empty)	Volume					****	****				
	Drainage					**	**	**	**		
	Bubble Size	*		***	****	****	***	*	****		*
	Distribution	*		****			***	***	****	****	***
Sterile (Empty) vs Sterile (Combined)	Volume				****	****	****	****	*		
	Drainage				**	****	****	*			
	Bubble Size		*			****	*	**	*	*	*
	Distribution		**	*	**			****	*	****	***
Sterile (Empty) vs Sterile (10 mg/mL TXA)	Volume				****	****	****	****	*		
	Drainage				****	****	****	**			
	Bubble Size	****	****	****	****	****	****	*	****		****
	Distribution	****	****	****	****	****	****	****	****	**	****
Sterile (Empty) vs Sterile (1 mg/mL vanc)	Volume				****	****	****	****	****		
	Drainage				****	****	****	***			*
	Bubble Size	****	****	***	****	****	****	****	****	****	****
	Distribution	****	****	***	****	****	****	****	****	****	****
Sterile (10 mg/mL TXA) vs Sterile (1 mg/mL vanc)	Volume										
	Drainage				**						
	Bubble Size	****	****	****	*	**				***	*
	Distribution	****	****	****						****	****

Time until volumetric loss onset decreased significantly when TXA and vancomycin were added to the MF (25 minutes, $p < 0.0001$). Accelerated volumetric breakdown is known to be related to larger bubble size, since large bubbles are more susceptible to coalescence and subsequent popping [98-100], leaving behind smaller bubbles after volume loss begins. As volume loss for therapeutic-loaded MFs was accelerated, bubble size measurements made at t = 25 minutes (optimized MF time until volume loss onset) were much smaller than bubble size measurements made at t = 25 minutes for non-sterile and sterile MF without TXA and/or vancomycin. Thus, it can be deduced that TXA and vancomycin MF likely demonstrated maximum bubble size at the time of volume loss onset (< 25 minutes).

4.2.3 MF Critical Bubble Size

To determine a critical bubble size that correlated with time until loss onset for therapeutic-loaded MF, average bubble sizes at 20 min (TXA), 18 min (vancomycin), and 20 min (combination) were determined (**Table 6**).

Table 6: Critical bubble diameters displayed as average diameters with standard deviations at time of volumetric loss onset.

Average Bubble Diameter at Time Until Volume Loss Onset [mm]	
MF (non-sterile)	1.048 ± 0.417
MF (sterile)	0.932 ± 0.283
MF (10 mg/mL TXA)	1.113 ± 0.331
MF (1 mg/mL vancomycin)	0.896 ± 0.294
MF (combination)	0.958 ± 0.369

Average bubble size was determined to rise before peaking at the observed time until loss onset and decreased after this point. This observation is consistent with the process of foam coarsening, where smaller bubbles transfer gas to larger bubbles causing growth, and the foam becomes less stable and more prone to volumetric collapse [102]. Thus, it can be reasonably

deduced that the longer the average bubble size is kept below these critical bubble sizes, the longer that volumetric loss onset can be delayed and the more volumetrically stable the MF will become.

Although most bubble size comparisons are deemed significantly different, this is likely due to the high sample size of bubbles per group per timepoint ($50 \leq N \leq 300$). Bubble diameters are on the scale of microns to millimeters, so significant differences may only be 100 microns.

4.2.4 Study Limitations

Limitations of this study include bubble size and volume loss measurements at limited time points and calculation of averages that were from samples of different solution ages. Bubble measurements and distributions were determined using 2D methods, which is not always representative of a 3D system. However, measurements were validated against 3D micro-computed tomography (uCT) measurements to ensure accuracy. Due to the time-sensitive nature of the MF breakdown and the time-consuming nature of uCT, this method was not chosen to characterize the MF.

5.0 Shelf-Life Determination

5.1 Materials and Methods

To determine the physical shelf-life of the optimal sterilized MF, the base MF bubble size, volume, and drainage were measured at 1, 10, 21, 42, and 112 days of refrigerated storage of the CMC solution using the same process as described in the previous section. Each time point was compared to Day 1 to determine if there were significant ($p < 0.05$) changes in volumetric stability over time. A fresh batch of CMC was produced, sterilized, and stored until each tested time point, with each experiment being conducted from the same batch.

5.2 Results

Sterilized MF bubble size, volumetric stability, drainage, and bubble distribution at different solution ages were compared to determine differences in measures of stability and if these differences could be related to bubble size and distribution (**Figure 13**).

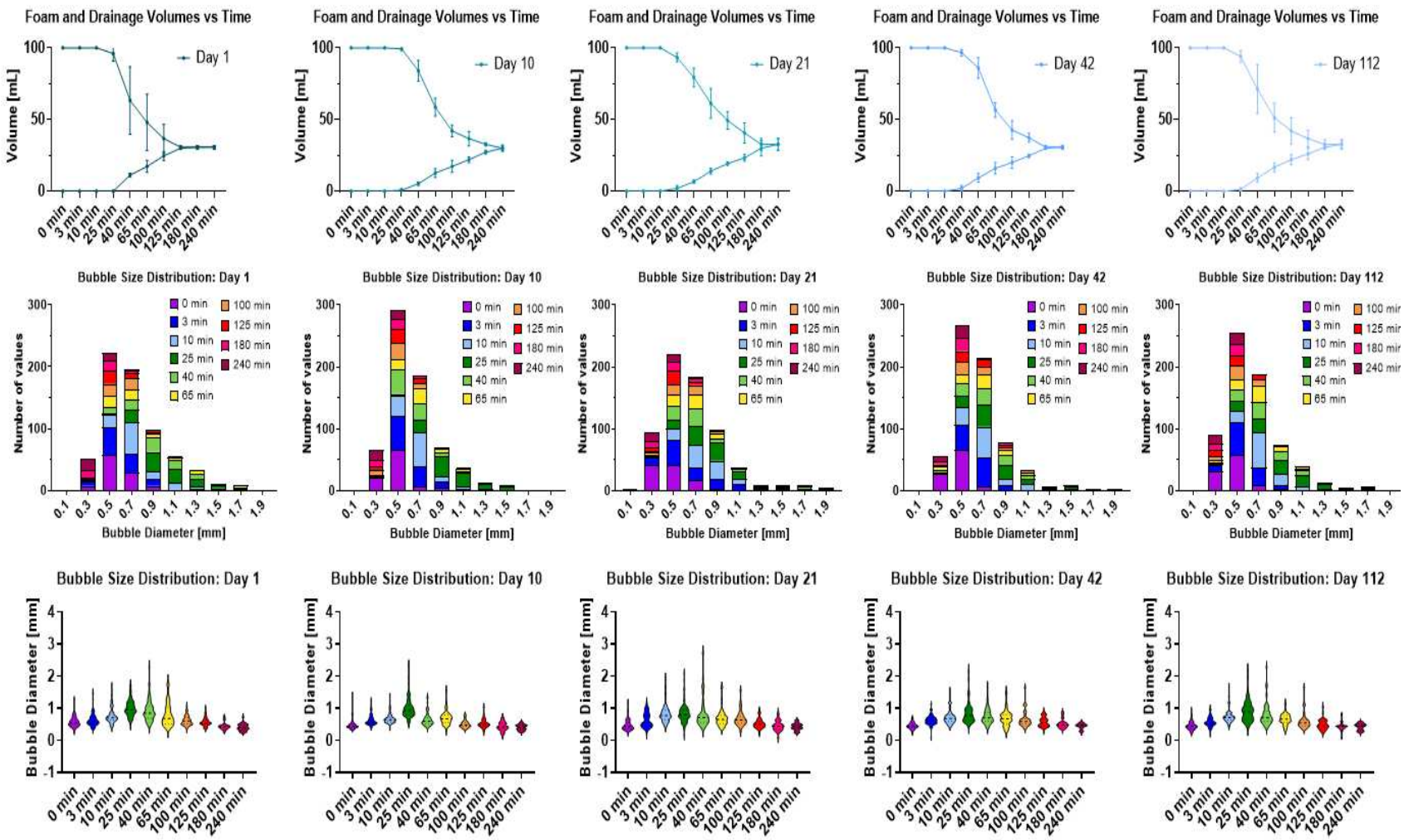

Figure 13: MF average volume loss and drainage with standard deviation (top row), bubble size distribution (middle row), and average bubble size (bottom row) over time for sterile formulations at 1, 10, 21, 42, and 112 days. N=3 samples.

There are a few discrepancies between the breakdown profiles of each MF at different solution ages and the Day 1 sample. The most similar behavior across all outputs is between Day 1 and Day 112, as demonstrated by the fewest significant differences (**Table 7**).

Table 7: Statistically significant comparisons for sterile MF formulations as compared to a Day 1 control. Statistical significance ($p < 0.05$*, $p < 0.01$ **, $p < 0.001$***, $p < 0.0001$****) was determined using Statistically significant comparisons for non-sterile, TXA, vancomycin, and combined MF formulations as compared to sterile MF formulations. Statistical significance ($p < 0.05$*, $p < 0.01$ **, $p < 0.001$***, $p < 0.0001$****) was determined using two-way ANOVA with Dunnett's multiple comparisons for volume, drainage, and bubble size and Kruskal-Wallis tests with Dunn's multiple comparisons for distribution.

Comparison	Outcome	T=0	T=3	T=10	T=25	T=40	T=65	T=100	T=125	T=180	T=240
Day 1 vs Day 10	Volume					***					
	Drainage					**	*	***	***		
	Bubble Size	*		*		****	*				
	Distribution	****		**				**			
Day 1 vs Day 21	Volume					*	*				
	Drainage					*		*	**		
	Bubble Size	**			****		*				
	Distribution	****			****	**					
Day 1 vs Day 42	Volume					***					
	Drainage							*	*		
	Bubble Size	**			***	****	*				
	Distribution	****			****	**					
Day 1 vs Day 112	Volume										
	Drainage										
	Bubble Size	**			*	**	**				
	Distribution	****			*	*			*		

5.3 Discussion

Although some significant differences exist in volume loss, liquid drainage, and bubble size/distribution, they are localized to a few time points. Moreover, fewer differences were noted across all variables at longer time points, indicating an approach back toward initial conditions over time. These data support that the physical foaming capabilities of the base CMC remain shelf-stable for at least 112 days (16 weeks) after sterilization. MF sterilized by autoclaving was utilized in all subsequent experiments, as sterilized MF is required for further *in vitro* studies. Limitations of this study include lower sample replicates than the previous study and evaluation of only non-therapeutic loaded MF.

6.0 Base Solution and MF Rheology

Flow behavior and viscoelasticity were characterized using rheology to give insight into traditional structural mechanics of the CMC solution and MF materials. CMC solution and MF rheology were conducted using a TA HR20 Discovery series rheometer (TA Instruments, New Castle, DE, USA) and analysis was conducted using TRIOS software (TA Instruments, New Castle, DE, USA).

6.1 Fluid Flow: Viscosity

6.1.1 Materials and Methods

Shear stress and viscosity curves were generated over shear rates ranging from 0.1-1000 s^{-1} at 25°C and a 0.1 mm test interval [103] to determine the influence of a) foaming the CMC to create the MF and b) adding clinically relevant (10 mg/mL TXA and 1 mg/mL vancomycin) concentrations of therapeutics. A 20 mm parallel-plate configuration was utilized for $N \geq 6$ 1 mL samples. Statistical significance was determined using two-way ANOVA with Tukey's multiple comparisons.

6.1.2 Results and Discussion

Average viscosity and shear stress curves were generated for CMC solution and MF with and without 10 mg/mL TXA and 1 mg/mL vancomycin (**Figure 14**).

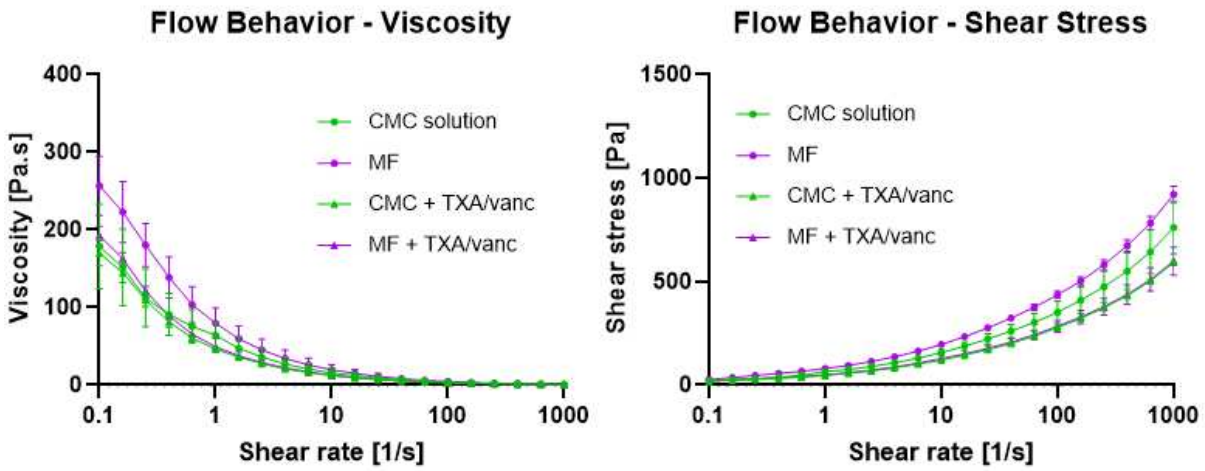

Figure 14: Average viscosity (left) and shear stress (right) vs shear rate curves for CMC solution and MF with and without TXA and vancomycin. N ≥ 6 samples, error bars represent standard deviations.

The resulting curves demonstrated non-Newtonian shear thinning behavior, characterized by decreased viscosity over increasing shear rate. This behavior was expected for the CMC solution and the MF, as it is well known that viscous CMC solutions demonstrate shear thinning behavior [79, 104].

At shear rates above 2.5 s^{-1}, the viscosities of all groups were not significantly different from each other ($p > 0.05$), indicating convergence at increased shear rates regardless of formulation or additives. At shear rates below 1 s^{-1}, the viscosities of MF without TXA or vancomycin were significantly greater than the other groups ($p \leq 0.001$), indicating that the addition of TXA and vancomycin decreases the viscosity of the MF as compared to the "empty" formulation. This behavior is accepted due to the extra PBS present in vancomycin and TXA-loaded MF which effectively reconstitutes the powders so they can be integrated into the MF. This reduced viscosity was hypothesized to be responsible for the increased volumetric breakdown rate demonstrated in the volumetric stability comparison data. The average viscosities of the MF with

TXA and vancomycin were greater than the average viscosities of the CMC solution with TXA and vancomycin at all shear rates, although not significantly so ($p > 0.05$). As shear stress is calculated as a function of the applied shear rate and measured viscosity, greater shear stresses at high shear rates indicate greater viscosity (**Equation 2**). Statistical significance was determined using two-way ANOVA with Tukey's multiple comparisons.

Equation 2: $Viscosity\ (\eta) * Shear\ rate\ (\gamma) = Shear\ stress\ (\tau)$

To validate the rheological data for each sample, viscosity data was fitted to the Cross model for shear thinning fluids (**Equation 3**), while shear stress data was fitted to the power law model for shear thinning fluids (**Equation 4**).

Equation 3: $\frac{\eta-\eta_\infty}{\eta_0-\eta_\infty} = \frac{1}{1+(k\gamma)^n}$

Equation 4: $\tau = K\left(\frac{du}{dy}\right)^n$

For the Cross model, η represents viscosity, η_0 represents Newtonian viscosity, η_∞ represents infinite viscosity, k represents a consistency factor, and n represents the power law index. For the power law model, τ represents shear stress, K and n represent power law constants, and du/dy represents shear rate.

The experimental data aligns exceptionally well with established shear thinning models ($R^2 \geq 0.998$), thus validating the non-Newtonian behavior of both CMC solution and MF formulations (**Table 8**) [105, 106].

Table 8: Goodness of fit (R^2) values for experimental data as compared to the Cross Model for non-Newtonian viscosity and Power Law for non-Newtonian shear stress. $N \geq 6$ samples.

Treatment		Cross Model R^2 (viscosity)	Power Law R^2 (shear stress)
Empty CMC	Solution	0.9981 ± 0.0014	0.9983 ± 0.0013
	Foam	0.9994 ± 0.0005	0.9995 ± 0.0002
10 mg/mL TXA + 1 mg/mL vancomycin	Solution	0.9998 ± 0.00003	0.9991 ± 0.0005
	Foam	0.9993 ± 0.0007	0.9988 ± 0.0009

6.2 Viscoelastic Behavior

6.2.1 Materials and Methods

Storage moduli (G') and loss moduli (G") curves for viscoelasticity were generated at 10 rad/s over shear strains ranging from 0.1-100% at 25°C [103] to determine the influence of a) foaming the CMC to create the MF and b) adding clinically relevant (10 mg/mL TXA and 1 mg/mL vancomycin) concentrations of therapeutics. The "flow point" of base solutions and MF were classified at crossover moduli and oscillatory strain values that were calculated using a modulus crossover model for viscoelastic materials. A 20 mm parallel-plate configuration was utilized for $N \geq 6$ 1 mL samples. Statistical significance was determined using one-way ANOVA with Tukey's multiple comparisons.

6.2.2 Results and Discussion

The flow points of CMC solutions and MF with and without TXA and vancomycin were determined (**Figure 15**).

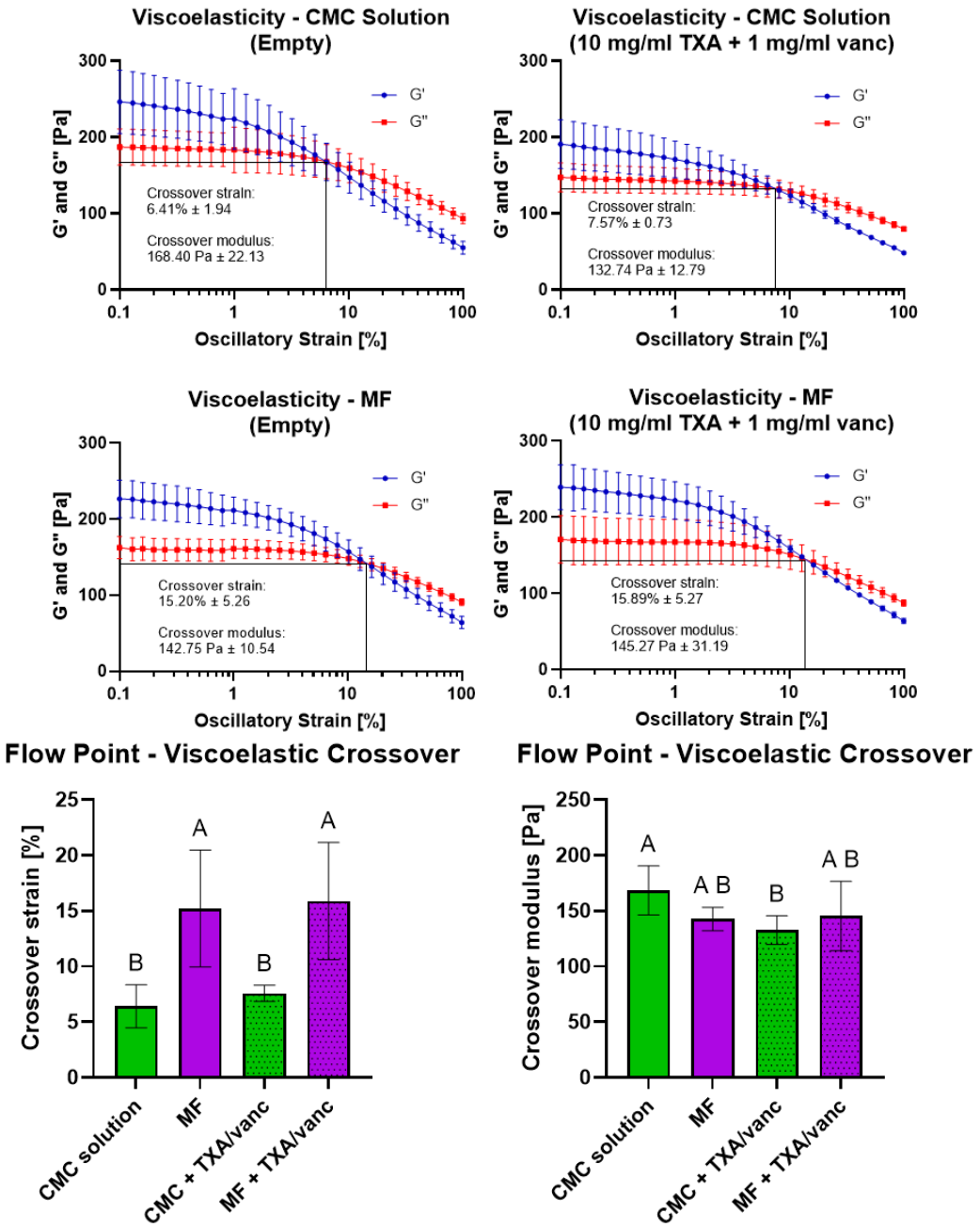

Figure 15: Average storage (G') and loss (G") modulus vs strain curves and crossover values (top) and crossover value comparisons (bottom) for CMC solution and MF with and without TXA and vancomycin. N ≥ 6 samples, error bars represent standard deviations. Statistical significance was defined as $p < 0.05$ and was determined by ordinary one-way ANOVA with Tukey's multiple comparisons. Columns with like letters are not statistically different.

The flow point of a viscoelastic foam was defined as the point where a foam transitions from elastic, gel-like behavior to viscous, fluid-like behavior [107, 108]. The flow points for MF and MF with TXA and vancomycin occur at significantly higher oscillation stresses than both CMC solution groups ($p \leq 0.01$), indicating MF can withstand higher deformation before significant structural breakdown occurs. This is hypothesized to enhance protective wound coverage during movement, pressure application, or undesirable treatment drainage.

Crossover moduli were only significantly different between CMC solution with and without TXA and vancomycin ($p = 0.012$). A decreased crossover modulus but similar crossover strain of the CMC solution with the addition of TXA and vancomycin would suggest that TXA and vancomycin decrease the stress tolerance of the CMC solution but do not influence the amount of deformation the material can withstand before the transition to primarily viscous behavior.

7.0 Conclusion

Through CMC solution and canister parameter manipulation, precise volumetric stability, breakdown, and expansion control was demonstrated over CMC-based MF and a wide working range of values was established. A formulation that optimized volumetric stability and expansion was chosen for subsequent experiments. The MF breakdown profile was further characterized by exploring the effects of sterilization and therapeutic loading on volume loss, drainage, bubble size, and bubble distribution over time. A critical bubble size range that corresponded to the time until volumetric loss onset was identified for each MF, and it was concluded that prolonging the bubble growth was important for increased volumetric stability. Proof-of-concept coating/adhesion and volumetric wound filling were demonstrated, indicating that MF is capable of total wound coverage while using less material than other formulations even during and after volumetric breakdown. Finally, enhanced rheological properties were demonstrated with the MF

as compared to the base CMC solution for both empty and therapeutic-loaded samples, giving insight into traditional mechanics of the MF and properties suspected to be beneficial for wound coverage and protection. Optimized MF sterilized by autoclaving was utilized in all subsequent chapters, as sterilized MF is required for *in vitro/ex vivo* studies.

Chapter 3 - Optimized MF *In Vitro* Cytotoxicity Studies

1.0 Background

1.1 *In Vitro* Biocompatibility

Demonstrating the biocompatibility of materials *in vitro* is crucial for ensuring their safety and efficacy before clinical or *in vivo* applications. *In vitro* cytotoxicity assays are an essential first step in this evaluation, as they assess the potential toxic effects of biomaterials, therapeutics, or a combination thereof on cultured cells. These assays measure parameters such as cell viability, proliferation, and metabolic activity following exposure to the 'material' or its extracts and help determine whether a material or drug induces cell death, inhibits growth, or disrupts normal cellular function [109]. By identifying potential toxic effects early in development, cytotoxicity assays help refine material formulations, minimize risks, and improve the likelihood of success in further preclinical and clinical testing stages.

1.2 Relevance for Topical Drug Delivery

This is particularly crucial in the context of topical drug delivery, where direct contact with tissues necessitates a thorough understanding of potential local cytotoxic effects. Unlike systemic administration, where drugs are metabolized before reaching target tissues, topical formulations interact immediately with skin or mucosal cells, increasing the importance of biocompatibility assessments [110]. Evaluating cytotoxicity *in vitro* provides insight into how a drug affects cellular bioactivity at the site of application, ensuring that it delivers the intended therapeutic benefits while minimizing inflammation or cell death.

1.3 Cytotoxicity Metrics

1.3.1 IC50 and LC50

Two common metrics utilized in cytotoxicity assays are the half maximal inhibitory concentration (IC50) and median lethal concentration (LC50). The IC50 value represents the concentration of a substance required to inhibit a specific biological or biochemical function by 50% [111]. In the context of cell viability, IC50 indicates the concentration at which cell proliferation, metabolic activity, or viability is reduced by half compared to untreated controls. A higher IC50 value indicates that higher concentrations of a drug can be safely used without risk of toxicity, thus a higher IC50 value is desirable. The LC50 value denotes the concentration of a substance that is lethal to 50% of the cell population [112]. It provides a measure of acute toxicity, indicating the concentration at which half of the exposed cells succumb to the toxic effects of the substance. LC50 values are essential for assessing the potential cytotoxic hazards of new compounds or materials.

1.3.2 ISO Guidelines

Standardized guidelines, such as ISO 10993-5: Tests for *in vitro* cytotoxicity, provide protocols to ensure reproducibility and reliability in cytotoxicity testing. ISO 10993-5 states "if the relative cell viability for the highest concentration… is ≥ 70% of the control group, then the material shall be considered non-cytotoxic". ISO 10993-5 also states that "if the relative cell viability for the highest concentration… is < 70 % of the control group, the concentration of a test chemical reflecting a 50 % inhibition of cell viability (i.e. IC50) is determined from the concentration-response" [113].

1.3.3 Available Toxicity Data

The individual cytotoxicities of vancomycin, TXA, and CMC are well characterized, particularly *in vitro* [31, 40, 114-118]. These studies examined cytotoxicity in chondrocytes, fibroblasts, keratinocytes, osteoblasts, and synovial cells for vancomycin, fibroblast and chondrocyte cells for TXA, and fibroblast and keratinocyte cells for CMC. Although all individual material components are FDA approved, off-label use requires biological evaluation when used in combination with other drugs or in methods not originally outlined for approval [119]. Thus, the *in vitro* cytocompatibility for MF was evaluated for individual and combined components.

2.0 Materials and Methods

Dose-response cytotoxicity profiles of the MF were generated in accordance with ISO 10993-5 using Trypan Blue (TB) live/dead staining over 4, 24, 48, and 72 hours, representing both acute and chronic time points. TB works by passing through the membrane of dead cells and staining the cytoplasm [120]. Both mouse embryonic fibroblast (MEFs, ATCC SCRC-1008) and adult human dermal fibroblast (HDFa, Thermo Fisher) cell lines were used for these analyses. ISO 10993-5 protocol requires the use of aseptic technique, sterile test samples, established cell lines, and a minimum of 3 replicates.

2.1 Overview

Dose-response curves for MEFs were generated first as preliminary data to support anticipated *in vivo* studies. Due to complete MF breakdown (see Chapter 2) by 4 hours and to minimize experiment complexity, material waste, and ensure accurate concentration dilutions, viability experiments were conducted with CMC solution rather than the volumetric MF to simplify experimental conditions. Treatments included individual and combined vancomycin and TXA delivery in CMC solution and phosphate-buffered saline (PBS). Limited experiments with the

volumetric MF were conducted as validation for the CMC solution delivery. *In vitro* cytotoxicity dose-response curves were then expanded to include HDFa, one of the prominent cell types that would affected by acute traumatic injuries [121]. Treatments included individual and combined vancomycin and TXA delivery in base MF solution and PBS.

2.2 Dosing and Experimental Controls

Complete vancomycin, TXA, and combination (equal concentrations) dose-response curves (0, 0.39, 0.78, 1.56, 3.12, 6.25, 12.5, 25 mg/mL) were generated for MEFs, while complete vancomycin and TXA (0, 0.39, 0.78, 1.56, 3.12, 6.25, 12.5, 25 mg/mL) and partial combination (select clinical concentrations, 1.56-3.23 mg/mL vancomycin and 12.5-25 mg/mL TXA) dose response curves were generated for HDFa. The doses selected for each agent were chosen based on similar studies conducted for vancomycin [114, 115, 117, 118] and TXA [40, 116] toxicity. Agents were delivered with PBS and CMC to determine any cytotoxic effects. This experimental design allows for the exploration of interactions between CMC, vancomycin, and TXA in equal concentrations and clinically relevant combinations. Complete media was used as a negative (blank) control and dimethyl sulfoxide (DMSO) was used as a positive control to induce cell death.

2.3 MEF Culture and Treatment Procedure

Frozen cell stocks were thawed quickly in a 37°C water bath and recovered in Dulbecco's Modified Eagle's Medium (DMEM) supplemented with 10% Fetal Bovine Serum (FBS) and 200 units penicillin, 0.2mg/mL streptomycin, and 0.5mg/mL amphotericin B (Abx, A5955; Sigma-Aldrich) for at least 48 hours under standard incubation conditions (37°C and 5% CO_2). Cells were sub-cultured at 80 to 100% confluency as necessary for culture expansion and were washed with PBS prior to plating (96-well plates, ~2000 cells/well) in antibiotic-free DMEM/FBS for 24

hours. Media from the wells was then discarded, and 100 µl/well of new antibiotic-free media was added. Treatments were then applied in a 1:1 ratio with the new media to the wells in technical triplicate and incubated for experiment duration (4, 24, 48,72 hours). Treatments were then carefully aspirated, and wells were washed with PBS to remove any residual treatments. Each cell layer was then stained with 0.2% TB (100 µl/well) and fixed with 4% paraformaldehyde [120]. Wells were then washed with PBS and viewed under an inverted phase contract microscope (Olympus CKX31). Percent cell viability was calculated using Error! Reference source not found. after manual counting.

Limited experiments with the volumetric MF were conducted and compared to the base CMC solution results to ensure that experimentation with CMC solution delivery was valid. MF was generated aseptically by autoclaving the CMC solution at 121°C for 15 minutes and adding the sterile agents in a laminar flow hood. Treatments were applied following the same procedure as outlined above.

2.4 HDFa Culture and Treatment Procedure

HDFa were plated in Human Fibroblast Expansion Basal Medium (Gibco, Thermo Fisher Scientific, MA, USA) supplemented with a Low Serum Growth Supplement Kit (Gibco LSGS Kit, Thermo Fisher Scientific, MA, USA) without antibiotics in 96-well plates (~15,000 cells/well) were generously obtained from cell stock used for a different study. Plates were incubated for 24 hours to allow monolayer formation. Media from the wells was then discarded, and 100 µl/well of new antibiotic-free media was added. Treatments were then applied in a 1:1 ratio with the new media to the wells in technical triplicate and incubated for experiment duration. Treatments were then carefully aspirated, and wells were washed with PBS to remove treatment remnants. Each cell layer was then stained with TB (100 µl/well) and fixed with 4%

paraformaldehyde [120]. Wells were then washed with PBS and viewed under a phase contract microscope (Olympus CKX31). Percent cell viability was calculated using **Equation 5** after manual counting.

$$\text{Equation 5: } Cell\ Viability\ \% = \left(1 - \frac{\#\ stained\ cells}{\#\ total\ cells}\right) * 100$$

2.5 IC50 determination

IC50 values were estimated using non-linear regression analyses in GraphPad Prism v10.4.1 (GraphPad Software Inc., CA, USA). Cell viability response vs. dose concentration data were entered and transformed into normalized dose response vs. concentration. Data was then fit to a four-parameter (variable slope) sigmoid function, implemented as "[Inhibitor] vs. normalized response – Variable slope". In instances where the cytotoxicity was ≥ 70% at the highest tested concentration, the IC50 was not calculated. 'Goodness of Fit' root-mean squared (R^2) values were recorded.

2.6 LC50 determination

LC50 values were estimated using linear regression analysis in GraphPad Prism v10.4.1 (GraphPad Software Inc., CA, USA). Cell viability response vs. dose concentration data were fit to a linear function. The concentration (x) at which 50% of cells were no longer viable was calculated and Goodness of Fit R^2 values were recorded.

2.7 Statistical Analyses

Statistical significance was defined as $p < 0.05$ and determined using one or two-way ANOVA with Tukey's multiple comparisons when appropriate.

3.0 Results

3.1 MEF Dose-Response

Over 4 hours, there were no significant differences in MEF viability between 1:1 ratios of 'empty' PBS, CMC solution, and MF (**Figure 16**).

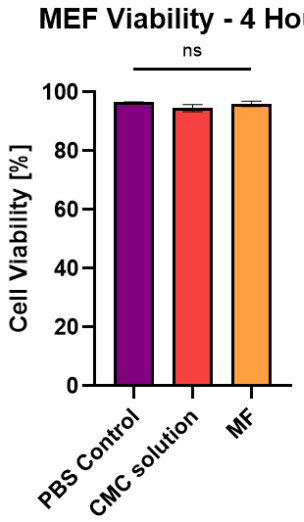

Figure 16: MEF viability carrier comparison. Statistical significance was determined using one-way ANOVA.

Thus, all subsequent dose-response curves were generated by evaluating CMC solution delivery rather than volumetric MF delivery. Vancomycin and TXA demonstrated time and dose-

dependent killing, both individually and in equal, combined concentrations (**Figure 17**).

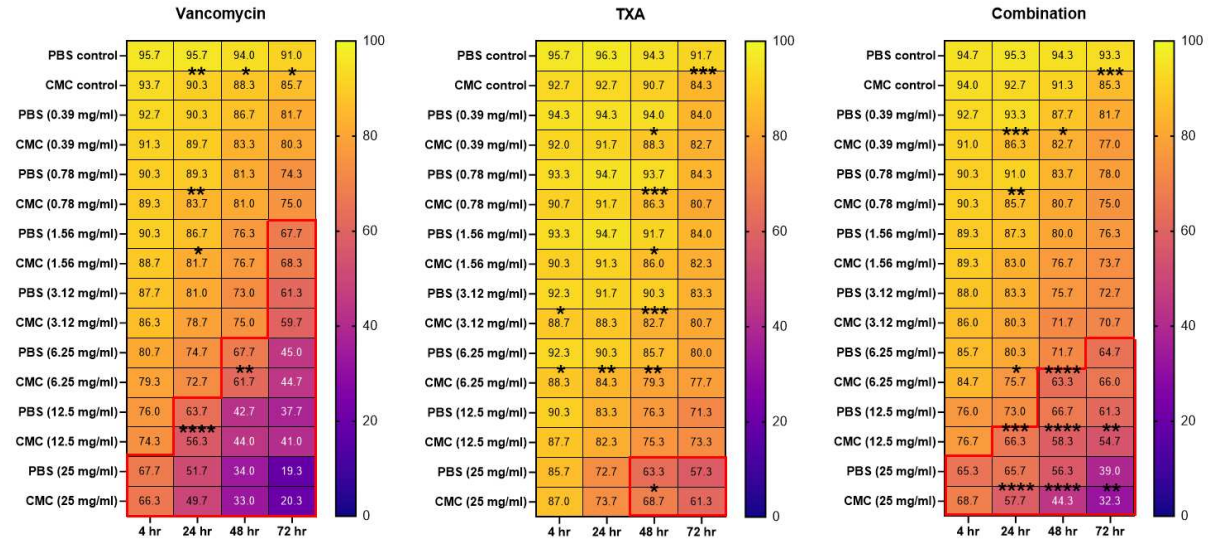

Figure 17: Comparative MEF viability of vancomycin, TXA, and combined treatments over 4, 24, 48, and 72 hours. Statistical significance between carriers for each time and concentration was determined with two-way ANOVA and Tukey's multiple comparisons.

Concentrations 0.78 mg/mL (vancomycin) and 12.5 mg/mL (TXA) were determined as the individual concentrations that were cytotoxic (< 70% viable) to MEFs after 72 hours for both PBS and MF delivery. The concentration 3.12 mg/mL was determined as the combined concentration that was cytotoxic to MEFs after 72 hours for both PBS and MF delivery. Overall, TXA demonstrated decreased cytotoxicity compared to vancomycin over both time and concentration. Combination treatments generally demonstrated the average toxicity values of individual vancomycin and TXA treatments, except at 4 hours (**Figure 18**).

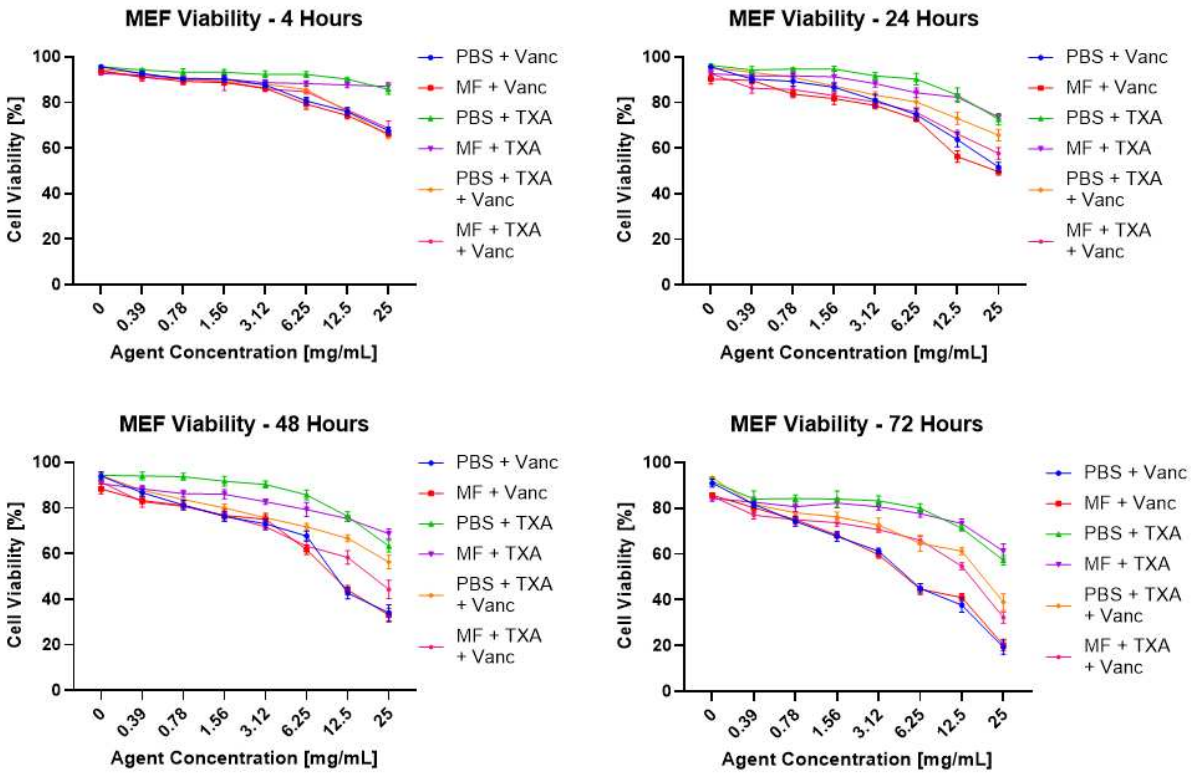

Figure 18: Temporal comparative MEF viability of vancomycin, TXA, and combined treatments.

Table 9 and **Table 10** shows the estimated IC50 and LC50 values, respectively, for each treatment at each time point. Overall, R^2 values for vancomycin treatments were generally greater than TXA treatments, indicating better estimates for these values.

IC50 and R^2 Values: Treatments Over Time					
Treatment		Time			
		4 hours	24 hours	48 hours	72 hours
PBS + Vanc	IC50	**5.21**	**5.22**	**4.35**	**3.40**
	R^2	0.94	0.94	0.91	0.96
MF + Vanc	IC50	**5.48**	**5.41**	**5.54**	**4.12**
	R^2	0.95	0.94	0.95	0.97
PBS + TXA	IC50	-	-	**9.56**	**6.84**
	R^2			0.95	0.80
MF + TXA	IC50	-	-	**4.79**	**10.14**
	R^2			0.91	0.86
PBS + TXA + Vanc	IC50	**7.76**	**4.43**	**2.94**	**4.17**
	R^2	0.90	0.94	0.95	0.87
MF + TXA + Vanc	IC50	**6.28**	**4.41**	**3.62**	**6.78**
	R^2	0.89	0.92	0.94	0.87

Table 9: Estimated IC50 values for MEFs dependent on treatment and time. Values could not be determined for cells without values.

Vancomycin treatment IC50 decreased over time for both PBS and MF delivery, while other treatment values did not follow this pattern.

LC50 and R^2 Values: Treatments Over Time					
Treatment		Time			
		4 hours	24 hours	48 hours	72 hours
PBS + Vanc	LC50	**39.51**	**23.67**	**14.77**	**10.02**
	R^2	0.91	0.91	0.87	0.84
MF + Vanc	LC50	**38.13**	**21.64**	**14.33**	**10.10**
	R^2	0.91	0.89	0.91	0.85
PBS + TXA	LC50	**129.71**	**49.38**	**34.70**	**30.84**
	R^2	0.83	0.95	0.97	0.92
MF + TXA	LC50	**213.70**	**55.84**	**45.81**	**38.57**
	R^2	0.51	0.92	0.87	0.93
PBS + TXA + Vanc	LC50	**37.62**	**36.24**	**27.40**	**17.99**
	R^2	0.96	0.86	0.82	0.87
MF + TXA + Vanc	LC50	**43.01**	**28.65**	**19.15**	**15.17**
	R^2	0.92	0.90	0.85	0.96

Table 10: Estimated LC50 values for MEFs dependent on treatment and time. Values in red have a Goodness of Fit R^2 value < 0.70.

LC50 values decreased over time for all treatments, supporting the conclusion that vancomycin and TXA exhibit time and dose-dependent killing. Estimates have high R^2 values, and values that are within the explored range align with the plots (**Figure 18**).

3.2 HDFa dose-response

Similar to the MEFs, individual vancomycin and TXA treatments demonstrated time and dose-dependent killing for the HDFa (**Figure 19**).

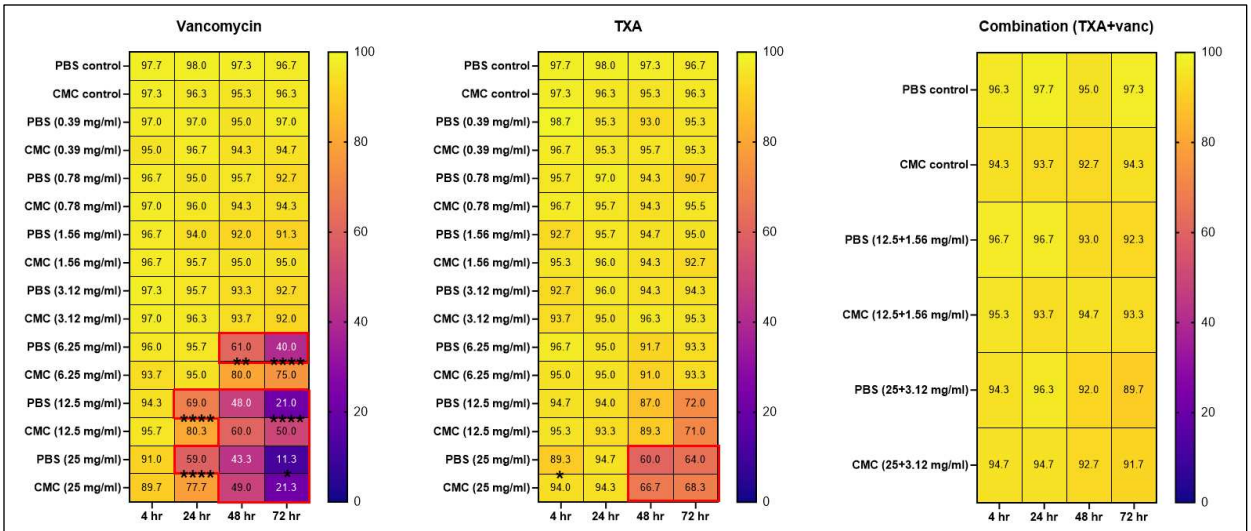

Figure 19: Comparative HDFa viability of vancomycin, TXA, and combined treatments over 4, 24, 48, and 72 hours. Statistical significance between carriers for each time and concentration was determined with two-way ANOVA and Tukey's multiple comparisons.

6.25 mg/mL (vancomycin) and 12.5 mg/mL (TXA) were determined as the individual concentrations delivered in base MF solution that were cytotoxic to HDFa after 72 hours, as compared to 3.12 mg/mL (vancomycin) and 12.5 mg/mL (TXA) delivered in PBS. Combinations of clinically relevant treatment concentrations (12.5 mg/mL TXA + 1.56 mg/mL vancomycin, 25 mg/mL TXA + 3.12 mg/mL vancomycin) were determined to be non-cytotoxic (> 70% viability) across all time points.

As also demonstrated in the MEFs, TXA was overall less cytotoxic than vancomycin in the HDFa. Across all time points, cell viability was not significantly impacted for vancomycin or TXA treatments up to 3.12 mg/mL (**Figure 20**).

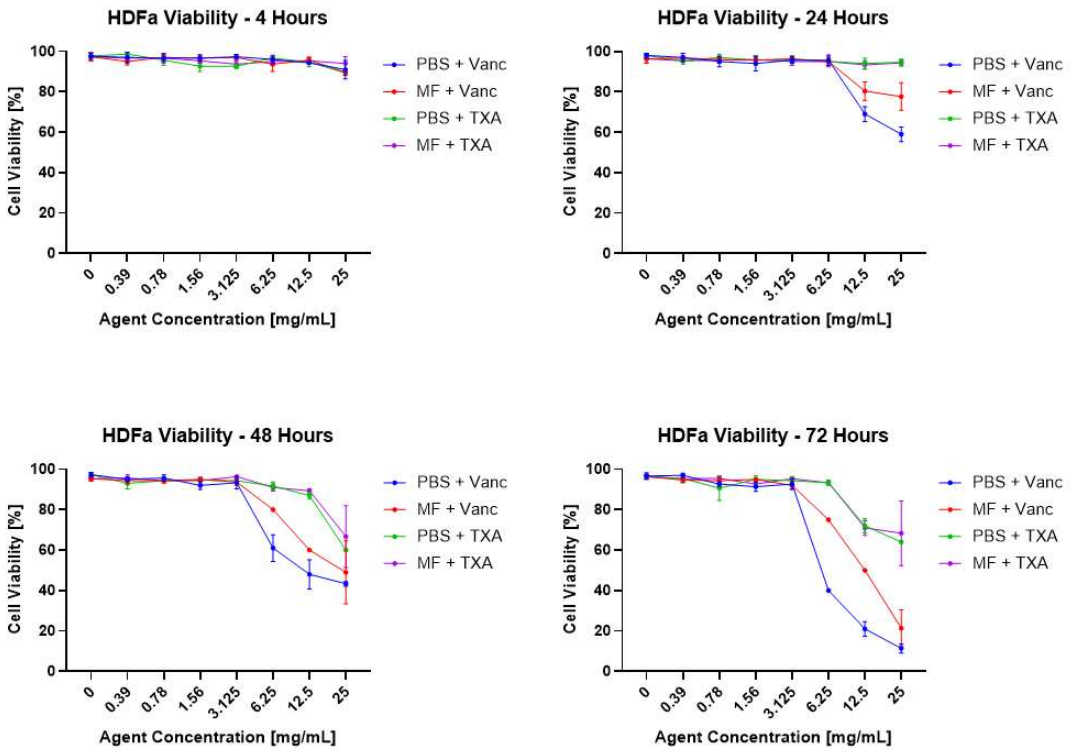

Figure 20: Temporal comparative HDFa viability of vancomycin, TXA, and combined treatments.

Table 11 and **Table 12** show the estimated IC50 and LC50 values, respectively, for each treatment at each time point. R^2 values for vancomycin treatments were generally greater than TXA treatments, indicating better estimates for these values.

IC50 and R^2 Values: Treatments Over Time					
Treatment		Time			
		4 hours	24 hours	48 hours	72 hours
PBS + Vanc	IC50	-	**10.28**	**5.32**	**5.70**
	R^2		0.96	0.97	0.99
MF + Vanc	IC50	-	-	**8.12**	**9.22**
	R^2			0.94	0.98
PBS + TXA	IC50	-	-	**15.06**	**9.83**
	R^2			0.80	0.88
MF + TXA	IC50	-	-	**14.61**	**8.74**
	R^2			0.76	0.82

Table 11: Estimated IC50 values for HDFas dependent on treatment and time. Values could not be determined for cells without values, as viability for all treatment groups remained above 70%.

Similar to MEFs, vancomycin treatment IC50 decreased over time for both PBS and MF delivery, while other treatment values did not follow this pattern. LC50 values with $R^2 > 0.70$ decreased over time for all treatments, supporting the conclusion that vancomycin and TXA exhibit time and dose-dependent killing.

LC50 and R^2 Values: Treatments Over Time					
Treatment		Time			
		4 hours	24 hours	48 hours	72 hours
PBS + Vanc	LC50	189.44	29.17	17.90	11.48
	R^2	0.52	0.88	0.79	0.86
MF + Vanc	LC50	182.01	55.09	23.25	15.34
	R^2	0.52	0.78	0.90	0.98
PBS + TXA	LC50	184.43	485.68	40.96	31.86
	R^2	0.40	0.16	0.83	0.79
MF + TXA	LC50	511.55	577.85	43.31	37.08
	R^2	0.14	0.13	0.74	0.71

Table 12: Estimated LC50 values for HDFas dependent on treatment and time. Values in red have a Goodness of Fit R^2 value < 0.70.

4.0 Discussion

MF did not induce decreased viability to MEFs relative to PBS and CMC solutions. Only the 4-hour time point was tested in these experiments, as the optimized MF breaks back down into CMC solution by the later time points regardless (see Chapter 2). As there were no significant differences ($p > 0.05$) between CMC solution and MF delivery, CMC solution was used in subsequent dose-response experiments.

4.1 MEF Responses

General trends for MEF responses indicate that agent delivery through CMC solution is associated with increased cytotoxicity compared to PBS delivery, except at high concentrations of TXA. The statistically significant differences between PBS and CMC is highest for the combination treatments. At equally high concentrations of agents, PBS offers significantly decreased cytotoxicity, however, it is highly unlikely that these combination concentrations would be used clinically. Vancomycin is known to be inherently more cytotoxic than TXA [122].

Without any vancomycin or TXA, PBS is significantly less cytotoxic to MEFs than CMC over time. As the CMC solution itself is acting as a drug, this decrease in viability is valid, especially at the viscous, high-potency, 1:1 treatment ratio.

At 24, 48, and 72 hours, the combination treatments demonstrate nearly average MEF cytotoxicity of the individual treatments at each concentration across both PBS and CMC delivery. This suggests that combination treatments do not have additive cytotoxicity and may have some synergistic, positive functional effect on monolayer cultures *in vitro*. This is supported by studies that demonstrate constant or increased cell function in combined treatments compared to individual drug treatments. Wagenbrenner et al. (2024) found no negative combined treatment effects in chondrocyte monolayers until 48 hours [122], while Benjumea et al. (2024) found that the addition of TXA to vancomycin treatments increased efficacy against staphylococcal cells [123] .

The data generated from these dose-response studies demonstrated the *in vitro* safety of individual and combined vancomycin and TXA delivery with the base MF solution on MEFs, thus beginning the transition to *in vivo* murine studies.

4.2 HDFa responses

General trends for HDFa cytotoxicity show increased viability with individual CMC treatments as compared to the same PBS treatments. This is the opposite of what was observed for the MEFs, indicating that HDFa are less sensitive to MF application and favor agent delivery through CMC over PBS. This conclusion is supported by Zhang et al (2024) through studies that demonstrate similar or increased cell viability in drug delivery with a CMC component as compared to the delivery vehicle without the CMC [124]. These results are also favorable for future studies that will focus on human participants and the eventual product use in the field.

Clinically relevant combination treatments demonstrated increased viability from the average individual cytotoxicities at each time point. This again suggests that TXA and vancomycin have a non-additive cytotoxic effect. It is also supported that human cell lines can be more robust than murine or other animal cell lines [31], potentially explaining the overall increased cell viability of HDFa compared to MEFs.

There is limited literature available on reported IC50 or LC50 values for these experimental conditions. IC50 is most often reported for vancomycin delivered directly into cell media, and has been experimentally determined as 7.306 mg/mL (equine chondrocytes) and 7.812 mg/mL (equine synovial cells) after 24 hours [114], 3.5 mg/mL (human fibroblasts) after 48 hours [118], and 1.775-5.541 mg/mL (human tenocytes) after 1 hour [125]. These results are highly variable yet agree with the MEF IC50 range of 3.40-5.54 mg/mL and the HDFa IC50 range of 5.32-10.28 mg/mL for the PBS/MF vancomycin treatments over 4-72 hours.

Overall, IC50 and LC50 values for HDFa had lower R^2 values than MEFs. This can be attributed to the delayed time and dose dependent killing, as viability does not significantly decrease until both vancomycin and TXA concentrations exceed 3.12 mg/mL across all time points.

A narrative review by Gkiatas et al. (2022) outlined a range of topical TXA doses typically investigated for *in vitro* and *in vivo* toxicity studies as 0-100 mg/mL [40]. This range supports clinically relevant doses of TXA, including 100 mg/mL for acute epistasis treatment [41], 25 mg/mL for temporary moistening of surgical wounds [42], and 10 mg/mL for sustained treatment of surgical wounds [43]. Although the effects of 100 mg/mL were not explored, 25 mg/mL at acute time points and 10 mg/mL at chronic time points yielded similar toxicity results to the discussed studies. Namely, sustained treatment of 10 mg/mL was deemed non-cytotoxic for both

cell types, while sustained treatment of 25 mg/mL TXA was deemed cytotoxic past 24 hours for MEFs and 48 hours for HDFa.

4.3 Limitations

Limitations of these studies include no biological replicates and only fibroblast experimentation. A larger range of clinically relevant concentration combinations will need to be explored to fully capture the interactions between CMC, vancomycin, and TXA.

5.0 Conclusion

MF was less cytotoxic to HDFa than MEFs. 0.78 mg/mL (vancomycin) and 12.5 mg/mL (TXA) were determined as the individual concentrations that were cytotoxic to MEFs after 72 hours for both PBS and MF delivery. 3.12 mg/mL was determined as the combined concentration that was cytotoxic to MEFs after 72 hours for both PBS and MF delivery. CMC had decreased viability compared to PBS delivery for these studies. 6.25 mg/mL (vancomycin) and 12.5 mg/mL (TXA) were determined as the individual concentrations delivered in base MF solution that were cytotoxic to HDFa after 72 hours, as compared to 3.12 mg/mL (vancomycin) and 12.5 mg/mL (TXA) delivered in PBS. Combinations of clinically relevant treatment concentrations (12.5 mg/mL TXA + 1.56 mg/mL vancomycin, 25 mg/mL TXA + 3.12 mg/mL vancomycin) were determined to be non-cytotoxic across all time points.

Overall, individual and combined delivery of MF was not cytotoxic to both murine and human fibroblasts in monolayer cell culture at clinically relevant concentrations. This conclusion is critical for the transition of product application into *in vivo* models and further exploration of dose-response curves *in vitro*.

1.0 Background

1.1 Hemorrhage in Civilian and Military Populations

Uncontrolled hemorrhage is a leading cause of preventable deaths in both civilian and military settings. Globally, trauma-related bleeding results in over 1.5 million annual deaths, and in the United States, hemorrhage accounts for over 60,000 potentially preventable deaths each year [126]. In battlefield contexts, hemorrhage is one of the primary causes of potentially preventable fatalities. Studies analyzing United States combat deaths from 2001-2011 found that up to 25% of these deaths were potentially preventable, and that 87% of deaths occurred before reaching a medical facility [127]. While the absolute number of hemorrhage-related deaths is higher in the civilian sector due to a larger population base, preventable deaths due to hemorrhage are significant in both settings. The military faces unique challenges, such as the tactical environment and potentially delayed medical evacuation, which contribute to a higher percentage of potentially survivable hemorrhage-related deaths occurring before hospital care. Most hemorrhagic deaths occur within the first 2 hours after injury [128], underscoring the critical need for effective pre-hospital hemorrhage control measures in both civilian and military arenas to reduce the incidence of preventable fatalities.

1.2 Current Standards of Care (SOC)

EMS professionals treat trauma patients utilizing the ABCDEs of triage care: Airway, Breathing, Circulation, Disability, Exposure [24, 129]. Along with establishing a clear airway and regular breathing pattern, stopping bleeding is the most crucial aspect of triage care. Wound packing,

bandages, pressure dressings, and tourniquets are common mechanisms for establishing bleeding control (see Chapter 1).

Tactical Combat Casualty Care (TCCC) guidelines dictate specific protocols for battlefield management of large open wounds, with emphasis on triage care to attempt hemorrhage prevention. Primary hemostasis interventions include wound packing with hemostatic gauze, pressure bandage application, and tourniquet application, when appropriate [130]. Although these emergency hemostatic interventions are relatively effective, especially in triage or emergency situations, traumatic injuries are often susceptible to abnormal bleeding and clotting pathways [131, 132].

1.3 Trauma-Induced Coagulopathy and Hyperfibrinolysis

Trauma-induced coagulopathy (TIC) is the title given to the overarching abnormal bleeding phenomenon that often accompanies traumatic open wounds. TIC is characterized by a complex interplay of factors such as hypoperfusion, systemic anticoagulation, and hyperfibrinolysis, leading to uncontrolled bleeding [133]. Hyperfibrinolysis, in particular, results from an overactivation of plasminogen to plasmin, causing rapid breakdown of fibrin clots and exacerbating hemorrhage [12]. Thus, any hemorrhage control that is achieved by these emergent TCCC protocols is susceptible to re-bleed due to the absence of blood clot formation or rapid breakdown of clots that do form.

1.4 Tranexamic Acid Mechanisms and Historical Use

Tranexamic acid (TXA) is a synthetic antifibrinolytic agent that has been utilized for decades to mitigate excessive bleeding in various medical contexts. Its primary mechanism involves the reversible blockade of lysine-binding sites on plasminogen molecules, thereby inhibiting their activation to plasmin. This inhibition prevents the degradation of fibrin clots, effectively

stabilizing hemostasis and reducing blood loss [38]. The efficacy of TXA has been demonstrated across multiple clinical scenarios, including surgical procedures and trauma care, where it significantly decreases mortality when administered promptly. For example, in the CRASH-2 trial aimed at determining the effect of TXA administration on death and transfusion requirements, patient mortality was significantly reduced ($p = 0.0035$, $N > 10{,}000$ patients) when TXA was delivered within 3 hours of injury [134]. Intravenous TXA administration is currently promoted by TCCC protocols but is often not a primary treatment in triage care, especially under duress [135, 136].

Thus, it was hypothesized that TXA delivery with the MF would stabilize blood clots, rather than directly promote hemostasis, by preventing clot breakdown and allowing continual fibrin network maturation throughout clot formation. Insight into TXA efficacy was established by monitoring changes in ovine blood clot breakdown and viscoelasticity *ex vivo* and comparing delivery through the MF to other treatment formulations.

2.0 Materials and Methods

Whole ovine blood obtained from the Preclinical Surgical Research Laboratory (Colorado State University) was collected from skeletally mature female Rambouillet sheep on holding protocol (not enrolled in preclinical studies). Blood drawn from the jugular vein was collected in standard 10 mL collection tubes without anticoagulant immediately before experimental use (< 5 minutes). Collections were performed by Animal Care Coordinators at Preclinical Surgical Research Laboratory. A total of N = 6 collections from N = 9 sheep were conducted.

2.1 Clot Breakdown Inhibition: Simulated Hyperfibrinolysis

The ability to inhibit simulated hyperfibrinolysis was evaluated on fresh blood (i.e. collection volume was applied directly to the treatment; designated 'fresh blood' clots) and blood that was allowed to form clots naturally before treatment (i.e. 15 minute formation after collection; designated 'clotted blood', **Figure 21**) using a modified procedure [137]. The primary outcome parameter of these analyses was normalized mass loss of blood clots (% of original mass) following lysing with streptokinase, a clot breakdown agent. 3 biological replicates were utilized for these experiments, each conducted in technical triplicate. Statistical significance was defined as $p < 0.05$ and determined by ordinary one-way ANOVA with Tukey's multiple comparisons.

Figure 21: Representative image of ‘clotted blood’ sample. Ovine blood was allowed to clot in the collection tube for 15 minutes before being placed in treatment conicals.

2.1.1 Treatments

Treatments for ‘fresh blood’ experiments included a lysed control, PBS + 10 mg/mL TXA, CMC solution + 10 mg/mL TXA, MF + 10 mg/mL TXA, and a non-lysed control. Treatments for the ‘clotted blood’ experiments included a lysed control, PBS + 10 mg/mL TXA, CMC solution + 10 mg/mL TXA, Quik-Clot, MF + 10 mg/mL TXA, TXA powder, and a non-lysed control.

2.1.2 Procedure

First, 2 g of whole ovine blood without anticoagulant was introduced into individual conical tubes (50 mL, VWR Centrifuge Tube) containing 25 mL of each treatment as ‘fresh blood’ (via pouring) or ‘clotted blood’ (via scoopula) as defined above. For Quik-Clot and TXA powder treatments, ‘clotted blood’ was wrapped in 15 cm of Quik-Clot gauze or fully coated in 250 mg of TXA powder, respectively, before being placed in empty conical tubes. Each conical was then incubated at 37°C for 4 hours. ‘Fresh blood’ and ‘clotted blood’ clots were then collected from the treatments and cut into ~3 x 3 x 3 mm samples. Each sample was then weighed (OHAUS PR

Series, 1 mg resolution), and placed in pre-weighed, individual 600 µL Eppendorf tubes (clear, polypropylene, Eppendorf). 100 µL of 1 mg/mL streptokinase (lyophilized powder, Sigma Aldrich, CAS 9002-01-1) was pipetted into the tubes and left to lyse at 37°C for 120 minutes (**Figure 22**). Excess liquid from breakdown was aspirated using a pipette and clots were then reweighed. Clot breakdown was expressed as a relative percentage of the pre-lysed clot weight for each treatment (**Equation 6**).

Equation 6: $Relative\ Clot\ Mass = \left(\frac{Intial\ mass - Final\ mass}{Initial\ mass}\right) * 100\%$

Figure 22: Representative image of induced lysis procedure. Non-lysed control (left) and streptokinase-lysed control (right). Streptokinase dissolves blood clots and leaves behind liquid where breakdown occurs.

2.2 Clot Breakdown Inhibition: Natural Lysis

The ability to inhibit natural blood clot lysis over time was evaluated for 'fresh blood' clots and 'clotted blood' using a modified procedure [137]. The primary outcome parameter of these analyses was normalized mass loss of blood clots (% of original mass) after 4, 24, 48, and 72 hours of treatment. 3 biological replicates were utilized for these experiments. Statistical

significance was defined as $p < 0.05$ and determined by repeated measures two-way ANOVA with Tukey's multiple comparisons.

2.2.1 Treatments

Treatments for 'fresh blood' experiments included a non-treated (negative) control, PBS, "empty" MF, PBS + 10 mg/mL TXA, MF + 10 mg/mL TXA, PBS + 10 mg/mL TXA + 1 mg/mL vancomycin, and MF + 10 mg/mL TXA + 1 mg/mL vancomycin. 'Clotted blood' treatments included a non-treated (negative) control, PBS, "empty" MF, PBS + 10 mg/mL TXA, MF + 10 mg/mL TXA, PBS + 10 mg/mL TXA + 1 mg/mL vancomycin, and MF + 10 mg/mL TXA + 1 mg/mL vancomycin, TXA powder, and Quik-Clot.

2.2.2 Procedure

First, 3 g of whole ovine blood without anticoagulant was introduced into individual 50 mL conical tubes containing 25 mL of each treatment as 'fresh blood' (via pouring) or 'clotted blood' (via scoopula) as defined above. For Quik-Clot and TXA powder treatments, 'clotted blood' was wrapped in 15 cm of Quik-Clot gauze or fully coated in 250 mg of TXA powder, respectively, before being placed in empty conical tubes. Each conical was then incubated at 37°C for 4, 24, 48, or 72 hours. 'Fresh blood' and 'clotted blood' clots were then collected from the treatments and weighed at each time point before being returned to individual treatments. Clot breakdown was expressed over time as a percent of the maximum clot weight for each treatment (**Equation 7**).

Equation 7: $$Relative\ Clot\ Mass_{treatment\ time} = \left(\frac{Clot\ mass}{Maximum\ clot\ mass}\right) * 100\%$$

2.3 Clot Rheological Assessment

Blood clot viscoelasticity was determined for 'fresh blood' and 'clotted blood' clots using rheology (TA HR20 Discovery Series). A combination of modified procedures [138, 139] was

utilized to monitor the change in clot viscoelasticity over time. Clot viscoelasticity is an important hemostatic parameter, as it can give insight into clot strength, deformation, and structural integrity. Clot viscoelasticity is also one of the parameters used to identify clotting disorders and can guide treatment options [139]. At least 1 biological replicate was utilized for these experiments in technical triplicate. Statistical significance was defined as $p < 0.05$ and assessed using multiple ordinary one-way ANOVAs.

2.3.1 Treatments

Treatments for 'fresh blood' experiments included a non-treated (negative) control, PBS, "empty" MF, PBS + 10 mg/mL TXA, MF + 10 mg/mL TXA, PBS + 10 mg/mL TXA + 1 mg/mL vancomycin, and MF + 10 mg/mL TXA + 1 mg/mL vancomycin. 'Clotted blood' treatments included a non-treated (negative) control, PBS, "empty" MF, PBS + 10 mg/mL TXA, MF + 10 mg/mL TXA, PBS + 10 mg/mL TXA + 1 mg/mL vancomycin, and MF + 10 mg/mL TXA + 1 mg/mL vancomycin, TXA powder, and Quik-Clot.

2.3.2 Procedure

First, 2 mL of whole ovine blood without anticoagulant was introduced into individual 50 mL conical tubes containing 25 mL of each treatment as 'fresh blood' (via pouring) or 'clotted blood' (via scoopula) as defined above. For Quik-Clot and TXA powder treatments, 'clotted blood' was wrapped in 15 cm of Quik-Clot gauze or fully coated in 250 mg of TXA powder, respectively, before being placed in empty conical tubes. Each conical was then incubated at 37°C for 4, 24, 48, or 72 hours. 'Fresh blood' and 'clotted blood' clots were then collected from the treatments and cut into ~6 x 3 mm circular samples. Samples were then placed in an 8 mm parallel-plate rheometer geometry (**Figure 23**), where an oscillatory time sweep was conducted

within the linear viscoelastic region (1 Hz, 1% strain) [140] over 5 minutes at physiological temperature (37°C).

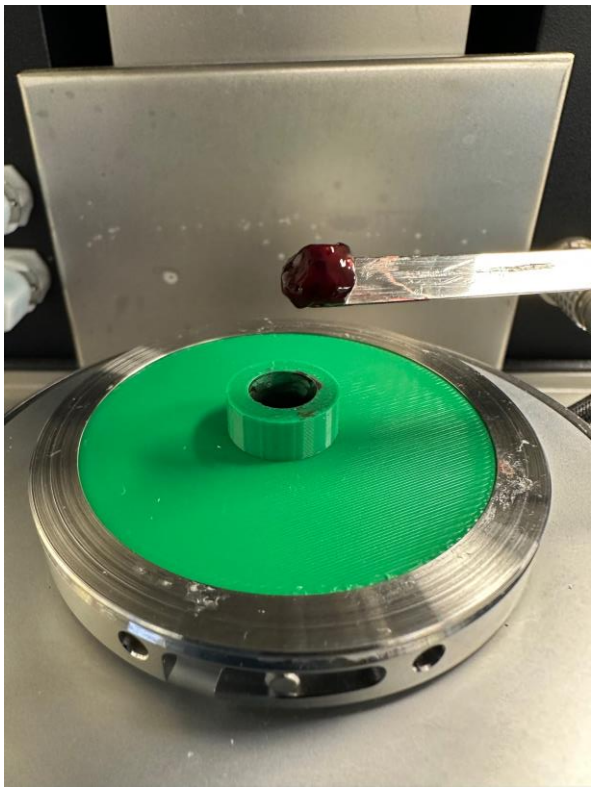

Figure 23: Representative image of a blood clot sample being placed in an 8 mm parallel-plate rheometer geometry.

The percent change in phase angle over the last 4 minutes was calculated and averaged for each treatment. Values obtained in the first minute were not included in the calculation to allow sample conditioning (**Equation 8**).

Equation 8: $$Phase\ Angle\ Change = \left(\frac{Phase\ angle_{5\ min} - Phase\ angle_{\ 1\ min}}{Phase\ angle_{5\ min}}\right) * 100\%$$

2.4 Reduced Flow Assessment

The ability of MF to slow blood flow was evaluated using a dual syringe pump (Pump33DDS, Harvard Apparatus). 3 biological replicates were utilized for these experiments, each conducted in technical triplicate.

2.4.1 Treatments

Treatments included PBS, CMC solution, MF, MF + 10 mg/mL TXA, and MF + 10 mg/mL TXA + 1 mg/mL vancomycin.

2.4.2 Procedure

10 mL of anticoagulated, whole ovine blood were drawn into luer-lock syringes attached to 1/8" ID plastic tubing (Soft Tygon PVC, McMaster-Carr) and deposited on top of 25 mL treatment volumes in a 50 mL conical tube at a rate of 2 mL/min (**Figure 24**). The time for the blood to reach the bottom of each container and the time the entire blood volume took to settle were measured and recorded.

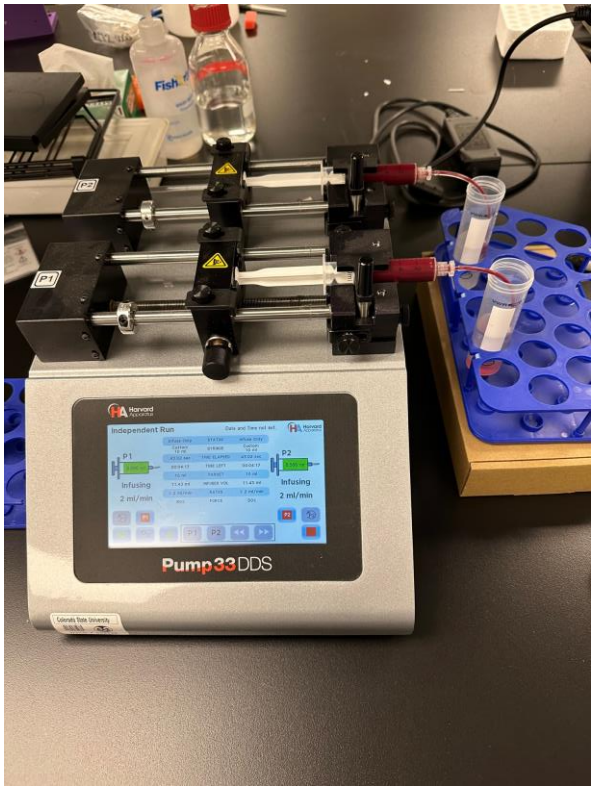

Figure 24: Representative image of reduced flow assessment setup. Luer-lock syringes filled with anticoagulated ovine blood are placed in a double-barrel syringe pump set at a volumetric flow rate of 2 mL/min.

3.0 Results

3.1 Clot Breakdown Inhibition: Simulated Hyperfibrinolysis

Streptokinase, a thrombolytic medication, works by activating plasminogen which is then converted to plasmin, which is directly responsible for dissolving blood clots [141]. After induced short-term hyperfibrinolysis of treated 'fresh' and 'clotted' blood clots, relative clot mass was calculated and averaged for each treatment (**Figure 25**).

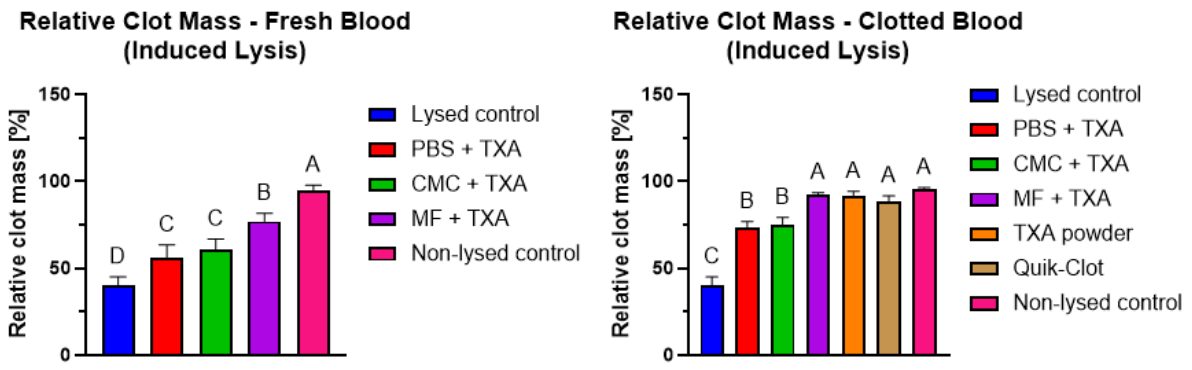

Figure 25: Relative clot mass per treatment for the induced lysis of fresh ovine blood (left) and clotted ovine blood (right). Columns that share the same letter are not statistically significant from each other ($p < 0.05$) as determined by one-way ANOVA with Tukey's multiple comparisons. N = 3 biological replicates, each conducted in technical triplicate. Columns represent averages ± standard deviations of biological replicates.

All 'fresh blood' clots in the TXA treatments had significantly more mass present (decreased breakdown) after induced lysis than the lysed, non-treated control ($p < 0.029$), indicating TXA was effective at stabilizing blood clots when delivered via all examined carriers. TXA delivered with PBS and CMC solutions were not significantly different ($p = 0.77$), indicating similar efficacy. TXA delivered with MF had significantly decreased breakdown compared to both PBS ($p = 0.005$) and CMC solution ($p = 0.028$) TXA treatments, indicating increased TXA efficacy compared to these carriers. However, TXA delivery through MF demonstrated significantly more ($p = 0.015$) breakdown than the non-lysed control.

All 'clotted blood' placed in TXA treatments had significantly decreased breakdown after induced lysis than the lysed, non-treated control ($p < 0.0001$), indicating TXA was effective across all carriers. Similar to the fresh blood treatments, PBS and CMC solution carriers were not significantly different from each other ($p = 0.99$). PBS and CMC solution carriers had significantly more breakdown than MF + TXA ($p < 0.0003$), TXA powder ($p < 0.0005$), and Quik-clot ($p < 0.0036$) treatments, indicating inferior efficacy. MF + TXA ($p = 0.85$), TXA

powder ($p = 0.74$), and Quik-Clot ($p = 0.17$) had non-significant differences to the non-lysed control, indicating inhibited clot breakdown for these experimental conditions.

Table 13 and **Table 14** outline the detailed statistical analysis for 'fresh blood' and 'clotted blood' experimental results, respectively.

Table 13: Ordinary one-way ANOVA with Tukey's multiple comparisons for 'fresh blood' induced clot lysis. N = 3 biological replicates conducted in technical triplicate. ($p \leq 0.05$ *, $p \leq 0.01$ **, $p \leq 0.001$ ***, $p < 0.0001$ ****).

One-Way ANOVA Tukey's Multiple Comparisons Relative Clot Mass – Fresh Blood (Induced Lysis)		
Treatment	Significance	
Lysed control vs. PBS + TXA	*	0.0293
Lysed control vs. CMC + TXA	**	0.0051
Lysed control vs. MF + TXA	****	<0.0001
Lysed control vs. Non-lysed control	****	<0.0001
PBS + TXA vs. CMC + TXA	ns	0.7707
PBS + TXA vs. MF + TXA	**	0.0049
PBS + TXA vs. Non-lysed control	****	<0.0001
CMC + TXA vs. MF + TXA	*	0.0283
CMC + TXA vs. Non-lysed control	***	0.0001
MF + TXA vs. Non-lysed control	*	0.0152

Table 14: Ordinary one-way ANOVA with Tukey's multiple comparisons for 'clotted blood' induced clot lysis. N = 3 biological replicates conducted in technical triplicate. ($p \leq 0.05$ *, $p \leq 0.01$ **, $p \leq 0.001$ ***, $p < 0.0001$ ****).

One-Way ANOVA Tukey's Multiple Comparisons Relative Clot Mass – Clotted Blood (Induced Lysis)		
Treatment	Significance	
Lysed control vs. PBS + TXA	****	<0.0001
Lysed control vs. CMC + TXA	****	<0.0001
Lysed control vs. MF + TXA	****	<0.0001
Lysed control vs. TXA powder	****	<0.0001
Lysed control vs. Non-lysed control	****	<0.0001
Lysed control vs. Quik-Clot	****	<0.0001
PBS + TXA vs. CMC + TXA	ns	0.9893
PBS + TXA vs. MF + TXA	***	0.0001
PBS + TXA vs. TXA powder	***	0.0001
PBS + TXA vs. Non-lysed control	****	<0.0001
PBS + TXA vs. Quik-Clot	**	0.001
CMC + TXA vs. MF + TXA	***	0.0003
CMC + TXA vs. TXA powder	***	0.0005
CMC + TXA vs. Non-lysed control	****	<0.0001
CMC + TXA vs. Quik-Clot	**	0.0036
MF + TXA vs. TXA powder	ns	>0.9999
MF + TXA vs. Non-lysed control	ns	0.8527
MF + TXA vs. Quik-Clot	ns	0.7923
TXA powder vs. Non-lysed control	ns	0.7452
TXA powder vs. Quik-Clot	ns	0.8889
Non-lysed control vs. Quik-Clot	ns	0.1754

'Fresh blood' clots formed in the treatments overall had increased lysis rates as compared to clotted blood as demonstrated by the lower relative clot masses. All TXA treatment formulations had significantly reduced clot breakdown as compared to the lysed control ($p < 0.05$) regardless of 'fresh blood' or 'clotted blood' status.

3.2 Clot Breakdown Inhibition: Natural Lysis

3.2.1 'Fresh Blood'

To determine the antifibrinolytic effectiveness of TXA during natural blood clot lysis, relative clot mass was monitored for each treatment. The relative mass of 'fresh blood' clots was calculated and averaged over 4, 24, 48, and 72 hours (**Figure 26**).

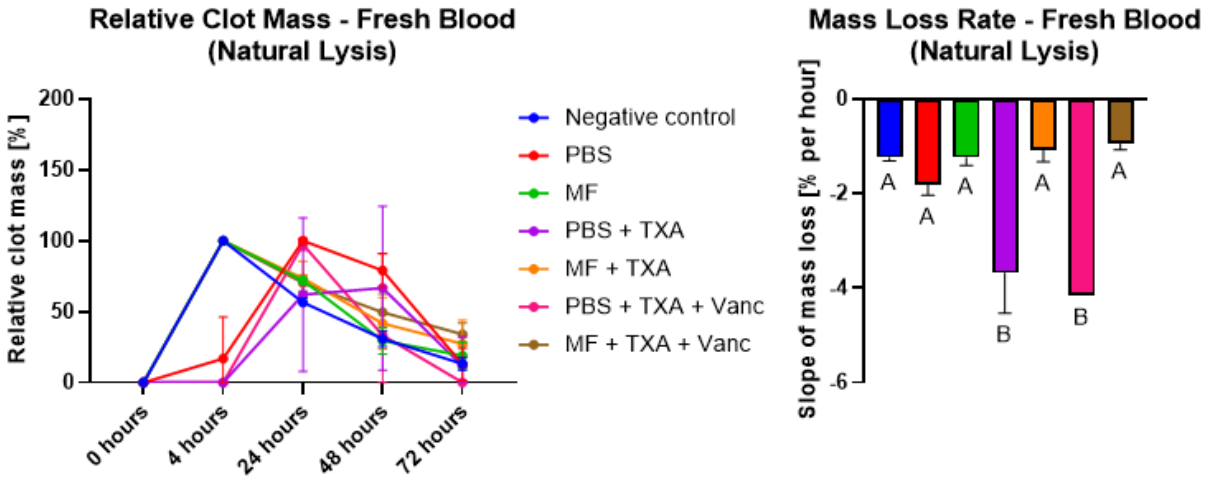

Figure 26: Relative clot mass of 'fresh' ovine blood clots (N = 3 biological replicates) due to natural lysis over 4, 24, 48, and 72 hours. Average clot masses and standard deviations were normalized as a percent of the maximum mass per treatment (left). Linear regression was used to estimate the rate of mass loss after clots reached their maximum mass. Statistical significance was defined as $p \leq 0.05$ and determined by one-way ANOVA with Tukey's multiple comparisons (right). Columns with shared letters were not deemed significantly different. N = 3 biological replicates. Data points represent averages ± standard deviations of biological replicates.

For 'fresh blood', mass loss rates were significantly higher for PBS + TXA and PBS + TXA + Vanc groups when compared to the other treatment groups ($p \leq 0.0002$). Clots in all PBS treatments did not fully form until at least 24 hours, while all MF groups had fully formed by 4 hours. This difference in relative clot mass between the treatments was statistically significant ($p < 0.0001$) except for MF treatments compared to the PBS group ($p \geq 0.15$). Detailed relative mass loss significance is outlined in **Table 15**.

Table 15: Repeated measures two-way ANOVA with Tukey's multiple comparisons for relative clot mass of 'fresh' ovine blood clots due to natural lysis over 4, 24, 48, and 72 hours. Blank spaces indicate that no comparison could be made. ($p \leq 0.05$ *, $p \leq 0.01$ **, $p \leq 0.001$ ***, $p < 0.0001$ ****).

Two-Way ANOVA Tukey's Multiple Comparisons Relative Clot Mass – Fresh Blood (Natural Lysis)					
	0 hours	4 hours	24 hours	48 hours	72 hours
Negative control vs. PBS		ns	**	*	ns
Negative control vs. MF			*	ns	ns
Negative control vs. PBS + TXA		****	ns	ns	ns
Negative control vs. MF + TXA			ns	ns	ns
Negative control vs. PBS + TXA + Vanc		****	**	ns	ns
Negative control vs. MF + TXA + Vanc			ns	ns	ns
PBS vs. MF		ns	***	*	ns
PBS vs. PBS + TXA		ns	ns	ns	ns
PBS vs. MF + TXA		ns	ns	ns	ns
PBS vs. PBS + TXA + Vanc		ns	ns	ns	ns
PBS vs. MF + TXA + Vanc		ns	*	ns	ns
MF vs. PBS + TXA		****	ns	ns	ns
MF vs. MF + TXA			ns	ns	ns
MF vs. PBS + TXA + Vanc		****	*	ns	ns
MF vs. MF + TXA + Vanc			ns	ns	ns
PBS + TXA vs. MF + TXA		****	ns	ns	ns
PBS + TXA vs. PBS + TXA + Vanc			ns	ns	ns
PBS + TXA vs. MF + TXA + Vanc		****	ns	ns	ns
MF + TXA vs. PBS + TXA + Vanc		****	ns	ns	ns
MF + TXA vs. MF + TXA + Vanc			ns	ns	ns
PBS + TXA + Vanc vs. MF + TXA + Vanc		****	*	ns	ns

When comparing treatments with identical doses of TXA or identical carriers, treatment differences become more apparent (**Figure 27**).

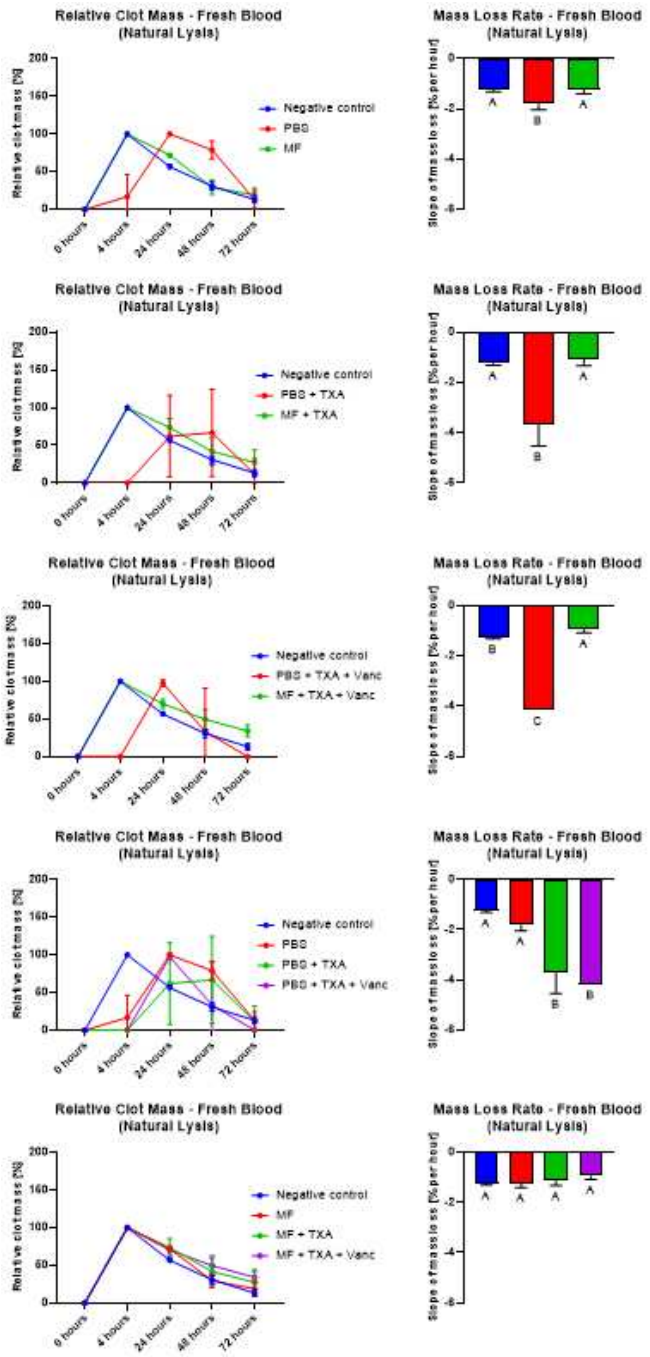

Figure 27: Selective comparisons of relative clot mass of 'fresh' ovine blood clots due to natural lysis over 4, 24, 48, and 72 hours. Average clot masses and standard deviations were normalized as a percent of the maximum mass per treatment (left). Linear regression was used to estimate the rate of mass loss after clots reached their maximum mass. Statistical significance was defined as $p \leq 0.05$ and determined by one-way ANOVA with Tukey's multiple comparisons (right). Columns that share a letter are not statistically different. N = 3 biological replicates. Data points represent averages ± standard deviations of biological replicates.

In carrier comparisons for TXA + Vanc treatments, MF demonstrated a significantly lower rate of lysis than PBS ($p < 0.0001$) and the negative control ($p = 0.014$). Across all carrier comparisons, MF demonstrated significantly lower rates of lysis than PBS groups ($p \leq 0.014$). Detailed statistical analyses of mass loss rates are demonstrated in **Table 16.**

Table 16: Selective one-way ANOVA with Tukey's multiple comparisons for 'fresh blood' mass loss rates. N = 3 biological replicates conducted in technical triplicate. ($p \leq 0.05$ *, $p \leq 0.01$ **, $p \leq 0.001$ ***, $p < 0.0001$ ****).

Selective One-Way ANOVA Tukey's Multiple Comparisons Mass Loss Rates – Fresh Blood (Natural Lysis)		
Treatment	Significance	
Negative control vs. PBS	*	0.0136
Negative control vs. MF	ns	>0.9999
PBS vs. MF	*	0.0136
Negative control vs. PBS + TXA	**	0.0027
Negative control vs. MF + TXA	ns	0.9322
PBS + TXA vs. MF + TXA	**	0.0020
Negative control vs. PBS + TXA + Vanc	****	<0.0001
Negative control vs. MF + TXA + Vanc	*	0.0139
PBS + TXA + Vanc vs. MF + TXA + Vanc	****	<0.0001
Negative control vs. PBS	ns	0.4394
Negative control vs. PBS + TXA	***	0.0006
Negative control vs. PBS + TXA + Vanc	***	0.0002
PBS vs. PBS + TXA	**	0.0037
PBS vs. PBS + TXA + Vanc	***	0.0008
PBS + TXA vs. PBS + TXA + Vanc	ns	0.5553
Negative control vs. MF	ns	>0.9999
Negative control vs. MF + TXA	ns	0.6806
Negative control vs. MF + TXA + Vanc	ns	0.2049
MF vs. MF + TXA	ns	0.6806
MF vs. MF + TXA + Vanc	ns	0.2049
MF + TXA vs. MF + TXA + Vanc	ns	0.7224

Although relative mass loss for “empty” and TXA + Vanc carrier comparisons is significantly less for MF treatments than PBS treatments at 24 hours ($p \leq 0.0065$), the blood clot in PBS has only just fully formed. This indicates that although the relative clot mass is greater for PBS groups, the ‘fresh’ clots took much longer to form, which is not desirable for bleeding control. Detailed statistical analyses for other relative clot mass comparisons are demonstrated in **Table 17**.

Table 17: Combined selective repeated measures two-way ANOVA with Tukey's multiple comparisons for relative clot mass of 'fresh' ovine blood clots due to natural lysis over 4, 24, 48, and 72 hours. Blank spaces indicate that no comparison could be made. ($p \leq 0.05$ *, $p \leq 0.01$ **, $p \leq 0.001$ ***, $p \leq 0.0001$ ****).

Selective Two-Way ANOVA Tukey's Multiple Comparisons Relative Clot Mass – Fresh Blood (Natural Lysis)					
	0 hours	4 hours	24 hours	48 hours	72 hours
Negative control vs. PBS		ns	**	*	ns
Negative control vs. MF			*	ns	ns
PBS vs. MF		ns	****	*	ns
Negative control vs. PBS + TXA		****	ns	ns	ns
Negative control vs. MF + TXA			ns	ns	ns
PBS + TXA vs. MF + TXA		****	ns	ns	ns
Negative control vs. PBS + TXA + Vanc		****	***	ns	ns
Negative control vs. MF + TXA + Vanc		ns	ns	ns	ns
PBS + TXA + Vanc vs. MF + TXA + Vanc		****	**	ns	*
Negative control vs. PBS		ns	**	*	ns
Negative control vs. PBS + TXA		****	ns	ns	ns
Negative control vs. PBS + TXA + Vanc		****	**	ns	ns
PBS vs. PBS + TXA		ns	ns	ns	ns
PBS vs. PBS + TXA + Vanc		ns	ns	ns	ns
PBS + TXA vs. PBS + TXA + Vanc		ns	ns	ns	ns
Negative control vs. MF			*	ns	ns
Negative control vs. MF + TXA			ns	ns	ns
Negative control vs. MF + TXA + Vanc			ns	ns	ns
MF vs. MF + TXA			ns	ns	ns
MF vs. MF + TXA + Vanc			ns	ns	ns
MF + TXA vs. MF + TXA + Vanc			ns	ns	ns

3.2.2 'Clotted Blood'

The relative mass of 'clotted blood' samples was calculated and averaged over 4, 24, 48, and 72 hours (**Figure 28**).

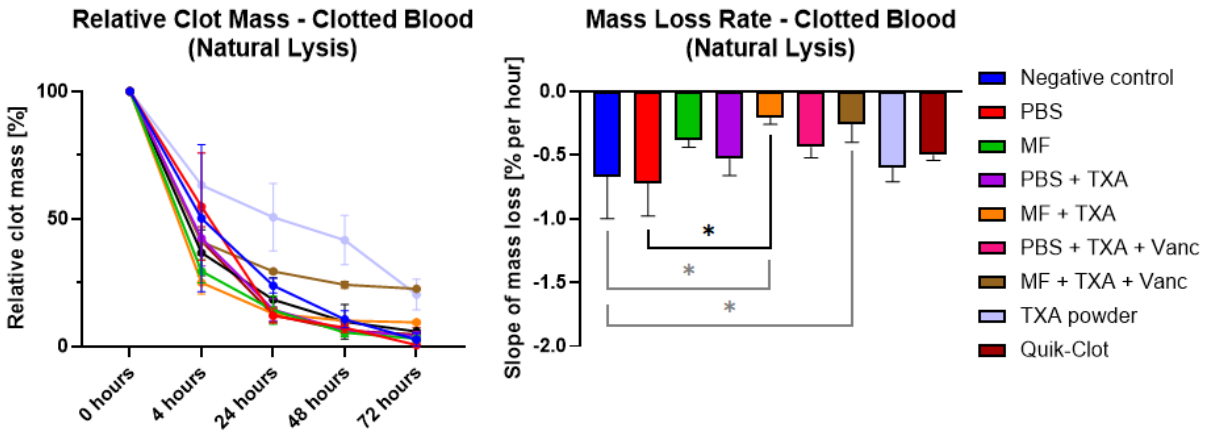

Figure 28: Relative clot mass of 'clotted' ovine blood treatments (N = 3 biological replicates) formed in each treatment due to natural lysis over 4, 24, 48, and 72 hours. Average clot masses and standard deviations were normalized for biological replicates as a percent of the maximum mass per treatment (left). Linear regression was used to estimate the rate of mass loss after clots reached their 4-hour mass. Statistical significance was defined as $p \leq 0.05$ and determined by one-way ANOVA with Tukey's (black) and Dunnett's (grey) multiple comparisons (right).

For 'clotted blood' experiments, all treatments exhibited continual mass loss over 72 hours. No new clot formation was observed over experiment duration. MF + TXA ($p = 0.017$) and MF + TXA + Vanc ($p = 0.037$) mass loss rates were significantly less than the negative control, and MF + TXA mass loss rate was significantly less than PBS ($p = 0.026$) indicating slower clot degradation. Although TXA powder treatments yielded the highest relative clot masses for 4, 24, and 48 hours, the rate of mass loss was not significantly different than that of the negative control ($p = 0.99$).

Multiple comparisons (two-way ANOVA) for relative clot mass over time were conducted to determine time and treatment-dependent significant differences (**Table 18**).

Table 18: Repeated measures two-way ANOVA with Tukey's multiple comparisons for relative clot mass of 'clotted' ovine due to natural lysis over 4, 24, 48, and 72 hours. Comparisons could not be determined for blank spaces. N = 3 biological replicates. ($p \leq 0.05$ *, $p \leq 0.01$ **, $p \leq 0.001$ ***, $p < 0.0001$ ****).

Two-Way ANOVA Tukey's Multiple Comparisons Relative Clot Mass – Clotted Blood (Natural Lysis)					
	0 hours	4 hours	24 hours	48 hours	72 hours
Negative control vs. PBS		ns	ns	ns	ns
Negative control vs. MF		ns	ns	ns	ns
Negative control vs. PBS + TXA		ns	ns	ns	ns
Negative control vs. MF + TXA		ns	ns	ns	ns
Negative control vs. PBS + TXA + Vanc		ns	ns	ns	ns
Negative control vs. MF + TXA + Vanc		ns	ns	ns	*
Negative control vs. TXA powder		ns	ns	ns	ns
Negative control vs. Quik-Clot		ns	ns	ns	ns
PBS vs. MF		ns	ns	ns	ns
PBS vs. PBS + TXA		ns	ns	ns	ns
PBS vs. MF + TXA		ns	ns	ns	**
PBS vs. PBS + TXA + Vanc		ns	ns	ns	ns
PBS vs. MF + TXA + Vanc		ns	*	**	****
PBS vs. TXA powder		ns	ns	ns	ns
PBS vs. Quik-Clot		ns	ns	ns	ns
MF vs. PBS + TXA		ns	ns	ns	ns
MF vs. MF + TXA		ns	ns	ns	*
MF vs. PBS + TXA + Vanc		ns	ns	ns	ns
MF vs. MF + TXA + Vanc		ns	ns	**	**
MF vs. TXA powder		ns	ns	ns	ns
MF vs. Quik-Clot		ns	ns	ns	ns
PBS + TXA vs. MF + TXA		ns	ns	ns	ns
PBS + TXA vs. PBS + TXA + Vanc		ns	ns	ns	ns
PBS + TXA vs. MF + TXA + Vanc		ns	ns	***	*
PBS + TXA vs. TXA powder		ns	ns	ns	ns
PBS + TXA vs. Quik-Clot		ns	ns	ns	ns
MF + TXA vs. PBS + TXA + Vanc		ns	ns	ns	ns
MF + TXA vs. MF + TXA + Vanc		ns	***	*	**
MF + TXA vs. TXA powder		ns	ns	ns	ns
MF + TXA vs. Quik-Clot		ns	ns	ns	ns
PBS + TXA + Vanc vs. MF + TXA + Vanc		ns	ns	ns	ns
PBS + TXA + Vanc vs. TXA powder		ns	ns	ns	ns
PBS + TXA + Vanc vs. Quik-Clot		ns	ns	ns	ns
MF + TXA + Vanc vs. TXA powder		ns	ns	ns	ns
MF + TXA + Vanc vs. Quik-Clot		ns	*	**	*
TXA powder vs. Quik-Clot		ns	ns	ns	ns

Although TXA powder samples appear to demonstrate high relative clot mass compared to other treatment groups, differences were not found to be significant ($p \geq 0.11$). MF + TXA + Vanc treatments had significantly decreased relative mass loss compared to PBS ($p \leq 0.033$), MF + TXA ($p \leq 0.015$), and Quik-Clot ($p \leq 0.048$) treatments from 24-72 hours and PBS + TXA ($p \leq 0.011$) and MF ($p \leq 0.005$) treatments from 48-72 hours. These data indicate that overall, MF + TXA + Vanc inhibits natural clot lysis the most out of the tested treatment groups.

Further comparisons of 'clotted' blood treatments with identical therapeutic doses or identical carriers were conducted to identify any additional significant differences (**Figure 29**).

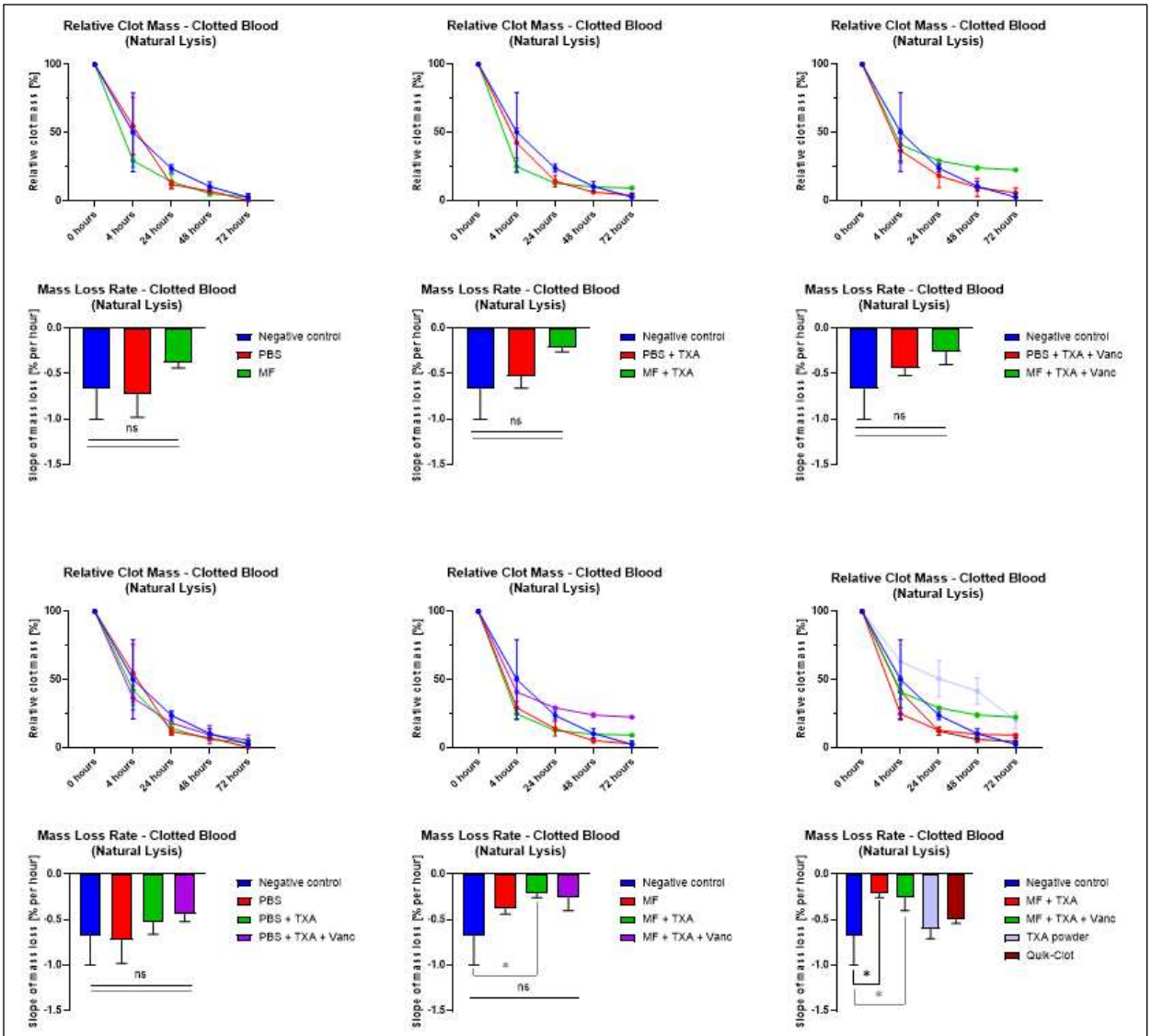

Figure 29: Selective comparisons of relative clot mass of 'clotted' ovine blood due to natural lysis over 4, 24, 48, and 72 hours. Average clot masses and standard deviations were normalized as a percent of the maximum mass per treatment (left). Linear regression was used to estimate the rate of mass loss after clots reached their 4-hour mass. Statistical significance was defined as $p \leq 0.05$ and determined by one-way ANOVA with Tukey's (black) and Dunnett's (grey) multiple comparisons (right). N = 3 biological replicates. ($p \leq 0.05$ *, $p \leq 0.01$ **, $p \leq 0.001$ ***, $p < 0.0001$ ****).

Further select comparisons of mass loss rates did not reveal additional significant differences.

Selective relative clot mass comparisons are outlined in **Table 19**.

Table 19: Combined selective repeated measures two-way ANOVA with Tukey's multiple comparisons for relative clot mass of clotted ovine blood placed in each treatment due to natural lysis over 4, 24, 48, and 72 hours. N = 3 biological replicates. ($p \leq 0.05$ *, $p \leq 0.01$ **, $p \leq 0.001$ ***, $p \leq 0.0001$ ****).

Selective Two-Way ANOVA Tukey's Multiple Comparisons Relative Clot Mass – Clotted Blood (Natural Lysis)					
	0 hours	4 hours	24 hours	48 hours	72 hours
Negative control vs. PBS		ns	*	ns	ns
Negative control vs. MF		ns	ns	ns	ns
PBS vs. MF		ns	ns	ns	ns
Negative control vs. PBS + TXA		ns	ns	ns	ns
Negative control vs. MF + TXA		ns	*	ns	ns
PBS + TXA vs. MF + TXA		ns	ns	*	*
Negative control vs. PBS + TXA + Vanc		ns	ns	ns	ns
Negative control vs. MF + TXA + Vanc		ns	ns	*	**
PBS + TXA + Vanc vs. MF + TXA + Vanc		ns	ns	ns	*
Negative control vs. PBS		ns	*	ns	ns
Negative control vs. PBS + TXA		ns	ns	ns	ns
Negative control vs. PBS + TXA + Vanc		ns	ns	ns	ns
PBS vs. PBS + TXA		ns	ns	ns	ns
PBS vs. PBS + TXA + Vanc		ns	ns	ns	ns
PBS + TXA vs. PBS + TXA + Vanc		ns	ns	ns	ns
Negative control vs. MF		ns	ns	ns	ns
Negative control vs. MF + TXA		ns	ns	ns	ns
Negative control vs. MF + TXA + Vanc		ns	ns	*	*
MF vs. MF + TXA		ns	ns	ns	**
MF vs. MF + TXA + Vanc		ns	ns	***	**
MF + TXA vs. MF + TXA + Vanc		ns	****	**	***
Negative control vs. MF + TXA		ns	ns	ns	ns
Negative control vs. MF + TXA + Vanc		ns	ns	*	*
Negative control vs. TXA powder		ns	ns	ns	ns
Negative control vs. Quik-Clot		ns	*	ns	ns
MF + TXA vs. MF + TXA + Vanc		ns	****	*	***
MF + TXA vs. TXA powder		ns	ns	ns	ns
MF + TXA vs. Quik-Clot		ns	ns	ns	ns
MF + TXA + Vanc vs. TXA powder		ns	ns	ns	ns
MF + TXA + Vanc vs. Quik-Clot		ns	*	**	*
TXA powder vs. Quik-Clot		ns	ns	ns	ns

Similar to the initial analysis, MF + TXA + Vanc demonstrated superior ability to inhibit relative mass loss of 'clotted blood' during natural lysis, despite the appearance of TXA powder having the greatest relative clos mass average.

3.3 Clot Rheological Assessment

In materials that exhibit both elastic (recoverable energy) and viscous (dissipated energy) behavior under deformation, like blood clots [142], phase angle is a direct relationship between the ability of the material to elastically deform (storage modulus) and the ability of the material to irreversibly deform (loss modulus) (**Equation 9**).

Equation 9: $$Phase\ Angle = tan^{-1}\left(\frac{Loss\ modulus}{Storage\ modulus}\right)$$

Thus, the lower the value of the phase angle, the more elastic behavior the material demonstrates, and the more resistant to deformation it becomes. In theory, a decrease in phase angle over time indicates that the blood clot is still forming, and that the fibrin network is maturing [138]. Blood clot viscoelasticity was monitored for both 'fresh' and 'clotted' blood treatments, and the change in phase angle was calculated and averaged for each treatment at 4, 24, 48, and 72 hours. Results for fresh blood clots are outlined in (**Figure 30**).

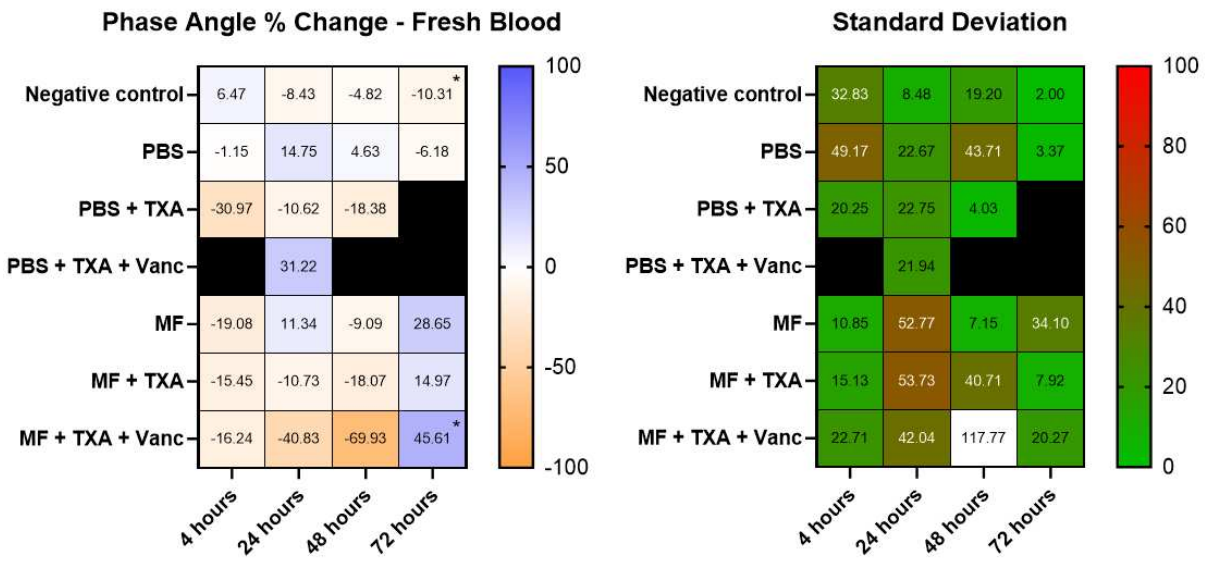

Figure 30: Average percent phase angle change (left) and standard deviations (right) for 'fresh' ovine blood clots at 4, 24, 48, and 72 hours. Positive percent changes indicate an increase in phase angle that corresponds to a decrease in clot elasticity. Negative percent changes indicate a decrease in phase angle that corresponds to an increase in elasticity. $N \geq 1$ biological replicate conducted in at least technical duplicate. Statistical significance was determined by multiple one-way ANOVAs and Tukey's multiple comparisons ($p \leq 0.05$ *). Black spaces indicate that sample replicates had dissolved at that treatment time point.

PBS + TXA + Vanc treatments did not form any clots at 4 hours, and the clots that formed at 24 hours were fully disintegrated by 48 hours. Blood clots formed in PBS + TXA were fully disintegrated by 72 hours. Due to these data blanks, running a full two-way ANOVA was not possible. Due to high sample variance, one-way ANOVAs for time and treatment only revealed a significant difference between MF + TXA + Vanc and negative control treatments ($p = 0.036$). All MF treatments and PBS + TXA demonstrated a negative change in phase angle at 4 hours, indicating the clot was still gaining elasticity at that time. This trend persists for PBS + TXA, MF + TXA, and MF + TXA + Vanc treatments until 72 hours, where a positive phase angle change for MF carriers indicates a decrease in elastic behavior, and clot disintegration for PBS + TXA

indicates full clot demise. The clots that did form in PBS + TXA + Vanc at 24 hours also demonstrated an increase in phase angle.

Similarly, phase angle changes for clotted blood treatment samples are presented in (**Figure 31**).

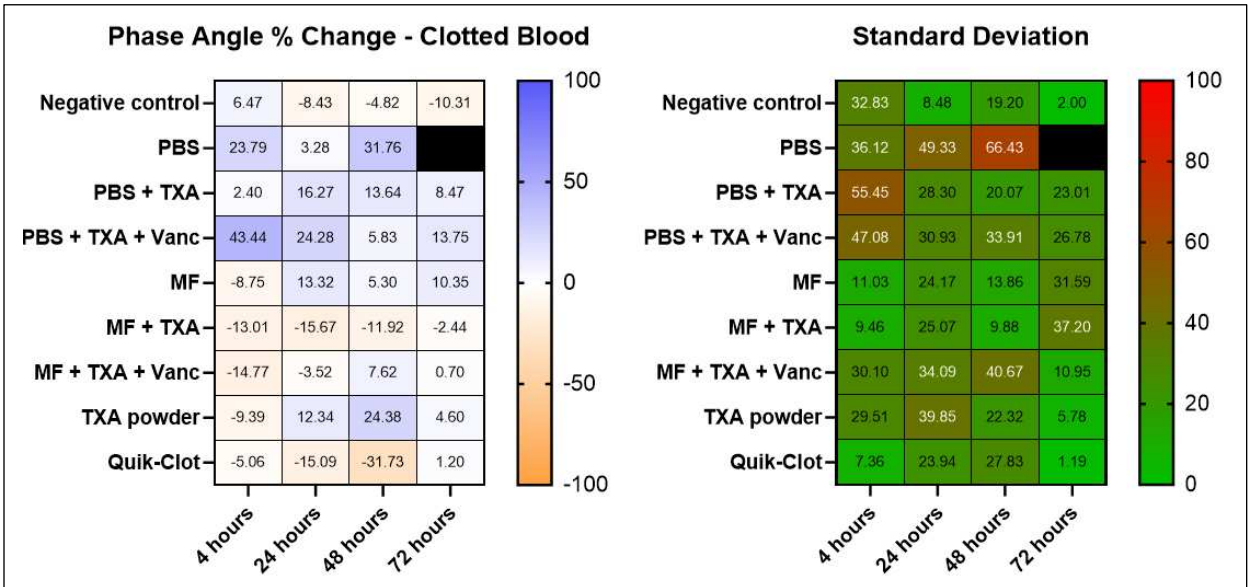

Figure 31: Average percent phase angle change (left) and standard deviations (right) for 'clotted' ovine blood at 4, 24, 48, and 72 hours. Positive percent changes indicate an increase in phase angle that corresponds to a decrease in clot elasticity. Negative percent changes indicate a decrease in phase angle that corresponds to an increase in elasticity. $N \geq 1$ biological replicate conducted in at least technical duplicate. Statistical significance was determined by multiple one-way ANOVAs and Tukey's multiple comparisons ($p \leq 0.05$ *). Black spaces indicate that sample replicates had dissolved at that treatment time point.

Blood clots treated with PBS were fully disintegrated by 72 hours, so no data could be collected. Due to this data blank, running a full two-way ANOVA was not possible. Due to high sample variance, one-way ANOVAs for time and treatment did not reveal any significant differences for any treatments ($p \geq 0.05$). Overall, MF treatments with TXA and vancomycin demonstrate more elastic behavior than PBS treatments with TXA and vancomycin. At 72 hours, all treatments except for the negative control appear to be losing elasticity as demonstrated by an increase in

phase angle. TXA powder treatments trend toward decreased elasticity after 4 hours, while Quik-Clot treatments trend toward increasing elasticity until 72 hours.

3.4 Reduced Flow Assessment

To assess the ability of the MF to slow blood flow and potentially aid in hemostasis, the amount of time it took for a set volume to travel through a known volume of solution was measured (**Table 20**).

Table 20: Time for ovine blood to travel to the bottom of each respective treatment and the time for ovine blood to completely settle at the bottom of each treatment. N = 3 biological replicates conducted in technical triplicate. Data is presented as average times ± standard deviations.

Whole Ovine Blood Volumetric Flow Rates and Settlement Times		
Treatment	Time to travel [min]	Time to settle [min]
PBS	0	-
CMC solution	28 ± 2.96	> 120
MF	1.33 ± 0.71	> 120
MF + TXA	1.11 ± 0.65	> 120
MF + TXA + Vanc	1.28 ± 0.56	> 120

N=9

Since blood flow through the PBS was immediate, the travel time was recorded as zero and the time to settle was recorded as negligible. Travel time of the blood through CMC solution (**Figure 32**) was significantly higher than all other groups ($p < 0.0001$, one-way ANOVA with Tukey's multiple comparisons) and took longer than 2 hours to fully settle. There were no statistically significant differences between all MF treatments or with PBS, although all MF groups took longer than 2 hours to fully settle.

Figure 32: Representative image of reduced flow experiment data. Blood volume through PBS (left) vs blood volume flow through CMC solution (right).

4.0 Discussion

Ovine blood was utilized for all experiments due to a matter of abundance, convenience, and sheep having similar coagulation profiles and clot stiffnesses to humans [143]. It was hypothesized that experimental behavior of ovine blood would be similar to what could be expected from human samples.

4.1 Clot Breakdown Inhibition

For induced and natural blood clot lysis experiments, TXA powder and Quik-Clot groups were not utilized for fresh blood clot treatments. Preliminary attempts of these treatments with fresh blood yielded paste rather than a clot (TXA powder) and a blood-soaked gauze (Quik-Clot), both of which were deemed unsuitable for the designed breakdown experiments. A preliminary experiment also included a combined MF and Quik-Clot fresh blood treatment to demonstrate

compatibility, but this treatment was not included in further experimentation due to the desire to first determine individualized treatment effects.

4.1.1 Induced Clot Lysis

For induced lysis experiments (simulated hyperfibrinolysis), the 1 mg/mL concentration of streptokinase was chosen because it is highly potent and was hypothesized to cause rapid blood clot breakdown, thus demonstrating the capabilities of TXA treatments to slow or stop this breakdown. The data supported this hypothesis, as the lysed streptokinase control demonstrated over 50% mass loss in 120 minutes, compared to the non-lysed control that only lost 5%. 1 mg/mL corresponds to approximately 2800 International Units (IU)/mL of streptokinase, a standardized unit of activity for streptokinase. The observed positive (streptokinase) and negative control mass loss was similar to the same controls of Prasad et al. (2006) who developed the basis for these experiments (62% mass loss over 90 minutes at 7500 IU/mL, 2.56% mass loss for non-lysed control) [137].

All TXA treatments had significantly less clot breakdown over the experiment duration than lysed controls, indicating TXA was effective at inhibiting hyperfibrinolysis to some extent. However, both ‘fresh’ and ‘clotted’ samples treated with PBS and CMC solution as carriers had significantly more breakdown than samples treated with MF treatments, indicating some mechanism of the MF that is favorable for robust blood clot formation and reinforcement. PBS and CMC solution treatments also visually delayed clot formation in the ‘fresh’ blood treatments, whereas MF did not. It is possible that this is attributed to the lack of calcium present in PBS, which plays an important role in blood clot formation [144]. PBS could dilute the calcium that is present in the whole blood, making it more difficult for clots to form. PBS is also the solvent in CMC solution, which would explain delayed formation there as well. However, this is also

contradictory because CMC solution is the base material for the MF. It is possible that the presence of air pockets (bubbles) in the MF may promote clot formation and strengthening in some way, but this is not supported directly in the literature.

TXA powder, Quik-Clot, and MF + TXA all demonstrated similar breakdown for the 'clotted' blood treatments ($p > 0.05$) and were not significantly different from the non-lysed control. These data indicate that these treatments are most conducive to structural clot reinforcement and inhibit the fibrinolysis process for these experimental conditions. TXA in powder formulation was expected to perform as such, due to the extremely high, localized concentration [145, 146] that exceeds those of any other treatment. The estimated effects of Quik-Clot were unknown, as Quik-Clot primarily works as a hemostatic agent by 1) acting as a gauze and 2) accelerating the body's natural clotting process rather than actively working to prevent clot breakdown [147].

4.1.1 Natural Clot Lysis

In natural clot lysis, relative clot mass was monitored for each 'fresh' and 'clotted' blood treatment over 4, 24, 48, and 72 hours, and the resulting rates of clot breakdown (linear regression slopes) were calculated and compared. For 'fresh' clots, PBS groups again hindered the formation of clots, with these samples not forming clots until at least 24 hours, where all MF groups had formed full clots by 4 hours, regardless of TXA presence. The rates of clot breakdown for MF + TXA + Vanc were significantly slower than other treatments in both large-scale and more targeted comparisons.

In 'clotted' treatment groups, MF + TXA and MF + TXA + Vanc rates of breakdown were the only groups determined to be significantly reduced compared to the negative control, indicating overall decreased temporal breakdown rates for clots formed before treatment. TXA powder demonstrated the highest overall clot mass until 72 hours, where relative mass decreased to the

same final values as the other treatments. The mass loss rate estimate did not include the 0-hour clot mass in the linear regression. This is because blood clots undergo significant shrinkage in this time not related to clot lysis [148], specifically when attempting to achieve homeostasis in the treatment environment.

These data suggest that the addition of vancomycin may have some synergistic or enhanced effect on the reduction of clot breakdown over time due to natural clot lysis. Some studies have confirmed the synergistic effects of TXA and vancomycin when co-delivered [123, 149, 150], yet they focus on determining if TXA has any effects on the vancomycin effectiveness, not the other way around.

Overall, MF + TXA and MF + TXA + Vanc treatments demonstrated increased performance in natural lysis clot mass and breakdown rate experiments. Future experiments would trend toward repetition of natural clot lysis experiments with hyper-lysed samples and induced lysis experiments with naturally-lysed samples to fully round out each data set. Combined effects of Quik-Clot and MF would also need to be explored further, as this would be a likely combination in trauma scenarios.

4.2 Clot Rheological Assessment

The goal of these experiments was to characterize the viscoelasticity of the blood clots for each respective treatment. Due to the *ex vivo* approach and highly variable kinetics of individual blood clots, no significant results between treatment groups were reported. It was hypothesized that blood clots treated with TXA would exhibit a significant decrease in or negligible phase angle change over longer treatment times than groups without TXA, which would indicate increasing clot firmness or structural stability, respectively [138, 139].

Thromboelastography (TEG) and Rotational Thromboelastometry (ROTEM) are two technologies that characterize clot formation and stability. They are typically found in hospitals, and monitor the clot formation progress by measuring resulting amplitude of oscillatory pin or cup movement that is directly related to clot structure [151, 152]. Increasing amplitudes over time correspond to clot formation and stiffening, while constant amplitudes and decreasing amplitudes correspond to clot stability and clot lysis over time, respectively [139].

Although not significant, fresh blood treatments containing TXA demonstrated a decrease in phase angle (increase in stiffness, indicator of structural integrity and resistance to deformation) at longer treatment times as opposed to treatments without TXA, apart from PBS + TXA + Vanc. These results are partially supported by Gosselin et al. (2022) who demonstrated that in models simulating trauma-induced coagulopathy, TXA effectively restores mechanical clot formation, thereby preserving clot integrity [12]. However, these results are not directly comparable to the ones obtained in this study, as they were conducted on human plasma and were conducted at a much higher frequency (7.8 Hz) to investigate clot recovery in simulated hyperfibrinolysis. Experimental modifications from the modeled studies [138, 139] include structural monitoring after full clot formation rather than during initial and continual formation. This approach could be responsible for variations in expected phase angle changes.

General trends for clotted blood treatments are more difficult to conclude, as no clear patterns emerge, and no statistically significant differences are demonstrated.

Performing the experiments under conditions within the linear viscoelastic region of blood clots is paramount to ensure that experimental outcomes are due to the inner blood clot mechanics and not influenced by machine input as much as possible [138]. The applied oscillatory shear strain amplitude and angular frequency were well within the published range for human blood (10%

strain, 2 Hz) [140], making the highly variable clot behavior unlikely to be caused by destructive conditions imposed by the rheometer.

Limitations for these studies include high sample variation and low sample size due to time sensitivity of *ex vivo* methods. Future experimentation would likely shift to focus on hyperfibrinolysis models in addition to natural lysis in an attempt to elicit more robust evidence of TXA efficacy.

4.3 Reduced Flow Assessment

TXA mechanisms of action are not responsible for active blood clotting or staunching, so no statistically significant difference was expected between MF groups with or without TXA. Treatments were only able to delay blood travel and not staunch, although blood had the slowest rate of travel through the CMC solution. These results are valid due to the high viscosity of the solution and absence of borders conducive to fluid flow like those present in the MF treatments. Although MF treatment groups were not as effective at slowing blood travel, these groups demonstrated long settling times. This is likely due to the MF turning back into solution and thus slowing the flow by eliminating the liquid-bubble borders that lead to high drainage rates (see Chapter 2).

CMC in hydrogel formulations has demonstrated exceptional ability to absorb wound exudates due to their absorption and expansion capabilities [153, 154], so it is plausible that CMC solution would act in a similar fashion by slowing the travel rate of blood through these treatments. However, as CMC solution and “empty” MF are not irreversibly crosslinked like hydrogels, the mechanism of blood slowing is not attributed to absorption for the CMC solution or MF. Although CMC solution was shown to slow blood flow the most, it also demonstrated decreased ability to stop induced clot lysis as compared to MF and took longer to form clots from fresh

blood than other treatments as demonstrated in the clot breakdown studies. Thus, as the primary goal of MF application is antifibrinolysis rather than direct hemostasis, these findings are informative of additional desirable qualities rather than hypothesized qualities. In preliminary findings, MF was also determined to be physically compatible with gauzes, including Quik-Clot. Limitations of these studies include the use of anticoagulated ovine blood at a relatively low flow rate (2 mL/min). This flow rate was chosen because it is representative of passive venous blood flow [155] and allowed for extended experimental duration. Realistically, this flow not indicative of massive hemorrhage or at risk of causing death by exsanguination [156]. However, if flow rate reduction of poor for low flow rates, it can be reasonably deduced that the reduction at higher flow rates would be poor as well. Due to the utilization of a syringe pump, anticoagulated blood was utilized to not cause mechanistic damage or backlogging due to clots forming in the tubing and in the syringe.

5.0 Conclusion

MF demonstrated blood clot formation and reinforcement, reduced mass loss and breakdown rate, and performed no worse than other treatment formulations in *ex vivo* ovine clotting experiments.

In induced lysis experiments, MF + TXA had significantly less breakdown than PBS + TXA and CMC + TXA for experiments on fresh blood clots and clotted blood, indicating superior TXA delivery. MF + TXA also did not have significant differences in clot breakdown from the non-lysed control, TXA powder, or Quik-Clot treatments for clotted blood, indicating similar efficacy and a complete inhibition of induced clotted blood lysis.

Overall, in natural lysis experiments, MF + TXA + Vanc and MF + TXA treatments demonstrated low mass loss and rates of mass loss, indicating effective delivery of TXA and a

potential synergistic relationship with vancomycin. All PBS groups, including those with TXA, took much longer to form clots and had increased breakdown compared to MF groups. Rates of mass loss for MF were not significantly different than those of TXA powder or Quik-Clot, again indicating similar effectiveness to high concentration, clinically relevant treatments.

MF reduced the rate at which blood traveled through it as compared to a non-viscous PBS solution but was not successful at achieving full stasis. This quality of the MF can be mitigated by potential combination with gauze for a multi-faceted approach to hemostasis.

1.0 Background

1.1 Overview

Infection prevention and control (IPC) are essential for reducing morbidity and mortality associated with open wounds. Objects responsible for causing open wounds, especially those causing penetrating trauma, allow pathogens and debris to enter deep into the wound, where they can then travel through the bloodstream or lodge deep into tissue [16]. An estimated 5-32% of acute wounds become infected, with surgical site and traumatic wounds being the most prone to infection [17].

1.2 Current Standards of Care

1.2.1 Advanced Clinical Environments

In clinical environments, wound irrigation and debridement are commonly conducted to mitigate infection potential, and prophylactic intravenous antibiotics are given to patients once they arrive at the hospital. Despite advanced antibiotic care in clinical settings, rates of post-operative surgical site infection still remain elevated in large wounds [52]. Specifically, there have been no significant declines in periprosthetic joint infections in total joint arthroplasties ($p \geq 0.63$) between 2005-2015 [157]. To combat this, the use of intrawound topical antibiotics (independent or combined with intravenous prophylactics) are being utilized by surgeons in an attempt to decrease the number of post-operative infections [50-52].

1.2.2 Austere Military Environments

The current standard of care (SOC) in military medicine outlines infection prevention and treatment strategies to mitigate the risk of combat-related infections, particularly from multidrug-

resistant organisms (MDROs) like methicillin-resistant *Staphylococcus aureus* (MRSA) [158]. These protocols include the use of single-dose, broad-spectrum antibiotics and/or limited intravenous antibiotics if supplies and Role of Care facilities (see Chapter 1) allow [21, 22]. Austere environments pose a multitude of challenges for combat-related injuries that exceed the already limited field treatment modalities, including but not limited to, multiple patient transfers, non-sterile environments, prolonged casualty care/evacuation, and triage mentality [159].

1.3 Methicillin-resistant *Staphylococcus aureus*

Many pathogens develop antibiotic resistance over time due to genetic mutation or inappropriate antibiotic use [160]. MRSA, specifically, has developed resistance to beta-lactam antibiotics through gene mutations that lower affinity for these antibiotics [161], leaving antibiotics like vancomycin, daptomycin, and linezolid as the primary antibiotics to combat MRSA infections [162].

It has been reported that 34% of combat-injured military personnel developed a trauma-related infection, with MRSA being a prevalent pathogen [163], although this is regionally variable. To combat MRSA infections in such settings, vancomycin remains a cornerstone of treatment if it is available to administer at the time of infection [22]. In clinical settings, MRSA is one of the leading causes of hospital infections with a reported infection incidence of 7-60% [161] depending on hospital region and level of care.

1.4 Vancomycin

Vancomycin is a Gram-positive, glycopeptide antibiotic that exerts its bactericidal effect by inhibiting bacterial cell wall synthesis. Importantly, vancomycin exhibits time-dependent, rather than concentration-independent, killing kinetics [45]. Thus, its efficacy is driven by the duration that the drug concentration remains above the minimum inhibitory concentration (MIC) of the

target pathogen, rather than achieving high peak concentrations. Therefore, maintaining adequate drug MIC levels over an extended period is crucial for optimal antibacterial activity [164]. This pharmacodynamic property underscores the importance of dosing strategies that ensure sustained exposure to the antibiotic, thereby enhancing its therapeutic effectiveness.

While traditionally administered intravenously, there is growing interest in the topical application of vancomycin for wound management [165, 166]. This approach not only delivers high local concentrations of the antibiotic directly to the wound site but also minimizes systemic exposure, potentially reducing adverse effects such as ototoxicity and nephrotoxicity [50, 167, 168]. However, optimized delivery of topical vancomycin remains elusive, and delivery strategies that can maintain adequate MIC levels remain an important area of research.

1.5 Carboxymethyl Cellulose

Carboxymethyl cellulose (CMC) has been effectively utilized as a delivery vehicle for therapeutics, enhancing efficacy through sustained and controlled release mechanisms [29, 80, 124, 169]. In a study by Meedecha et al., CMC/polycaprolactone (PCL) polymer films demonstrated a sustained release profile of vancomycin to reduce biofilms formed *in vitro* [170]. Similarly, research by Cerchiara et al. focused on the development of microparticles based on chitosan and CMC polyelectrolyte complexes for the targeted delivery of vancomycin to the colon [171]. This approach aimed to enhance the therapeutic efficacy of vancomycin against colonic infections by ensuring its localized and sustained release. These studies are examples of those that underscore the versatility and efficacy of CMC as a delivery matrix for vancomycin, facilitating sustained release and improved treatment outcomes in various medical applications. Thus, our group hypothesized that a viscous MF derived from CMC would deliver a prolonged and sustained release of vancomycin to tissue inoculated with MRSA, effectively reducing the

bacterial load over time. Pilot experiments were conducted to validate the chosen experimental approach, which was then further refined in pivotal, expanded data sets.

2.0 Materials and Methods

The ability of the MF containing vancomycin was assessed by a modified MRSA bacterial killing assay [172]. Canisters were sterilized by vaporized hydrogen peroxide (50°C, 60 minutes) and 3% CMC solution, 1x phosphate-buffered saline (PBS), instruments, and glassware were sterilized by autoclave (liquid cycle at 121°C, 15 minutes: CMC and PBS solutions, gravity cycle at 121°C, 45 minutes: instruments and glassware). Therapeutics were stored as sterile powders. Experimental conditions were executed in a laminar flow hood. Bacterial subcultures (USA300 MRSA) were grown to log phase on the day of tissue inoculation in antibiotic-free complete growth medium (Dulbecco's Modified Eagle Medium; DMEM with 1000 mg/L glucose, 10% fetal bovine serum; FBS, 1M hydroxyethyl piperazineethanesulfonic acid; HEPES) to OD600 of 0.6, corresponding to 7.5 $\log_{10}$ colony forming units (CFU)/mL. Bacterial inoculum (2.5×10^4 per muscle tissue sample) was calculated based on optical density and a previously determined growth curve equation.

2.1 Pilot Study for MF Bacterial Killing Experimentation

Aseptically-collected ovine bicep femoris muscle tissue samples (1 cm^3/sample) were individually inoculated with actively dividing log phase bacteria (2.5×10^4 per sample) for 10 minutes, then submerged in treatment groups (positive-inoculated control or MF with 0.5 mg/mL vancomycin). The submerged tissue samples were then incubated at 37°C for 30 minutes and 60 minutes. Following treatment, 1 mL of PBS was added to the sample tube and the muscle tissue was sonicated for 1 minute to release bacteria. Supernatant was then collected, diluted 10-fold in 96 well plates, plated on Luria-Bertani (LB) agar plates at 100 ul/quadrant, and incubated at

37°C overnight (~18 hours). CFU were counted manually (macroscopic) at that time and plotted as $\log_{10}$ bacterial colony count (CFU/mL)

Statistical significance was defined as $p \leq 0.05$ and determined using unpaired t-tests. N = 1 biological replicate conducted in technical triplicate.

2.2 Pivotal MF Bacterial Killing Experimentation

To more accurately mimic typical bacterial exposure conditions, the experimental approach was extended to include 4-, 24-, 48-, and 72-hour treatment times with an increased inoculation time (30 minutes) and alternate treatment application (tissue coated with treatment rather than submerged, **Figure 33**). Vancomycin concentration was increased to 1 mg/mL, and a combined tranexamic acid (TXA)/vancomycin treatment was introduced.

Figure 33: Representative image of MRSA-inoculated muscle tissue being coated with MF treatment. The tissue sample was dipped into MF, allowing the treatment to coat the surface. This sample was then placed in a sterile conical tube and incubated.

Aseptically-collected ovine bicep femoris muscle tissue samples (1 cm^3/sample) were inoculated with actively dividing log phase bacteria (2.5 x 10^4 per sample) for 30 minutes, then coated with

each treatment group (PBS (control), PBS/vancomycin (1 mg/mL), PBS/vancomycin (1 mg/mL)/TXA (10 mg/mL), base MF, MF/vancomycin (1 mg/mL), and MF/vancomycin (1 mg/mL)/TXA (10 mg/mL)). All materials were appropriately sterilized and experimental conditions executed in a laminar flow hood. The treated tissue samples were then incubated at 37°C for 4, 24, 48, and 72 hours. Following treatment, 1 mL of PBS was added to the sample tube and the muscle tissue was sonicated for 1 minute to release bacteria. Supernatant was then collected, diluted 10-fold in 96 well plates, plated on LB agar plates at 100 ul/quadrant, and incubated at 37°C overnight (~18 hours). CFU were counted manually (macroscopic) at that time. CFU were counted manually (macroscopic) at that time and plotted as $\log_{10}$ bacterial colony count (CFU/mL)

Statistical significance was defined as $p \leq 0.05$ and determined by ordinary one and two-way ANOVA with Tukey's or Sidak's multiple comparisons when appropriate. N = 1 biological replicate conducted in technical triplicate.

3.0 Results

3.1 Pilot Study for MF Bacterial Killing Experimentation

After a 10-minute inoculation period, the MF containing 0.5 mg/mL of vancomycin demonstrated a 44% reduction and 90% reduction in bacterial colonies from the positive inoculated control at 30 and 60 minutes, respectively. This reduction was not statistically significant at 30 minutes ($p = 0.26$) but was at 60 minutes ($p = 0.0002$) (**Figure 34**).

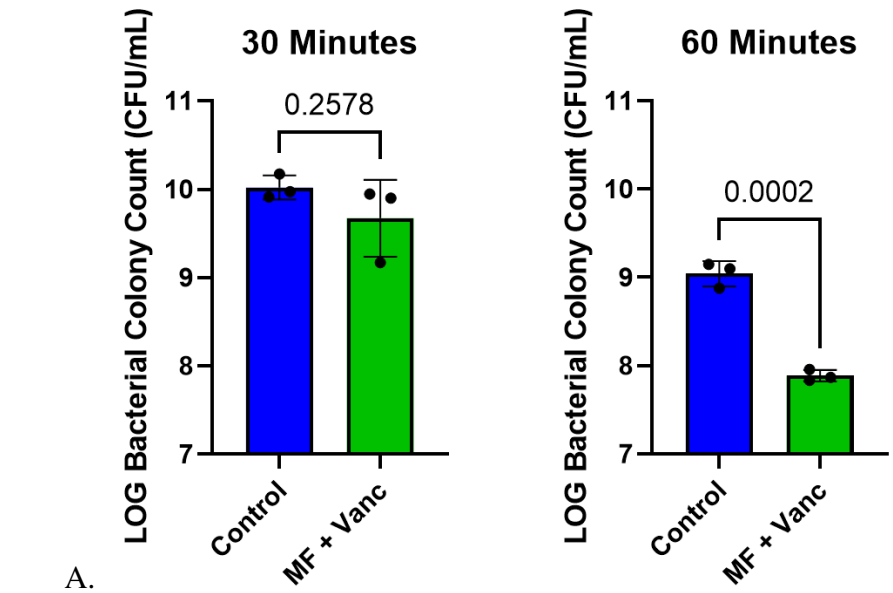

A.

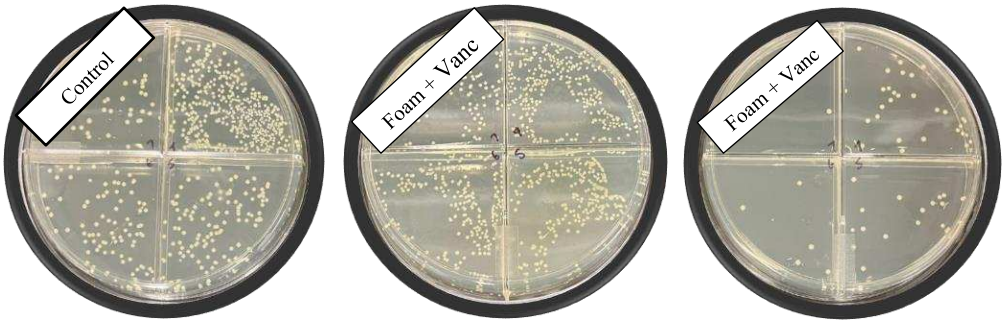

B.

Figure 34: Log MRSA colony count comparison over 30-minute ($p = 0.26$) and 60-minute ($p = 0.0002$) MF treatments with vancomycin. Statistical significance was defined as $p \leq 0.05$ and analyzed using unpaired t-tests (N = 1 biological replicate, conducted in technical triplicate, panel A). Representative images of bacterial CFUs for an untreated control (panel B, left). A 30-minute MF/vancomycin treatment (panel B, middle), and a 60-minutes MF/vancomycin treatment (panel B, right).

These preliminary data indicated that vancomycin to submerged tissue samples delivered through the MF was effective when compared to a positive control (inoculated, but not treated, muscle tissue), thus demonstrating proof-of-concept for further investigation of antibiotic delivery through the MF.

3.2 Pivotal MF Bacterial Killing Experimentation

After a 30-minute inoculation period and 4-, 24-, 48-, and 72-hour treatment times, the lowest bacterial load was observed following the treatment with the MF with vancomycin and TXA ($10^{5.5}$ CFU/mL) at 48 hours, and the highest bacterial load was achieved by the base MF ($10^{13.7}$ CFU/mL) at 72 hours (**Figure 35).**

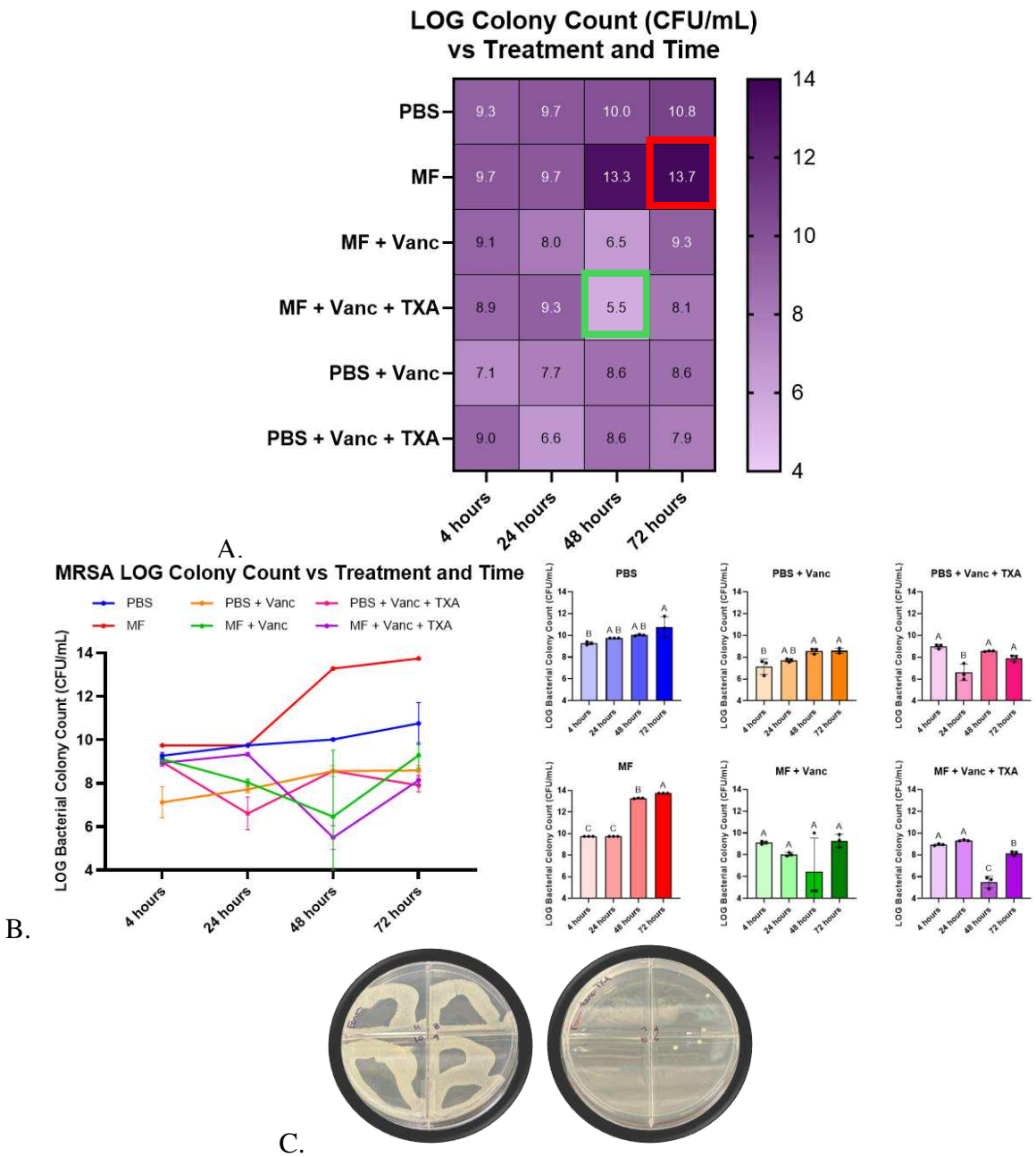

Figure 35: Compiled average MRSA colony counts for each treatment over 4, 24, 48, and 72 hours. Red outline corresponds to the highest observed bacterial load and green outline corresponds to the lowest observed bacterial load (panel A). Visualization of bacterial killing per treatment over time. Statistical significance defined as $p \leq 0.05$ and determined by one-way ANOVA with Tukey's multiple comparisons (panel B). Representative images of highest (panel C, left) and lowest (panel C, right) bacterial loads. N = 1 biological replicate conducted in technical triplicate.

3.2.1 Effect of MF with Vancomycin

The bacterial load of the MF with vancomycin did not decrease significantly over time, but did exhibit a 1 log (90%, p = 0.83) decrease from 4 to 24 hours and an additional 2 log (99%, p = 0.62) decrease from 24 to 48 hours. From 48 to 72 hours, the colony count increased by 3 log (99.9%, p = 0.20) back to the original count at 4 hours (**Figure 36**).

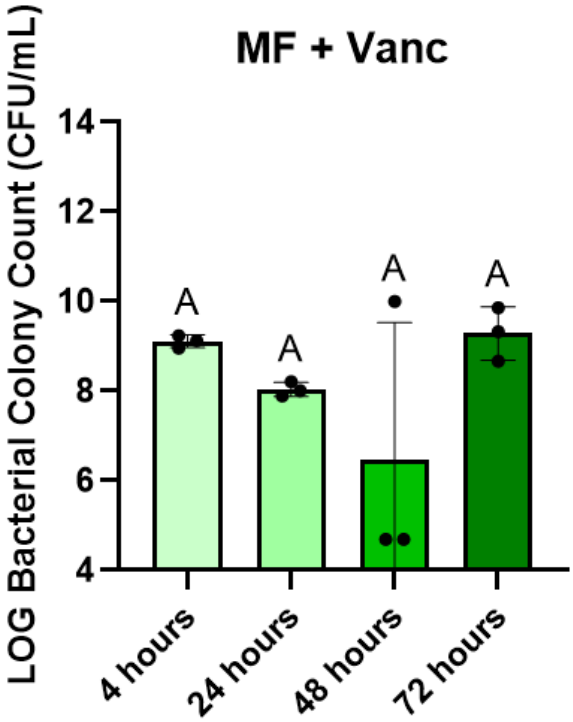

Figure 36: Observed MRSA bacterial load in tissue samples treated with MF with 1 mg/mL vancomycin over time. N = 1 biological replicate conducted in technical triplicate. Statistical significance was defined as $p \leq 0.05$ and determined with ordinary one-way ANOVA with Tukey's multiple comparisons. Columns with like letters are not statistically different.

When compared directly to the PBS with vancomycin treatment, MF with vancomycin killing was not significantly different at any time point ($p \geq 0.15$) as determined by two-way ANOVA with Sidak's multiple comparisons, indicating similar effectiveness (**Figure 37**).

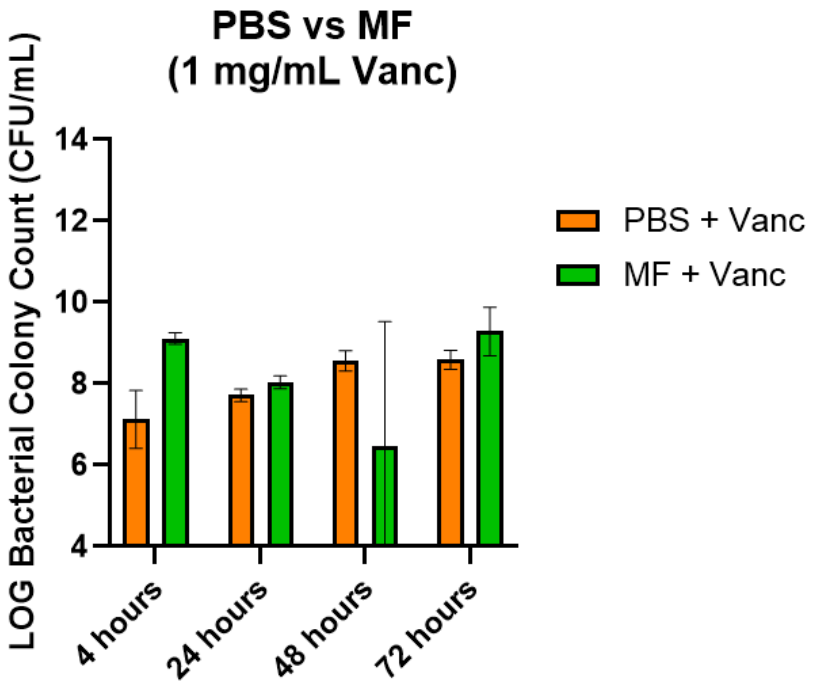

Figure 37: Observed MRSA bacterial load in tissue samples treated with 1 mg/mL vancomycin in PBS or MF over time. N = 1 biological replicate conducted in technical triplicate. Statistical significance was defined as $p \leq 0.05$ and determined with two-way ANOVA with Sidak's multiple comparisons.

3.2.2 Effect of MF with Vancomycin and TXA

The MF with vancomycin and TXA demonstrated a significant 3 log (99.9%, $p < 0.0001$) reduction in bacterial load from 24 to 48 hour treatment times as determined by ordinary one-way ANOVA with Tukey's multiple comparisons (**Figure 38**).

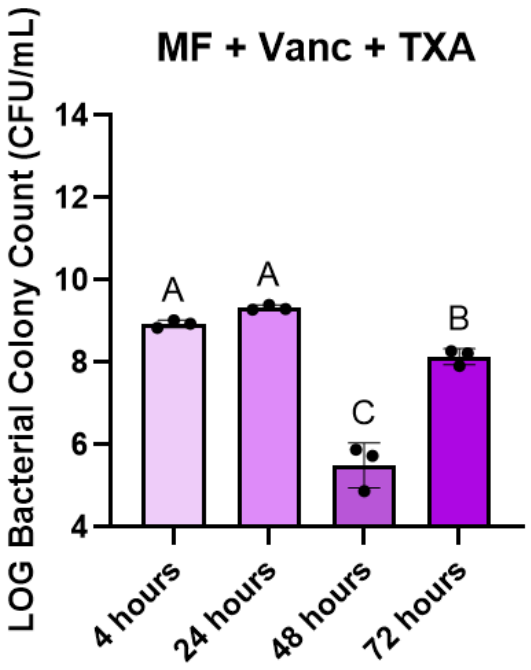

Figure 38: Observed MRSA bacterial load in tissue samples treated with MF with 1 mg/mL vancomycin and 10 mg/mL TXA over time. N = 1 biological replicate conducted in technical triplicate. Statistical significance was defined as $p \leq 0.05$ and determined with ordinary one-way ANOVA with Tukey's multiple comparisons. Columns with like letters are not statistically different.

Even after a significant bacterial increase from 48 to 72 hours ($p < 0.0001$) indicating reduced treatment efficacy, the bacterial load at 72 hours is still significantly less than at 4 ($p = 0.044$) or 24 ($p = 0.005$) hours.

When compared directly to the PBS with vancomycin and TXA treatment, the bacterial load of MF with vancomycin and TXA is significantly increased at 24 hours ($p < 0.0001$), but reduced at 48 hours ($p < 0.0001$) as determined by two-way ANOVA with Sidak's multiple comparisons (**Figure 39**).

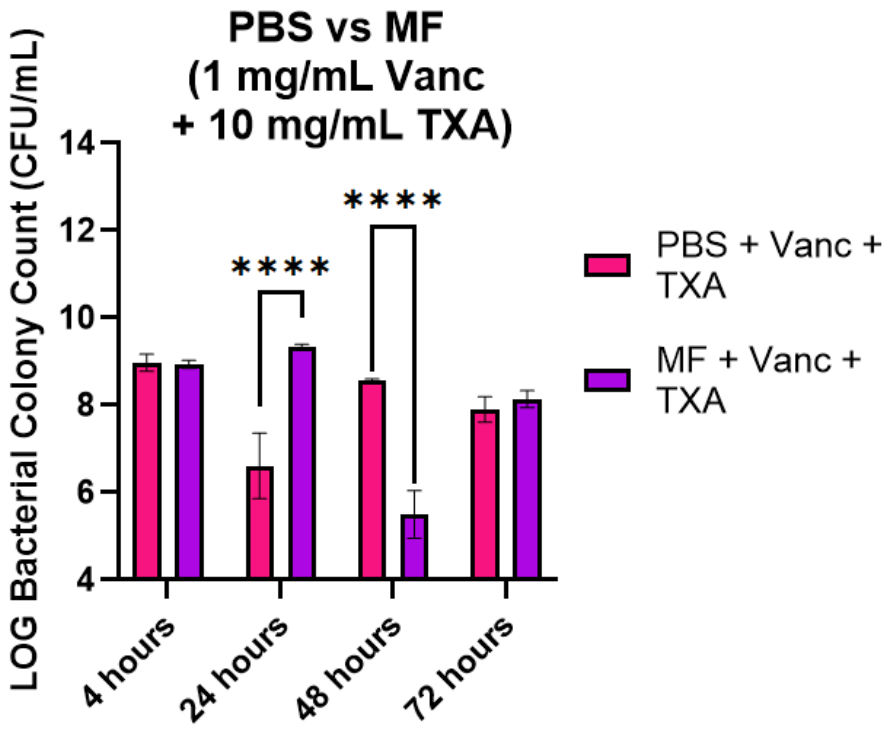

Figure 39: Observed MRSA bacterial load in tissue samples treated with 1 mg/mL vancomycin and 10 mg/mL TXA in PBS or MF over time. N = 1 biological replicate conducted in technical triplicate. Statistical significance was defined as $p \leq 0.05$ and determined with two-way ANOVA with Sidak's multiple comparisons. ($p < 0.0001$****).

These data indicate a comparable bacterial load at 4 and 72 hours but delayed therapeutic action in the MF when delivering combined vancomycin and TXA.

3.2.3 Effect of "Empty" MF

The base MF appeared to become a vehicle for increased bacterial growth at 48- and 72-hour time points, demonstrating a 3-4 log increase in MRSA colonies from the 24 hours treatment time (**Figure 40**).

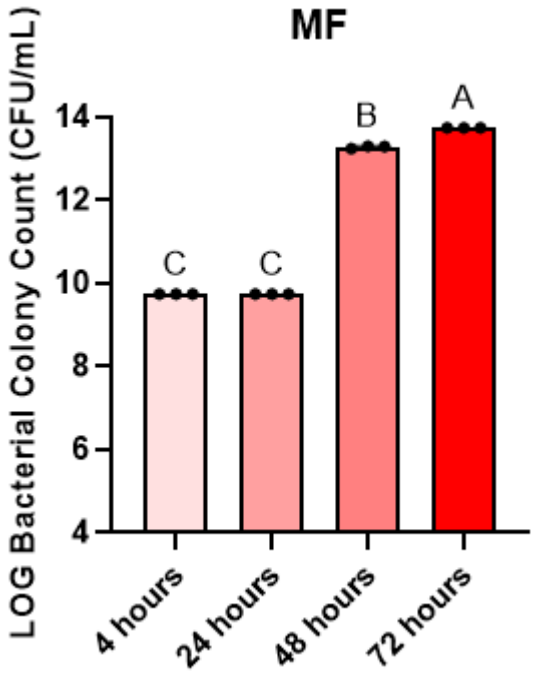

Figure 40: Observed MRSA bacterial load in tissue samples treated with "empty" MF over time. N = 1 biological replicate conducted in technical triplicate. Statistical significance was defined as $p \leq 0.05$ and determined with ordinary one-way ANOVA with Tukey's multiple comparisons. Columns with like letters are not statistically different.

Colony count in the MF increased significantly over time from 24 to 48 hours ($p < 0.0001$) and from 48 to 72 hours ($p < 0.0001$) as determined by ordinary one-way ANOVA with Tukey's multiple comparisons.

When compared directly to the PBS control treatment, MF demonstrated significantly increased bacterial load at 48 ($p < 0.0001$) and 72 ($p < 0.0001$) hour treatment times as determined by two-way ANOVA with Sidak's multiple comparisons (**Figure 41**).

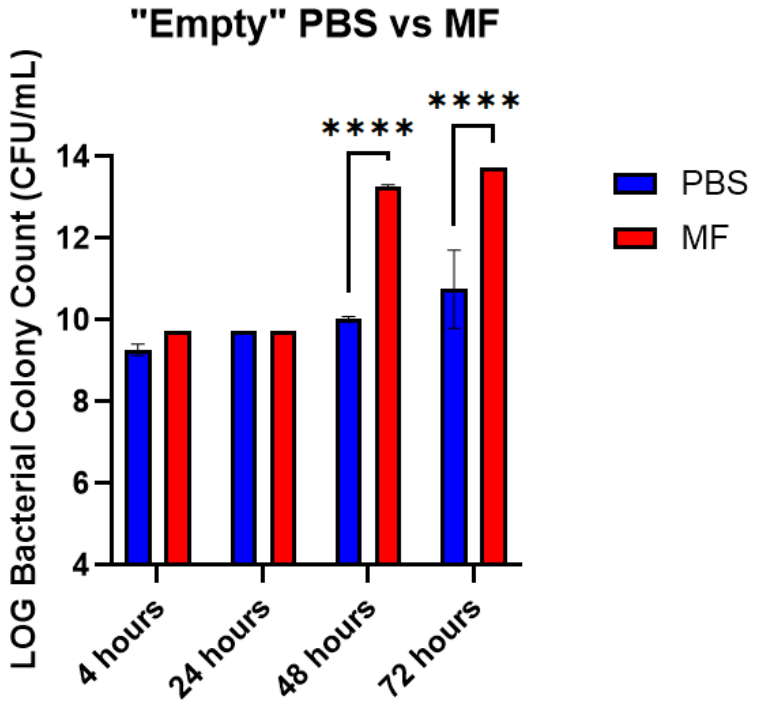

Figure 41: Observed MRSA bacterial load in tissue samples treated with "empty" MF or PBS over time. N = 1 biological replicate conducted in technical triplicate. Statistical significance was defined as $p \leq 0.05$ and determined with two-way ANOVA with Sidak's multiple comparisons. ($p < 0.0001$****).

3.2.4 Overall Treatment Comparisons

When all treatments were compared at each time point (one-way ANOVA, Tukey's multiple comparisons), the full range of bacterial killing efficacy was determined (**Figure 42**).

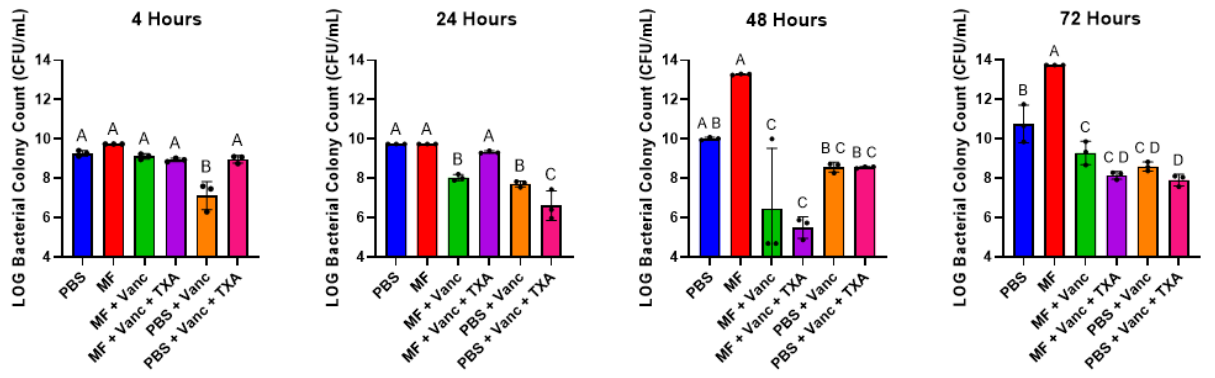

Figure 42: Observed bacterial load comparisons for PBS and MF treatments over time. Statistical significance was defined as $p \leq 0.05$ and determined using ordinary one-way ANOVAs with Tukey's multiple comparisons at each time point. N = 1 biological replicate conducted in technical triplicate. Columns that share letters are not significantly different. Letter comparisons do not expand outside of each time point.

At 4 hours, PBS with vancomycin was the only treatment to significantly reduce the bacterial load from the PBS control ($p = 0.0001$). All MF treatments were not significantly different from the PBS control ($p \geq 0.48$). At 24 hours, MF with vancomycin ($p = 0.0003$), PBS with vancomycin ($p < 0.0001$), and PBS with vancomycin and TXA ($p < 0.0001$) significantly reduced bacterial load compared to the PBS control. PBS with vancomycin and TXA demonstrated significantly more bacterial killing than MF with vancomycin (0.0016) and PBS with vancomycin (0.011). At 48 hours, MF with vancomycin and MF with vancomycin and TXA demonstrate significantly reduced bacterial load compared to the PBS control ($p = 0.045$ and $p = 0.009$, respectively). PBS with vancomycin and PBS with vancomycin and TXA are not significantly different to the PBS control at 48 hours ($p = 0.72$ and $p = 0.72$, respectively). At 72 hours, MF has significantly increased bacterial load compared to all other treatments ($p \leq 0.0001$).

4.0 Discussion

4.1 Pilot Study for MF Bacterial Killing Experimentation

When compared to an inoculated, untreated control, ovine tissue submerged in MF with 0.5 mg/mL vancomycin significantly reduced the MRSA bacterial load after 10 minutes of inoculation and 60 minutes of treatment. These preliminary data demonstrate that the MF is able to deliver vancomycin without altering the efficacy of the drug.

To directly compare MF to PBS delivery and because wound tissue would most likely not be fully submerged in topical antibiotic treatment, treatment application was changed from tissue submersion to tissue coating with the hypothesis that MF would better adhere to muscle tissue and thus provide superior vancomycin delivery.

To more accurately mimic typical bacterial exposure conditions, the experimental approach was extended to include 4-, 24-, 48-, and 72-hour treatment times with a safe (see Chapter 3), clinically relevant, increased vancomycin concentration (1 mg/mL) [45] and a 30-minute bacterial inoculation period. Treatments were also expanded to include combination vancomycin and TXA delivery and determine whether the antibacterial effect of MF would be promoted or inhibited.

S. aureus biofilm formation progresses through distinct stages, beginning with adhesion, followed by microcolony formation, and maturation into structured biofilms [173]. A 30-minute inoculation period mimics the early colonization phase of MRSA in acute wounds before the host immune response or external interventions would be anticipated to be initiated in prolonged treatment. The 10-minute inoculation performed in the pilot studies represents a quick time-to-treatment duration that is desired but often not attainable with traumatic injuries, especially in patients not in danger of immediate hemorrhage [174]. The 30-minute inoculation period

introduced MRSA in a viable planktonic or early adherent state before development into a mature biofilm, focusing this work on early contamination treatment with potential infection prevention.

Treatment times were expanded to determine the temporal efficacy of the MF in cases of extended application. This new range allowed for killing assessments before, during, and after infection strengthening and encompasses the likely range of time before advanced care is available in extreme cases [175].

4.2 Pivotal MF Bacterial Killing Experimentation

Under these revised experimental conditions, MF with vancomycin demonstrated significant MRSA bacterial killing compared to the PBS control at 24, 48, and 72 hours, supporting the hypothesis that MF can effectively deliver vancomycin without altering drug efficacy. Vancomycin was first reconstituted in 5 mL of PBS before integration into the MF. After the initial delay of vancomycin release (24 hours), MF treatments maintained effective treatment for 24 hours before bacterial colony counts begin to increase again. These data indicate that the MF has some protective capability over the vancomycin, both inhibiting initial release and still allowing for 24 hours of effective treatment. These interactions will need to be explored through further experimentation and characterization.

Based strictly on carrier viscosities alone, results of delayed vancomycin release with the MF make inherent sense and are supported by studies that have demonstrated this prolonged release through viscous carriers, thus enhancing therapeutic effectiveness over time [176, 177]. As expected, PBS treatments did not adhere to the tissue, but MF treatments did (see Chapter 2). This increased vancomycin presence during incubation is hypothesized to be responsible for the

extended efficacy due to increased contact time of the vancomycin as compared to the PBS groups, since vancomycin efficacy is known to be dependent on exposure time [45, 164].

The addition of TXA to the treatments did not significantly change the bacterial load compared to the vancomycin counterpart treatments for both PBS and MF except at 4 hours and 24 hours, respectively. Combination treatments of vancomycin and TXA have been shown to either have a synergistic effect against strains of bacteria including MRSA [150] or unaltered effects compared to individual vancomycin treatments [149]. These findings support the observed data trends for this study at 48 and 72 hours for both PBS and MF carriers, showing no statistical differences between combination treatments and vancomycin treatments. There is no available literature concerning the combination use of vancomycin, TXA, and CMC products, so further *in vitro/ex vivo* and *in vivo* experimentation will be necessary to fully comprehend the interactions of this complex, 3-component treatment.

Experimental results indicate that base MF without vancomycin does not have any inherent bacterial killing ability and significantly increases the bacterial load at chronic time points as demonstrated at 48 and 72 hours. This is neither contradictory not supportive to most literature on the use of CMC in healthcare, which rarely explore the antibacterial properties of CMC without other antibacterial or antimicrobial additives [35, 169, 178, 179]. One key difference between literature and this study is that the MF contains a non-crosslinked form of CMC rather than a true hydrogel or film formulation. In 2023, the FDA recalled a series of CMC-based eyedrops for bacterial contamination during production. This recall supports that once inoculated with bacteria, CMC alone does not have the ability to tame the infection and potentially amplifies the severity of the contamination [180]. However, these assays need to be rerun to confirm these results.

The diminished decrease in bacterial load with treatment over time (72 hours) is suspected to be related to the extended reconstitution time of the powdered agents in solution and continual bacterial replication overcoming initial treatment effects. As treatments begin to lose potency and contact time with the infected tissue, there is a high chance for bacterial recovery [181]. Delays or interruptions in therapy can allow bacterial populations to recover, especially if the initial treatment did not sufficiently reduce the bacterial load [182]. Moreover, the phenomenon of bacterial persistence, where a subset of bacteria survives antibiotic exposure, underscores the importance of maintaining effective drug concentrations. These cells can repopulate once antibiotic levels decrease, leading to infection recurrence [183].

4.3 Study Limitations

The assay will need to be rerun to confirm results and further explore the interactions of the combined vancomycin and TXA treatments. Study limitations include the use of only one biological ovine replicate and one representative MF formulation (1 mg/mL vancomycin with 10 mg/mL TXA). Alternate formulations time-kill curves need to be generated to fully characterize the temporal release and MRSA killing abilities of the medical foam *in vitro/ex vivo*.

5.0 Conclusion

MF containing vancomycin or vancomycin and TXA overall effectively reduced MRSA bacterial loads over 72 hours as compared to both positive inoculated controls and PBS counterpart treatments. Regardless of PBS or MF delivery, the least amount of bacteria were present at 24 and 48 hour time points, with the MF with vancomycin and MF with vancomycin and TXA performing the best at 48 hours. PBS with vancomycin performed the best at 4 and 24 hours, and PBS with vancomycin and TXA performed the best at 24 hours. The base MF without vancomycin or TXA significantly increased the bacterial load compared to the positive control at

48 hours, in stark contrast with the sharply reduced killing of the MF with vancomycin and MF with vancomycin and TXA. Thus, for this study and the chosen experimental parameters, MF treatments should be reapplied at 48 hours and PBS treatments should be reapplied at 24 hours.

Chapter 6: Conclusion

1.0 Summary of Work

This work details the material development, characterization, and safety and efficacy of a multifunctional Medical Foam (MF) for enhanced open wound care. To these ends, physical characteristics, toxicity profile, and antifibrinolytic/hemostatic and antibiotic properties of carboxymethyl cellulose-based MF containing tranexamic acid and vancomycin were characterized in *vitro/ex vivo*.

Chapter 2 detailed the investigation of the physical and mechanical properties of the MF with and without the chosen therapeutics, including temporal stability, volumetric expansion, 3D volume-filling and coating ability, breakdown kinetics, and rheology. Once the working limits and properties of the MF were defined, Chapter 3 moved on to explore the *in vitro* safety of the MF with and without the chosen therapeutics by evaluating fibroblast dose-response viability curves. Once the MF *in vitro* safety was categorized, Chapters 4 and 5 explored the *in vitro* efficacy of the chosen therapeutics on ovine samples.

MF demonstrated safe, effective delivery of tranexamic acid and vancomycin therapeutics in the outlined benchtop studies, indicating the potential for successful implementation in animal or human models.

2.0 Future Work

The results reported within this thesis work demonstrate proof-of-concept for development, characterization, and *in vitro/ex vivo* safety and efficacy of the multifunctional MF described herein. These efforts were instrumental in securing funding for *in vivo* murine and canine bleeding and infection wound studies. Future work will investigate these *in vivo* effects of the

MF as well as develop a range of formulations to incorporate additional or alternate therapeutics for expanded use ranging from backyard scrapes to battlefield scars.

References

1. Rossiter, N.D., *"Trauma-the forgotten pandemic?".* Int Orthop, 2022. **46**(1): p. 3-11.
2. Trauma, T.A.A.F.T.S.O. *Trauma Facts*. [cited 2025 March 14]; Available from: https://www.aast.org/resources/trauma-facts.
3. Scrushy, M., N. Lunardi, and J.V. Sakran, *Trauma Demographics and Injury Prevention.* Surg Clin North Am, 2024. **104**(2): p. 243-254.
4. Dumovich, J. and P. Singh, *Physiology, Trauma*, in *StatPearls*. 2025: Treasure Island (FL).
5. Lotfollahzadeh, S. and B. Burns, *Penetrating Abdominal Trauma*, in *StatPearls*. 2025: Treasure Island (FL).
6. D'Souza, E.W., et al., *Combat injury profiles among U.S. military personnel who survived serious wounds in Iraq and Afghanistan: A latent class analysis.* PLoS One, 2022. **17**(4): p. e0266588.
7. Harrington, B.M., et al., *Complications, outcomes, and management strategies of non-missile penetrating head injuries.* J Neurosurg, 2021. **134**(5): p. 1658-1666.
8. Huber, G.H. and B. Manna, *Vascular Extremity Trauma*, in *StatPearls*. 2025: Treasure Island (FL).
9. Whitehorne, M., R. Cacciola, and M.E. Quinn, *Multiple trauma: survival after the Golden Hour.* J Adv Med Surg Nurs, 1989. **2**(1): p. 27-9.
10. Kotwal, R.S., et al., *The Effect of a Golden Hour Policy on the Morbidity and Mortality of Combat Casualties.* JAMA Surg, 2016. **151**(1): p. 15-24.
11. Ma, X.Y., L.X. Tian, and H.P. Liang, *Early prevention of trauma-related infection/sepsis.* Mil Med Res, 2016. **3**: p. 33.
12. Gosselin, A.R., et al., *Hyperfibrinolysis drives mechanical instabilities in a simulated model of trauma induced coagulopathy.* Thromb Res, 2022. **220**: p. 131-140.
13. Moore, E.E., et al., *Author Correction: Trauma-induced coagulopathy.* Nat Rev Dis Primers, 2022. **8**(1): p. 25.
14. Nystrup, K.B., et al., *Reduced clot strength upon admission, evaluated by thrombelastography (TEG), in trauma patients is independently associated with increased 30-day mortality.* Scand J Trauma Resusc Emerg Med, 2011. **19**: p. 52.
15. Carroll, R.C., et al., *Early evaluation of acute traumatic coagulopathy by thrombelastography.* Transl Res, 2009. **154**(1): p. 34-9.
16. Petersen, K. and P. Waterman, *Prophylaxis and treatment of infections associated with penetrating traumatic injury.* Expert Rev Anti Infect Ther, 2011. **9**(1): p. 81-96.
17. Ding, X., et al., *Challenges and innovations in treating chronic and acute wound infections: from basic science to clinical practice.* Burns Trauma, 2022. **10**: p. tkac014.
18. Fleischmann-Struzek, C. and K. Rudd, *Challenges of assessing the burden of sepsis.* Med Klin Intensivmed Notfmed, 2023. **118**(Suppl 2): p. 68-74.
19. Schauer, S.G., et al., *A Conceptual Framework for Non-Military Investigators to Understand the Joint Roles of Medical Care in the Setting of Future Large Scale Combat Operations.* Prehosp Emerg Care, 2023. **27**(1): p. 67-74.
20. Handbook, N.L. *Medical Support - Role Support*. 1997 [cited 2025 March 14]; Available from: https://www.nato.int/docu/logi-en/1997/lo-1610.htm.

21. Trauma, J.T.S.-T.D.o.D.C.o.E.f. *Acute Traumatic Wound Management in the Prolonged Field Care Setting*. 2017 March 14, 2025; Available from: https://jts.health.mil/assets/docs/cpgs/Wound_Management_PFC_24_Jul_2017_ID62.pdf .
22. Trauma, J.T.S.-T.D.o.D.C.o.E.f. *Infection Prevention in Combat-Related Injuries*. 2021; Available from: https://jts.health.mil/assets/docs/cpgs/Infection_Prevention_in_Combat-related_Injuries_27_Jan_2021_ID24.pdf.
23. Cizman, M. and T. Plankar Srovin, *Antibiotic consumption and resistance of gram-negative pathogens (collateral damage).* GMS Infect Dis, 2018. **6**: p. Doc05.
24. Thim, T., et al., *Initial assessment and treatment with the Airway, Breathing, Circulation, Disability, Exposure (ABCDE) approach.* Int J Gen Med, 2012. **5**: p. 117-21.
25. Xu, Q., et al., *Monitoring the topical delivery of ultrasmall gold nanoparticles using optical coherence tomography.* Skin Res Technol, 2020. **26**(2): p. 263-268.
26. Simon, L., et al., *Recent advances and prospects in nano drug delivery systems using lipopolyoxazolines.* Int J Pharm, 2020. **585**: p. 119536.
27. Fan, D.Y., Y. Tian, and Z.J. Liu, *Injectable Hydrogels for Localized Cancer Therapy.* Front Chem, 2019. **7**: p. 675.
28. Rahman, M.S., et al., *Recent Developments of Carboxymethyl Cellulose.* Polymers (Basel), 2021. **13**(8).
29. Liao, W., et al., *Multifunctional nanogel based on carboxymethyl cellulose interfering with cellular redox homeostasis enhances phycocyanobilin photodynamic therapy.* Carbohydr Polym, 2024. **323**: p. 121416.
30. Priya, G., et al., *In Vitro and In Vivo Evaluation of Carboxymethyl Cellulose Scaffolds for Bone Tissue Engineering Applications.* ACS Omega, 2021. **6**(2): p. 1246-1253.
31. Yalcintas, E.P., et al., *Analysis of In Vitro Cytotoxicity of Carbohydrate-Based Materials Used for Dissolvable Microneedle Arrays.* Pharm Res, 2020. **37**(3): p. 33.
32. Zhang, H., et al., *Effects of Chitosan and Cellulose Derivatives on Sodium Carboxymethyl Cellulose-Based Films: A Study of Rheological Properties of Film-Forming Solutions.* Molecules, 2023. **28**(13).
33. Bohorquez-Moreno, C.D., et al., *Plant-inspired adhesive and injectable natural hydrogels: in vitro and in vivo studies.* Biotechnol Lett, 2023. **45**(9): p. 1209-1222.
34. Chen, Y., et al., *Mussel-inspired self-healing hydrogel form pectin and cellulose for hemostasis and diabetic wound repairing.* Int J Biol Macromol, 2023. **246**: p. 125644.
35. Al-Tarawneh, W.A., et al., *Synthesis of Cellulose-Based Hydrogel-Nanocomposites for Medical Applications.* Polymers (Basel), 2024. **16**(15).
36. Thewanjutiwong, S., et al., *Development of Film-Forming Gel Formulations Containing Royal Jelly and Honey Aromatic Water for Cosmetic Applications.* Gels, 2023. **9**(10).
37. Nho, Y.C., J.S. Park, and Y.M. Lim, *Preparation of hydrogel by radiation for the healing of diabetic ulcer.* Radiation Physics and Chemistry, 2014. **94**: p. 176-180.
38. Chauncey, J.M. and J.S. Wieters, *Tranexamic Acid*, in *StatPearls*. 2025: Treasure Island (FL).
39. Mitha, R., et al., *Topical tranexamic acid (TXA) is non-inferior to intravenous TXA in adult spine surgery: a meta-analysis.* Neurosurgical Review, 2024. **47**(1).
40. Gkiatas, I., et al., *Topical use of tranexamic acid: Are there concerns for cytotoxicity?* World J Orthop, 2022. **13**(6): p. 555-563.

41. Reuben, A., et al., *The Use of Tranexamic Acid to Reduce the Need for Nasal Packing in Epistaxis (NoPAC): Randomized Controlled Trial.* Ann Emerg Med, 2021. **77**(6): p. 631-640.
42. Ausen, K., et al., *Randomized clinical trial of topical tranexamic acid after reduction mammoplasty.* Br J Surg, 2015. **102**(11): p. 1348-53.
43. Kim, J.K., et al., *Optimal dose of topical tranexamic acid considering efficacy and safety in total knee arthroplasty: a randomized controlled study.* Knee Surg Sports Traumatol Arthrosc, 2021. **29**(10): p. 3409-3417.
44. Lavery, L.A., et al., *Bacterial pathogens in infected puncture wounds in adults with diabetes.* J Foot Ankle Surg, 1994. **33**(1): p. 91-7.
45. Patel, S., C.V. Preuss, and F. Bernice, *Vancomycin*, in *StatPearls*. 2025: Treasure Island (FL).
46. Cancienne, J.M., et al., *Applications of Local Antibiotics in Orthopedic Trauma.* Orthop Clin North Am, 2015. **46**(4): p. 495-510.
47. Ostermann, P.A., D. Seligson, and S.L. Henry, *Local antibiotic therapy for severe open fractures. A review of 1085 consecutive cases.* J Bone Joint Surg Br, 1995. **77**(1): p. 93-7.
48. Metsemakers, W.J., et al., *Infection after fracture fixation: Current surgical and microbiological concepts.* Injury, 2018. **49**(3): p. 511-522.
49. Wei, J., H. Gu, and K. Tong, *Intra-wound versus systemic vancomycin for preventing surgical site infection induced by methicillin-resistant S. aureus after spinal implant surgery in a rat model.* J Orthop Surg Res, 2023. **18**(1): p. 299.
50. Joshi, M., et al., *Does Topical Vancomycin Powder Use in Fracture Surgery Change Bacteriology and Antibiotic Susceptibilities? An Analysis of the VANCO Trial.* J Orthop Trauma, 2024. **38**(4): p. 183-189.
51. Patterson, J.T., et al., *The VANCO Trial Findings Are Generalizable to a North American Trauma Registry.* J Orthop Trauma, 2024. **38**(1): p. 10-17.
52. Schar, R.T. and S. Zimmerli, *VANCO Trial-Preliminary Results on the Safety Profile of Intrawound Vancomycin Powder in Complex Spine Surgery.* World Neurosurg, 2022. **162**: p. 7-8.
53. Wilcox, M., et al., *Reporting elevated vancomycin minimum inhibitory concentration in methicillin-resistant Staphylococcus aureus: consensus by an International Working Group.* Future Microbiol, 2019. **14**(4): p. 345-352.
54. Moses, V.K., V. Kandi, and S.K.D. Rao, *Minimum Inhibitory Concentrations of Vancomycin and Daptomycin Against Methicillin-resistant Staphylococcus Aureus Isolated from Various Clinical Specimens: A Study from South India.* Cureus, 2020. **12**(1): p. e6749.
55. Saint-Jalmes, A., *Physical chemistry in foam drainage and coarsening.* Soft Matter, 2006. **2**(10): p. 836-849.
56. Guidolin, C., et al., *Viscoelastic coarsening of quasi-2D foam.* Nat Commun, 2023. **14**(1): p. 1125.
57. Safouane, M., et al., *Viscosity effects in foam drainage: Newtonian and non-newtonian foaming fluids.* Eur Phys J E Soft Matter, 2006. **19**(2): p. 195-202.
58. Maurdev, G., A. Saint-Jalmes, and D. Langevin, *Bubble motion measurements during foam drainage and coarsening.* J Colloid Interface Sci, 2006. **300**(2): p. 735-43.

59. Krom, J., K. Meister, and T.A. Vilgis, *Simple Method to Assess Foam Structure and Stability using Hydrophobin and BSA as Model Systems.* Chemphyschem, 2024. **25**(15): p. e202400050.
60. Onffroy, P.R., et al., *Polylactic Acid Chemical Foaming Assisted by Solid-State Processing: Solid-State Shear Pulverization and Cryogenic Milling.* Polymers (Basel), 2022. **14**(21).
61. Li, Y., et al., *Comparative Study of the Foaming Behavior of Ethylene-Vinyl Acetate Copolymer Foams Fabricated Using Chemical and Physical Foaming Processes.* Materials (Basel), 2024. **17**(15).
62. Kaminska, K., et al., *The Effect of a Chemical Foaming Agent and the Isocyanate Index on the Properties of Open-Cell Polyurethane Foams.* Materials (Basel), 2022. **15**(17).
63. Jia, H., et al., *Thermal Insulation Properties and Simulation Analysis of Foam Concrete Regulated by Mechanical and Chemical Foaming.* ACS Omega, 2023. **8**(50): p. 48091-48103.
64. Damanpack, A.R., A. Sousa, and M. Bodaghi, *Porous PLAs with Controllable Density by FDM 3D Printing and Chemical Foaming Agent.* Micromachines (Basel), 2021. **12**(8).
65. Sitarz, M., et al., *Foaming and Physico-Mechanical Properties of Geopolymer Pastes Manufactured from Post-Metallurgical Recycled Slag.* Materials (Basel), 2024. **17**(6).
66. Liu, J., et al., *Preparation of microgel particles from egg yolk components by combining phospholipase A(2) with high-pressure homogenization: Physicochemical, structural properties and their effects on foaming, processing stability of egg white protein.* Int J Biol Macromol, 2024. **278**(Pt 2): p. 134833.
67. Fanovich, M.A., E. Di Maio, and A. Salerno, *Current Trend and New Opportunities for Multifunctional Bio-Scaffold Fabrication via High-Pressure Foaming.* J Funct Biomater, 2023. **14**(9).
68. Agustion, Y.H., et al., *High-Quality Foaming and Weight Reduction in Microcellular-Injection-Molded Polycarbonate Using Supercritical Fluid Carbon Dioxide under Gas Counter Pressure.* Polymers (Basel), 2024. **16**(18).
69. Yoo, Y.J. and J. Hong, *Bubble entrainment aeration for high-foaming fermentation.* Biotechnol Bioeng, 1986. **28**(5): p. 756-60.
70. Ohkawa, A., et al., *Mechanical control of foaming in a bubble column.* Biotechnol Bioeng, 1984. **26**(7): p. 702-13.
71. Tong, M. and S.J. Neethling, *The size of films in dry foams.* J Phys Condens Matter, 2010. **22**(15): p. 155109.
72. Stevenson, P., et al., *Measurement of bubble size distribution in a gas-liquid foam using pulsed-field gradient nuclear magnetic resonance.* J Colloid Interface Sci, 2010. **352**(1): p. 114-20.
73. Kraynik, A.M., D.A. Reinelt, and F. van Swol, *Structure of random foam.* Phys Rev Lett, 2004. **93**(20): p. 208301.
74. Schmideder, S., et al., *Inline imaging reveals evolution of the size distribution and the concentration of microbubbles in dissolved air flotation.* Water Res, 2022. **224**: p. 119027.
75. Pugh, R.J., *Experimental techniques for studying the structure of foams and froths.* Adv Colloid Interface Sci, 2005. **114-115**: p. 239-51.
76. Sangnim, T., et al., *Swallowing Gel for Patients with Dysphagia: A Novel Application of Chitosan.* Gels, 2021. **7**(3).

77. Zhang, W., et al., *Influence of Carboxymethyl Cellulose on the Stability, Rheological Property, and in-vitro Digestion of Soy Protein Isolate (SPI)-Stabilized Rice Bran Oil Emulsion.* Front Nutr, 2022. **9**: p. 878725.
78. Sabri, L.A., A.H. Khasraghi, and H.T. Sulaiman, *Preparation and evaluation of oral soft chewable jelly containing flurbiprofen.* J Adv Pharm Technol Res, 2022. **13**(4): p. 306-311.
79. Salehi, F., M. Inanloodoghouz, and M. Karami, *Rheological properties of carboxymethyl cellulose (CMC) solution: Impact of high intensity ultrasound.* Ultrason Sonochem, 2023. **101**: p. 106655.
80. Karmakar, R., et al., *Enhanced wound healing properties by sodium alginate-carboxymethyl cellulose hydrogel enriched with decellularized amniotic membrane.* Eur J Pharm Biopharm, 2025. **207**: p. 114621.
81. Xu, Y., et al., *Effect of carboxymethyl cellulose and/or wheat gluten on the pasting, rheological and quality properties of wheat starch-based batter for deep-fried products.* Food Chem X, 2025. **26**: p. 102262.
82. Pawar, P.K., R.D. Rathod, and S.R. Jagadale, *A review on topical ophthalmic drug delivery system: Reference to viscosity enhancer.* Polim Med, 2024. **54**(1): p. 71-84.
83. Cholakova, D., et al., *Hydroxypropyl Cellulose Polymers as Efficient Emulsion Stabilizers: The Effect of Molecular Weight and Overlap Concentration.* Gels, 2025. **11**(2).
84. Sayko, R., M. Jacobs, and A.V. Dobrynin, *Quantifying Properties of Polysaccharide Solutions.* ACS Polym Au, 2021. **1**(3): p. 196-205.
85. Ilyin, S.O., *Structural Rheology in the Development and Study of Complex Polymer Materials.* Polymers (Basel), 2024. **16**(17).
86. Cilindre, C., et al., *Foaming properties of various Champagne wines depending on several parameters: grape variety, aging, protein and CO2 content.* Anal Chim Acta, 2010. **660**(1-2): p. 164-70.
87. Etoc, A., et al., *Foam control in fermentation bioprocess: from simple aeration tests to bioreactor.* Appl Biochem Biotechnol, 2006. **129-132**: p. 392-404.
88. Noble, M., et al., *Protein recovery using gas-liquid dispersions.* J Chromatogr B Biomed Sci Appl, 1998. **711**(1-2): p. 31-43.
89. Ratusznei, S.M., et al., *Influence of agitation rate on the performance of a stirred anaerobic sequencing batch reactor containing immobilized biomass.* Water Sci Technol, 2001. **44**(4): p. 305-12.
90. Nasir, M.S., A.R.M. Yahya, and N.A.M. Noh, *Utilization of palm sludge oil for rhamnolipid biosynthesis by Pseudomonas aeruginosa USM-AR2 in a stirred tank reactor.* Bioprocess Biosyst Eng, 2025. **48**(2): p. 221-232.
91. Zolghadr, A., et al., *Study of the Viscosity and Thermal Characteristics of Polyolefins/Solvent Mixtures: Applications for Plastic Pyrolysis.* ACS Omega, 2021. **6**(48): p. 32832-32840.
92. Mine, T., et al., *Effects of temperature alteration on viscosity, polymerization, and in-vivo arterial distribution of N-butyl cyanoacrylate-iodized oil mixtures.* Jpn J Radiol, 2021. **39**(11): p. 1111-1118.
93. Ibar, J.P., *The Challenges Facing the Current Paradigm Describing Viscoelastic Interactions in Polymer Melts.* Polymers (Basel), 2023. **15**(21).

94. Morey, M.D., N.S. Deshpande, and M. Barigou, *Foam Destabilization by Mechanical and Ultrasonic Vibrations.* J Colloid Interface Sci, 1999. **219**(1): p. 90-98.
95. Li, S., et al., *Analysis of Flow Field Characteristics in a Mechanical Defoaming Device.* ACS Omega, 2024. **9**(42): p. 42850-42857.
96. Dorlac, G.R., et al., *Air transport of patients with severe lung injury: development and utilization of the Acute Lung Rescue Team.* J Trauma, 2009. **66**(4 Suppl): p. S164-71.
97. Maddry, J.K., et al., *Management of Combat Casualties during Aeromedical Evacuation from a Role 2 to a Role 3 Medical Facility.* Mil Med, 2024. **189**(5-6): p. e1003-e1008.
98. Langevin, D., *Recent Advances on Emulsion and Foam Stability.* Langmuir, 2023. **39**(11): p. 3821-3828.
99. Langevin, D., *On the different coalescence mechanisms in foams and in emulsions.* Adv Colloid Interface Sci, 2025. **340**: p. 103448.
100. Dehdari, B., et al., *Dimensionless analysis of foam stability for application in enhanced oil recovery.* Sci Rep, 2024. **14**(1): p. 29842.
101. Yegorov, A., et al., *Influence of Parameters Used to Prepare Sterile Solutions of Poloxamer 188 on Their Physicochemical Properties.* Polymers (Basel), 2024. **17**(1).
102. Galvani, N., et al., *Hierarchical bubble size distributions in coarsening wet liquid foams.* Proc Natl Acad Sci U S A, 2023. **120**(38): p. e2306551120.
103. Sheng, Y., et al., *Rheological Properties of Gel Foam Co-Stabilized with Nanoparticles, Xanthan Gum, and Multiple Surfactants.* Gels, 2023. **9**(7).
104. Gupta, S.K., A.P. Deshpande, and R. Kumar, *Rheological and dielectric behavior of sodium carboxymethyl cellulose (NaCMC)/Ca(2+) and esterified NaCMC/Ca(2+) hydrogels: Correlating microstructure and dynamics with properties.* Carbohydr Polym, 2024. **335**: p. 122049.
105. Martinez-Padilla, L.P., *Rheology of liquid foods under shear flow conditions: Recently used models.* J Texture Stud, 2023.
106. Vazquez-Quesada, A., R.I. Tanner, and M. Ellero, *Shear Thinning of Noncolloidal Suspensions.* Phys Rev Lett, 2016. **117**(10): p. 108001.
107. Wang, J., et al., *Strong and thermally insulating polylactic acid/glass fiber composite foam fabricated by supercritical carbon dioxide foaming.* Int J Biol Macromol, 2019. **138**: p. 144-155.
108. Simoes, A., et al., *Rheology by Design: A Regulatory Tutorial for Analytical Method Validation.* Pharmaceutics, 2020. **12**(9).
109. Rosa, V., et al., *Guidance on the assessment of biocompatibility of biomaterials: Fundamentals and testing considerations.* Dent Mater, 2024. **40**(11): p. 1773-1785.
110. Li, W., J. Zhou, and Y. Xu, *Study of the in vitro cytotoxicity testing of medical devices.* Biomed Rep, 2015. **3**(5): p. 617-620.
111. Soothill, J.S., R. Ward, and A.J. Girling, *The IC50: an exactly defined measure of antibiotic sensitivity.* J Antimicrob Chemother, 1992. **29**(2): p. 137-9.
112. Zhang, M., et al., *Measuring cytotoxicity: a new perspective on LC50.* Anticancer Res, 2007. **27**(1A): p. 35-8.
113. ISO, *Biological Evaluation of Medical Devices - Tests for In Vitro Cytotoxicity*. 2009, ISO.
114. Pezzanite, L., et al., *Use of in vitro assays to identify antibiotics that are cytotoxic to normal equine chondrocytes and synovial cells.* Equine Veterinary Journal, 2021. **53**(3): p. 579-589.

115. Hall, S., et al., *In Vitro Evaluation of Vancomycin-Induced Toxicity in Human Primary Knee Chondrocytes.* Int J Toxicol, 2024. **43**(2): p. 177-183.
116. Wang, F., et al., *Cytotoxicity and Effect of Topical Application of Tranexamic Acid on Human Fibroblast in Spine Surgery.* World Neurosurg, 2021. **153**: p. e380-e391.
117. Liu, J.X., et al., *Topical vancomycin and its effect on survival and migration of osteoblasts, fibroblasts, and myoblasts: An in vitro study.* J Orthop, 2018. **15**(1): p. 53-58.
118. Damour, O., et al., *Cytotoxicity evaluation of antiseptics and antibiotics on cultured human fibroblasts and keratinocytes.* Burns, 1992. **18**(6): p. 479-85.
119. Howland, R.H., *Off-label medication use.* J Psychosoc Nurs Ment Health Serv, 2012. **50**(9): p. 11-3.
120. Perry, S.W., L.G. Epstein, and H.A. Gelbard, *In situ trypan blue staining of monolayer cell cultures for permanent fixation and mounting.* Biotechniques, 1997. **22**(6): p. 1020-1, 1024.
121. Tracy, L.E., R.A. Minasian, and E.J. Caterson, *Extracellular Matrix and Dermal Fibroblast Function in the Healing Wound.* Adv Wound Care (New Rochelle), 2016. **5**(3): p. 119-136.
122. Wagenbrenner, M., et al., *Does Combined Treatment with Tranexamic Acid and Vancomycin Affect Human Chondrocytes In Vitro?* Pharmaceuticals (Basel), 2024. **17**(12).
123. Benjumea, A., et al., *Validation of the antibacterial effect of topically applied tranexamic acid using in vitro and in vivo models.* Front Microbiol, 2024. **15**: p. 1367884.
124. Zhang, X., et al., *Poloxamer 407 modified collagen/beta-tricalcium phosphate scaffold for localized delivery of alendronate.* J Biomater Appl, 2024. **39**(3): p. 179-194.
125. Papalia, R., et al., *Does Vancomycin Wrapping in Anterior Cruciate Ligament Reconstruction Affect Tenocyte Activity In Vitro?* Antibiotics (Basel), 2021. **10**(9).
126. Latif, R.K., et al., *Traumatic hemorrhage and chain of survival.* Scand J Trauma Resusc Emerg Med, 2023. **31**(1): p. 25.
127. Mabry, R.L. and R. DeLorenzo, *Challenges to improving combat casualty survival on the battlefield.* Mil Med, 2014. **179**(5): p. 477-82.
128. Kotwal, R.S., et al., *United States Special Operations Command fatality study of subcommands, units, and trends.* J Trauma Acute Care Surg, 2020. **89**(2S Suppl 2): p. S213-S224.
129. Williamson, K., R. Ramesh, and A. Grabinsky, *Advances in prehospital trauma care.* Int J Crit Illn Inj Sci, 2011. **1**(1): p. 44-50.
130. Puryear, B., J. Roarty, and C. Knight, *EMS Tactical Combat Casualty Care*, in *StatPearls*. 2025: Treasure Island (FL).
131. Petros, S., *Trauma-Induced Coagulopathy.* Hamostaseologie, 2019. **39**(1): p. 20-27.
132. Katrancha, E.D. and L.S. Gonzalez, 3rd, *Trauma-induced coagulopathy.* Crit Care Nurse, 2014. **34**(4): p. 54-63.
133. Hanke, A.A. and N. Rahe-Meyer, *[Trauma-induced coagulopathy].* Unfallchirurg, 2014. **117**(2): p. 95-8.
134. Roberts, I., et al., *The CRASH-2 trial: a randomised controlled trial and economic evaluation of the effects of tranexamic acid on death, vascular occlusive events and transfusion requirement in bleeding trauma patients.* Health Technol Assess, 2013. **17**(10): p. 1-79.

135. Care, T.C.C. *Tactical Combat Casualty Care Quick Reference Guide*. 2017 [cited 2025 March 16]; Available from: https://emsa.ca.gov/wp-content/uploads/sites/71/2017/07/TCCC_Quick_Reference_Guide_2017.pdf.
136. Care, T.C.C. *Tactical Combat Casualty Care Course - Module 6: Massive Hemorrhage Control*. [cited 2025 March 16]; Available from: https://tccc.org.ua/files/downloads/module-06-massive-hemorrhage-control-in-tfc.pdf.
137. Prasad, S., et al., *Development of an in vitro model to study clot lysis activity of thrombolytic drugs.* Thromb J, 2006. **4**: p. 14.
138. Windberger, U. and J. Lauger, *Blood Clot Phenotyping by Rheometry: Platelets and Fibrinogen Chemistry Affect Stress-Softening and -Stiffening at Large Oscillation Amplitude.* Molecules, 2020. **25**(17).
139. Volod, O., et al., *Viscoelastic Hemostatic Assays: A Primer on Legacy and New Generation Devices.* J Clin Med, 2022. **11**(3).
140. Yeh, H.H., et al., *Rheological and clot microstructure evaluation of heparin neutralization by UHRA and protamine.* J Mech Behav Biomed Mater, 2021. **124**: p. 104851.
141. Reddy, K.N. and G. Markus, *Mechanism of activation of human plasminogen by streptokinase. Presence of active center in streptokinase-plasminogen complex.* J Biol Chem, 1972. **247**(6): p. 1683-91.
142. Weisel, J.W., *Biophysics. Enigmas of blood clot elasticity.* Science, 2008. **320**(5875): p. 456-7.
143. Siller-Matula, J.M., et al., *Interspecies differences in coagulation profile.* Thromb Haemost, 2008. **100**(3): p. 397-404.
144. Boyer, M.H., J.R. Shainoff, and O.D. Ratnoff, *Acceleration of fibrin polymerization by calcium ions.* Blood, 1972. **39**(3): p. 382-7.
145. Xi, C., et al., *Experimental Evaluation of Tranexamic Acid-Loaded Porous Starch as a Hemostatic Powder.* Clin Appl Thromb Hemost, 2018. **24**(2): p. 279-286.
146. Wakasa, J., et al., *Perioperative bleeding control in total hip arthroplasty: hemostatic powder vs. tranexamic acid-a prospective randomized controlled trial.* Arch Orthop Trauma Surg, 2024. **144**(8): p. 3797-3805.
147. Ran, Y., et al., *QuikClot Combat Gauze use for hemorrhage control in military trauma: January 2009 Israel Defense Force experience in the Gaza Strip--a preliminary report of 14 cases.* Prehosp Disaster Med, 2010. **25**(6): p. 584-8.
148. Guilbeau, A. and R. Majumder, *Systemic Review of Clot Retraction Modulators.* Int J Mol Sci, 2023. **24**(13).
149. Schwerdt, C., et al., *The bactericidal effect of vancomycin is not altered by tranexamic acid, adrenalin, dexamethasone, or lidocaine in vitro.* Sci Rep, 2021. **11**(1): p. 10739.
150. Benjumea, A., et al., *Tranexamic Acid in Combination With Vancomycin or Gentamicin Has a Synergistic Effect Against Staphylococci.* Front Microbiol, 2022. **13**: p. 935646.
151. Wikkelso, A., et al., *Thromboelastography (TEG) or rotational thromboelastometry (ROTEM) to monitor haemostatic treatment in bleeding patients: a systematic review with meta-analysis and trial sequential analysis.* Anaesthesia, 2017. **72**(4): p. 519-531.
152. Hunt, H., et al., *Thromboelastography (TEG) and rotational thromboelastometry (ROTEM) for trauma induced coagulopathy in adult trauma patients with bleeding.* Cochrane Database Syst Rev, 2015. **2015**(2): p. CD010438.

153. Kanikireddy, V., et al., *Carboxymethyl cellulose-based materials for infection control and wound healing: A review.* Int J Biol Macromol, 2020. **164**: p. 963-975.
154. Zhang, W., et al., *Synthesis and Applications of Carboxymethyl Cellulose Hydrogels.* Gels, 2022. **8**(9).
155. Klarhofer, M., et al., *High-resolution blood flow velocity measurements in the human finger.* Magn Reson Med, 2001. **45**(4): p. 716-9.
156. Hooper, N. and T.J. Armstrong, *Hemorrhagic Shock*, in *StatPearls*. 2025: Treasure Island (FL).
157. Kurtz, S.M., et al., *Are We Winning or Losing the Battle With Periprosthetic Joint Infection: Trends in Periprosthetic Joint Infection and Mortality Risk for the Medicare Population.* J Arthroplasty, 2018. **33**(10): p. 3238-3245.
158. Saeed, O., et al., *Infection Prevention in Combat-Related Injuries.* Mil Med, 2018. **183**(suppl_2): p. 137-141.
159. Keenan, S. and J.C. Riesberg, *Prolonged Field Care: Beyond the "Golden Hour".* Wilderness Environ Med, 2017. **28**(2S): p. S135-S139.
160. Habboush, Y. and N. Guzman, *Antibiotic Resistance*, in *StatPearls*. 2025: Treasure Island (FL).
161. Siddiqui, A.H. and J. Koirala, *Methicillin-Resistant Staphylococcus aureus*, in *StatPearls*. 2025: Treasure Island (FL).
162. Hou, Z., et al., *Progress in the Prevalence, Classification and Drug Resistance Mechanisms of Methicillin-Resistant Staphylococcus aureus.* Infect Drug Resist, 2023. **16**: p. 3271-3292.
163. Tribble, D.R., et al., *After the Battlefield: Infectious Complications among Wounded Warriors in the Trauma Infectious Disease Outcomes Study.* Mil Med, 2019. **184**(Suppl 2): p. 18-25.
164. Cunha, B.A., *Vancomycin revisited: a reappraisal of clinical use.* Crit Care Clin, 2008. **24**(2): p. 393-420, x-xi.
165. Sinkler, M.A., et al., *Complications and Outcomes After Fixation of Lisfranc Injuries at an Urban Level 1 Trauma Center.* J Orthop Trauma, 2024. **38**(5): p. e169-e174.
166. Awad, M.E., et al., *Prophylactic Intrawound Antibiotics Significantly Reduce the Risk of Deep Infections in Fracture Fixation: Subgroup Meta-analyses of the Type of Fracture, Antibiotics, and Organism.* J Orthop Trauma, 2023. **37**(10): p. e400-e409.
167. Xu, S.J., et al., *The Effect of Topical Vancomycin Powder Application on the Rate of Intervertebral Fusion Following Lumbar Fusion: A Retrospective Study.* World Neurosurg, 2024. **185**: p. e1216-e1223.
168. DeFrancesco, C.J., et al., *Clinically apparent adverse reactions to intra-wound vancomycin powder in early onset scoliosis are rare.* J Child Orthop, 2017. **11**(6): p. 414-418.
169. Orhan, B., et al., *Foam-based antibacterial hydrogel composed of carboxymethyl cellulose/polyvinyl alcohol/cerium oxide nanoparticles for potential wound dressing.* Int J Biol Macromol, 2025. **291**: p. 138924.
170. Meedecha, P., et al., *Preparation and evaluation of blend polymer films for wound dressing using vancomycin-loaded polycaprolactone and carboxymethyl cellulose via crosslinking methods: Effect of mechanical strength, antibacterial activity, and cytotoxicity.* J Mech Behav Biomed Mater, 2024. **151**: p. 106339.

171. Cerchiara, T., et al., *Microparticles based on chitosan/carboxymethylcellulose polyelectrolyte complexes for colon delivery of vancomycin.* Carbohydr Polym, 2016. **143**: p. 124-30.
172. Pezzanite, L.M., et al., *Toll-like receptor activation of equine mesenchymal stromal cells to enhance antibacterial activity and immunomodulatory cytokine secretion.* Vet Surg, 2021. **50**(4): p. 858-871.
173. Otto, M., *Staphylococcal Biofilms.* Microbiol Spectr, 2018. **6**(4).
174. Siripakarn, Y., L. Triniti, and W. Srivilaithon, *Association of Scene Time with Mortality in Major Traumatic Injuries Arrived by Emergency Medical Service.* J Emerg Trauma Shock, 2023. **16**(4): p. 156-160.
175. Rapp, J., et al., *Sepsis Management in Prolonged Field Care: 28 October 2020.* J Spec Oper Med, 2020. **20**(4): p. 27-39.
176. Censi, R., et al., *Thermosensitive hybrid hydrogels for the controlled release of bioactive vancomycin in the treatment of orthopaedic implant infections.* Eur J Pharm Biopharm, 2019. **142**: p. 322-333.
177. Gustafson, C.T., et al., *Controlled Delivery of Vancomycin via Charged Hydrogels.* PLoS One, 2016. **11**(1): p. e0146401.
178. Sadeghi, S., et al., *Carboxymethyl cellulose-human hair keratin hydrogel with controlled clindamycin release as antibacterial wound dressing.* Int J Biol Macromol, 2020. **147**: p. 1239-1247.
179. Thakur, S., et al., *Antibacterial properties enhancement tropical fruit waste biopolymer hydrogel loaded Nephelium Lappaceum leaf extract for sanitizing applications.* Int J Biol Macromol, 2024. **281**(Pt 3): p. 136297.
180. Sundermann, A.J., et al., *Two Artificial Tears Outbreak-Associated Cases of Extensively Drug-Resistant Pseudomonas aeruginosa Detected Through Whole Genome Sequencing-Based Surveillance.* J Infect Dis, 2024. **229**(2): p. 517-521.
181. Stokes, J.M., et al., *Bacterial Metabolism and Antibiotic Efficacy.* Cell Metab, 2019. **30**(2): p. 251-259.
182. Gjini, E., F.F.S. Pauperio, and V.V. Ganusov, *Treatment timing shifts the benefits of short and long antibiotic treatment over infection.* Evol Med Public Health, 2020. **2020**(1): p. 249-263.
183. Balaban, N.Q., et al., *Definitions and guidelines for research on antibiotic persistence.* Nat Rev Microbiol, 2019. **17**(7): p. 441-448.